# Prediction of Noise Propagation on Board a Motor Yacht Using Statistical Energy Analysis (SEA)

**AUNG HTUT KHAUNG**

**Master Thesis Report**

presented in partial fulfillment

of the requirements for the double degree:

"Advanced Master in Naval Architecture" conferred by University of Liege

"Master of Sciences in Applied Mechanics, specialization in Hydrodynamics, Energetics and Propulsion" conferred by Ecole Centrale de Nantes

developed at University of Genoa, Italy

in the framework of the

**"EMSHIP"**

**Erasmus Mundus Master Course**

**in "Integrated Advanced Ship Design"**

Internship company: Cerri Cantieri Navali, La Spezia, Italy

Supervisor: Prof. Dario Boote, University of Genoa, Italy

# Declaration of Authorship

I, AUNG HTUT KHAUNG, declare that this thesis and the work presented in it are my own and have been generated by me as the result of my own original research.

**Prediction of Noise Propagation on Board a Motor Yacht Using Statistical Energy Analysis (SEA)**

I confirm that:

1. This work was done wholly or mainly while in candidature for a research degree at the University of Genoa (UNIGE);
2. Where any part of this thesis has previously been submitted for a degree or any other qualification at this University or any other institution, this has been clearly stated;
3. Where I have consulted the published work of others, this is always clearly attributed;
4. Where I have quoted from the work of others, the source is always given. With the exception of such quotations, this thesis is entirely my own work;
5. I have acknowledged all main sources of help;
6. Where the thesis is based on work done by myself jointly with others, I have made clear exactly what was done by others and what I have contributed myself;
7. Either none of this work has been published before submission, or parts of this work have been published in the reference list.
8. I cede copyright of the thesis in favor of the University of Genoa (UNIGE)

Signed:

Date:

# AKNOWLEDGEMENTS

Special thanks to people who made this work possible:

Prof. Dario Boote and Ing. Gianmarco Vergassola, from the University of Genoa

Ing. Guido Penco and Ing. Nicolo Morando, from Cerri Cantieri Navali in La Spezia, Italy

**Contents**

**List of figures**

**List of tables**

## ABSTRACT

The purpose of this report is the study of the prediction of noise propagation generated on board a motor yacht (40m) still under the construction at Cerri Cantieri Navali shipyard. This investigation is carried out because of the shipyard's necessity to collect the information about the dynamic and vibration behavior of the structures of the motor yacht. The structure of the yacht is not a conventional one: it is considerably stiffer than the regular semi-displacement motor yacht of nearly the same size because it is of Ice Class.

Prediction of noise propagation is of great importance in luxury ships like motor yachts. It is more or less concerned with the vibration of the structures on the ship. Generally, the more vibration there is, the more is the noise production and propagation. Noise propagation issues are determinant not only for the structural reasons but also when the high standards are expected on comfort and well-being. If the limits established by the standards are not exceeded, the habitability will be good which means no health damage will occur.

For this study, the complete motor yacht including hull, decks, structures and insulations are going to be finished. Because it is a perfect condition to perform the predictions, measurements and analyze the comparison of the generated results with the noise criteria from RINA measurements, considering that there is less uncertainties regarding the damping in the vibration analysis and induced errors in the input data. The objective of this study is to know the nature of the Vibroacoustic One software which is applied to perform the SEA analysis, to know the acoustic theory of the structures, to make the prediction of noise in each room throughout the analyzed yacht model, to check whether the estimated sound pressure level of noise satisfy the criteria proposed by RINA and whether the created yacht model can be used to make further investigations on this particular field of study. And the behavior of the glass windows especially around the owner's cabin such that how they contribute to the sound pressure level according to the variation of particular thickness and the behavior of changes in insulation thickness surrounding the acoustic cavity of interest. Moreover, the transmission loss behavior around the critical coincidence frequency of one of the SEA plate panels which contributes the highest power input to the acoustic cavity of interest will be analyzed. The design of yacht, construction plans and technical information will be provided by the shipyard's responsible office. On the side of software, the analysis of this study is developed through the application of VA One (Vibroacoustic One) software. The creation of yacht model is done through the marine modeler tab inside the software.

# 1. INTRODUCTION

The main title of this document is to present noise propagation prediction of the motor yacht of 40m which is still under the construction, by means of SEA analysis of the corresponding yacht model created and to see whether the generated results satisfy the criteria proposed by RINA. This is a useful phase to be employed as first step for further analysis. The analysis is performed using the model created in Marine Modeler in the Vibroacoustic One software from ESI group.

Noise and vibration of the structures are the problems that a ship usually faces after the construction unless a proper study is not performed during the design stages. And it is difficult to find the solution of reducing them after the yacht has been already launched. Moreover, it would cost a lot if there is necessary to change parts of the structure at the time after launching. The sooner the problems are detected, the better it is in order to reduce the cost.

Ship on-board noise propagation is one of the most important issues which shipyards and ship-owners have to deal with. This issue begins during the early stage of designing a new vessel or rebuilding. Noise treatment and thermal insulation of walls, ceilings and floors are being selected in order to fulfill the noise criteria. This activity is done based on noise and vibration propagation analysis. Correct noise and vibration analysis is the only way to achieve a goal - optimized costs and noise criteria fulfillment. Noise analysis is one of the steps one has to take during designing a ship - it's obvious when one takes into account that outfitting costs are very high with respect to overall costs.

This research has been demanded by Cerri Cantieri Navali (CCN), La Spezia, Italy. The 40m yacht to perform the analysis is under the construction in the shipyard. Since it is a kind of luxury yacht, the comfort and well-being of passengers and crew is the most important thing to consider, resulting in the need to predict the noise propagation and noise level due to the vibration of the structures and if the measured noise levels are higher than the accepted level, then the possible solutions to reduce them and the information about the behavior of the yacht will be searched in the further analysis.

All the units used in the whole of this thesis are SI units.

## 2. OBJECTIVE OF THE STUDY

The objectives of this report are as follows.

- To understand the basis of the noise propagation mechanisms
- To get familiar with the simplified methods and associated software for the analysis
- To make a brief review of the noise propagation and associated vibration problems that the yacht usually faces after the construction
- To emphasize the underlying theories mainly based on statistical energy analysis (SEA)
- To evaluate the advantages and difficulties of the applied method and software
- To declare the predicted achievement at the end of the master thesis and the internship period

## 3. SCOPE OF THE STUDY

In last 10 years, there has been a major development on anti-noise and vibration treatment materials used in shipping industry, starting from passive elements such as mineral wool, elastic mountings up to active noise reduction systems based on real-time processors. Simultaneously, the demands of ship owners for silencing their ships have also evolved. Hence, noise limits get more restricted (especially when comfort class is important i.e. passenger ships, yachts, etc.). In order to fulfill those demands, noise propagation analyses have to be performed. For many years, wave propagation model or statistical model has been incorporated for this purpose. Statistical Energy Analysis method has been used especially for high frequency range. In this report, the noise propagation SEA method which will be used for the Master thesis is briefly presented in order to get familiar with this method and noise analysis will be performed and then the generated results after satisfying the noise criteria will become new reliable database for new direction for further research and development.

# 4. METHODOLIGES AND EXPECTED OUTCOMES

First of all when starting the internship, a meeting with the supervisor and the representatives from the shipyard should be held in order to confirm the expectations of the study subject and available resources and data in the shipyard. If there is similar noise and vibration analysis of different ships or yachts, then they should be studied so as to provide more data to be explored. Next, a mapping of the process should take place in order to verify ensure that all possible factor that can influence the process are covered. Subsequently, the study of contribution of the contributing factors will be done together with the collection of the data. Then, according to the requirements of the shipyard and allowed time frame, the selected tools (VA One and Marine Modeler) will be studied and applied to make the noise analysis of the desired yacht through the proposed operating conditions (here in this thesis – navigation condition at cruise speed) recommended by the shipyard. Finally the results will be checked by the proposed standards and the nature of how the structures surrounding the acoustic cavity of interest contribute the sound pressure level by increasing the thickness of particular structures and insulations.

The execution of this work is actually aimed to generate the information as a database for the next generation of yachts. From this database, the correction of the structures and operating functions and the use of the materials of the analyzed yacht will be learned to increase comfort and well-being of passengers and crew and to reduce the noise level with the reduced amount of work, cost, material and time.

# 5. BACKGROUND STUDY OF NOISE PROPAGATION THEORY

From the acoustical point of view, ship is a very difficult object to analyze. It is a rigid structure with many noise sources, flanking paths, discontinuities etc. As far as ship is concerned, noise in compartment is a result of different kind of equipment and machinery noise influence. These noise sources are commonly located in aft part of the ship or in the mid ship part which affects all compartments. The most important noise sources on a yacht are as follows.

- Main engines and generator sets
- Gearboxes
- Propulsion system (cavitation effect)

- Exhaust systems with engine room ventilation
- Auxiliary mechanism such as hydraulic systems, pumps, compressors
- Ventilation and air-conditioning systems
- Side thrusters if there exists one

Participation of particular noise source on total noise in analyzed compartment depends on a ship structure, power and structure of mechanisms, their foundation, distance between noise source and analyzed compartment. In compartments, where noise sources are installed in (i.e. engine room, pump room, bow thrusters room), the most influence on total noise is a machinery airborne noise (noise which is fundamentally transmitted by the way of the air).

In compartments that are located at some distance from noise sources, structure borne noise (noise which is generated by the vibrations induced in the structure - these vibrations excite partitions in ship structure and cause them to radiate noise) dominates. The structure borne sound is directly induced by any mechanical force. The mechanical power transmitted from a source through its connection to the foundation propagates into the structure as flexural, longitudinal, transverse and torsional waves. The longer the distance from the noise sources, the lower the structure borne noise level meaning that the energy flux is attenuated as the function of distance from the disturbance. The attenuation depends on losses in the structure and also on the number of obstructions or discontinuities (decks, platforms, frames) in the propagation path. At the receiving end, the acoustical power radiated from a structure depends on the velocity level and the material parameters and dimensions of the structure. To make a prediction of resulting noise levels in an accommodation space possible, the following quantities must be known.

- Source strengths
- Transmission properties of the structure
- Radiation properties of structure at the receiving end

Generally, noise present on a ship is mostly structure-borne noise. Airborne noise is present especially in compartments, which are adjacent to engine room, exhaust system, or on decks in the chimney neighborhood. These are shown in the figure (1).

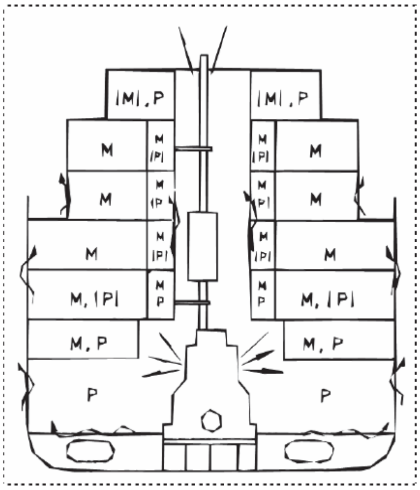


Figure 1: Structure-borne (M) and airborne (P) noise influence on the compartments

The noise propagation analysis can be done through the different methods depending on the interested frequency range. The applications of different methods depending on the frequency range are summarized as shown in the following figure (2).

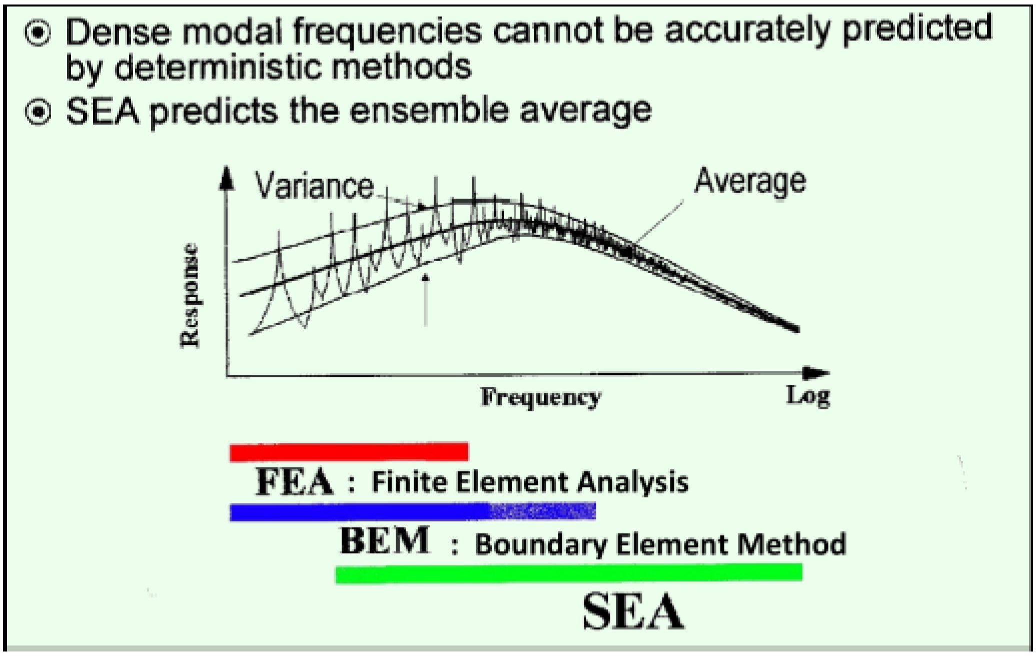


Figure 2: Comparison of noise propagation prediction methods

Classification Societies recommend Statistical Energy Analysis (SEA) noise prediction method for ship's high noise requirements. This method is also recommended at the time of an advanced design that is in a situation when one has a sufficient number of input data. In the absence of such data, the problem of reliability of the results raises. In this case, the measurement data will be applied to certain standard structures. The brief review of Statistical Energy Analysis (SEA) is presented as follows. Statistical Energy Analysis (SEA), numerical analysis based on numerical model, is developed specially for the purpose of noise analysis in the small ships. This numerical model enables the analysis of both the structural elements and the acoustic spaces (acoustic cavities). Statistical Energy Analysis (SEA) is a method for studying the diffusion of acoustic and vibration energy in a system. It is based on energy dissipation. “Statistical” means, that the variables are extracted from statistical population and all the results are expected values. The main idea of SEA method is that one has to divide the analyzed structure into “subsystems”. All energy analysis is done between those subsystems. What is the subsystem? It’s a part or physical element of a structure (system) being analyzed. At high frequencies, modes of a system become localized to various subsystems. Flow of vibrational energy between coupled subsystems is proportional to the difference in modal energies (average energy per mode). To be a subsystem, one has to comply with some conditions as:

- Part of structure considered as a subsystem should have a capability of vibrating quite independently from other parts, where quite means that as long as the element is not separated from the structure, its vibration is not independent.
- Part of structure considered as a subsystem should vibrate in resonant mode, i.e. if the excitation is suddenly switched off, the vibrational energy stored in subsystem should decay rather than drop to zero immediately.

One of the basic advantages of SEA method is namely that the structures or acoustical cavities involved are represented by general geometrical and material data from which properties like average modal densities, average modal damping and average coupling data may be derived. Also the dynamic field variables are represented by simple spatial and temporal averages, corresponding to the total vibratory energy of the subsystems. The coupling leads to energy flow between subsystems in order to maintain an energy balance in the presence of dissipative losses.

The most obvious disadvantage of SEA is that the energy levels obtained for different subsystem are statistical estimates of the true levels, and therefore afflicted with some degree of uncertainty. Usually this problem will be less pronounced when the number of modes is sufficiently high for all subsystem. This will set limits for the practical use of SEA at low frequencies. However no physical limitations can be formulated as long as the subsystem can vibrate resonantly.

# 6. NUMERICAL MODEL

In the past, the marine industry has extensively used the empirical models to predict transfer functions between the source location and noise sensitive cabins. These methods work well for standard construction types, standard materials and small number of cabin. Nowadays, there are also challenges such as unusual hull shapes, use of sophisticated materials like composites and trend of building larger and larger yacht (ships) with huge number of cabins. Current challenges related to on board noise prediction models are cost, quality and time. Cost constraints require computationally efficient techniques to accurately predict on board noise. Luxury vessel owners are of a demanding nature and are extremely sensitive to noise quality and quietness of their purchases. Noise predictions are needed early in the proposal process to support design to meet cost and the noise level constraints. In order to overcome these challenges, an automated means of creating the accurate noise prediction models is therefore necessary. By using a model based on SEA method which can be created with ease, it allow users to make design changes such as construction, material, physical properties, acoustic insulation, loadings and so on. The resulting model can also be used for more detailed analysis by including more details in the geometry, physical properties, insulations and sources.

SEA method is based on an assumption that at a given frequency $\omega$, there is a minimum modal density. In every frequency band, there should be at least 5 vibration modes and all modes are energetically equal. Energy can be transferred from subsystem with higher modal energy to the subsystem with lower modal energy. In order to calculate transferred energy, one has to build an SEA model composed of acoustic cavities, plates etc. SEA is a method where one can distinguish certain steps:

- Structural division for subsystem determination
- Applying excitation (input power sources)
- SEA parameters estimation (modal density, coupling loss factor, damping loss factor)
- Energy transferred calculation
- Resulting response levels calculation (i.e. sound pressures, vibration velocity levels)

# 7. BRIEF THEORETICAL REVIEW OF SEA METHOD

## 7.1. Theoretical SEA Calculation

The following figure (3) is the general SEA model consisting of N subsystems, each of which may receive power $P_{in}$ from an external source and dissipated power $P_{diss}$ due to the damping of the subsystem. Moreover, there is the transferred power $P_{ij}$ between subsystems by the action of coupling forces at the junctions between these subsystems. The energy of each subsystem here is denoted by $E$ and it is the set of energy values that is intended to be solved. Since $E$ is the vibrational energy of the subsystem in a frequency band $\Delta f$, it is the energy that will be used to make the subsystem response estimates later on.

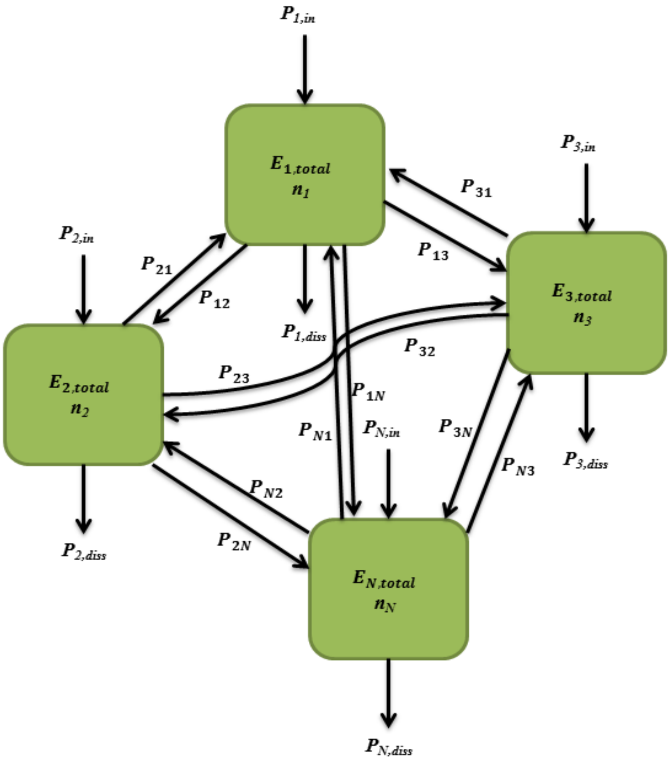


Figure 3: N-Subsystems SEA model

The fundamental relation which is applied is the conservation of energy for each subsystem or a balance between the input power and output power of the subsystem. For the i[th] subsystem, the power balance equation is as follows.

$$P_{i,in} = P_{i,out} \tag{1}$$

$$P_{i,in} = P_{i,diss} + \sum_{j \neq i}^{N} P_{ij} \tag{2}$$

The dissipated power is calculated as follows.

$$P_{i,diss} = \omega \cdot \eta_i \cdot E_{i,total} \tag{3}$$

$\omega = 2\pi f$ is the center frequency of the band of interest,

$\eta_i$ is the damping loss factor,

$E_{i,total}$ is the total energy stored in the i$^{th}$ subsystem.

The power transferred from subsystem i to subsystem j can be shown by the following relation.

$$P_{ij} = \omega \cdot \eta_{ij} \cdot E_{i,total} - \omega \cdot \eta_{ji} \cdot E_{j,total} \; or \; P_{ij} = \omega \cdot \beta \left(\frac{E_{i,total}}{n_i} - \frac{E_{j,total}}{n_j}\right) \tag{4}$$

$\eta_{ij}$ and $\eta_{ji}$ are the coupling loss factors,

$n$ is the modal density.

The connections between the subsystems are described by the coupling loss factors. They are not all independent because they must satisfy the consistency relation as shown below.

$$\beta = n_i \cdot \eta_{ij} = n_j \cdot \eta_{ji} \tag{5}$$

By substituting the equations (3) and (4) into the equation (2), it results in the following set of equations.

$$\frac{P_{1,in}}{\omega} = \left(\eta_1 + \sum_{j\neq 1}^{N} \eta_{1j}\right) E_{1,total} - \sum_{j\neq 1}^{N} \eta_{j1} E_{j,total}$$

$$\frac{P_{2,in}}{\omega} = \left(\eta_2 + \sum_{j\neq 2}^{N} \eta_{2j}\right) E_{2,total} - \sum_{j\neq 2}^{N} \eta_{j2} E_{j,total}$$

$$\frac{P_{3,in}}{\omega} = \left(\eta_3 + \sum_{j\neq 3}^{N} \eta_{3j}\right) E_{3,total} - \sum_{j\neq 3}^{N} \eta_{j3} E_{j,total}$$

$$\frac{P_{N,in}}{\omega} = \left(\eta_N + \sum_{j\neq N}^{N} \eta_{Nj}\right) E_{N,total} - \sum_{j\neq N}^{N} \eta_{jN} E_{j,total}$$

The solutions of these simultaneous equations are found in the conventional way. They are expressed in the matrix form as below.

$$\begin{bmatrix} \eta_{1,total} & -\eta_{21} & -\eta_{31} & \cdots & -\eta_{N1} \\ -\eta_{12} & \eta_{2,total} & -\eta_{32} & \cdots & -\eta_{N2} \\ -\eta_{13} & -\eta_{23} & \eta_{3,total} & \cdots & -\eta_{N3} \\ \vdots & \vdots & \vdots & \ddots & \vdots \\ -\eta_{1N} & -\eta_{2N} & -\eta_{3N} & \cdots & \eta_{N,total} \end{bmatrix} \times \begin{Bmatrix} E_{1,total} \\ E_{2,total} \\ E_{3,total} \\ \vdots \\ E_{N,total} \end{Bmatrix} = \begin{Bmatrix} \frac{P_{1,in}}{\omega} \\ \frac{P_{2,in}}{\omega} \\ \frac{P_{3,in}}{\omega} \\ \vdots \\ \frac{P_{N,in}}{\omega} \end{Bmatrix} ---------- (6)$$

Here in the above matrix equation (6), the diagonal terms of the coefficient matrix (the first matrix) are total loss factors for each subsystem which include not only dissipative losses but also the effects of transfer losses to other subsystems. This total loss factor can be written as below.

$$\eta_{i,total} = \eta_i + \sum_{j \neq i}^{N} \eta_{ij} \qquad (7)$$

If the coefficient matrix is denoted by C, then the above matrix equation (6) can be written as follows where the matrix of energy of vibration is intended to be solved to allow the estimation of subsystem response such as velocity, acceleration, sound pressure and so on.

$$[\mathrm{C}] \,.\, [\mathrm{E_{total}}] = [\frac{\mathrm{P_{in}}}{\omega}] \text{ and therefore, } [\mathrm{E_{total}}] = [\mathrm{C}]^{-1}.\left[\frac{\mathrm{P_{in}}}{\omega}\right]$$

Knowing the values of $P_{in}$ and $\eta$, by the above expression, $E_{total}$ must be carried out for each frequency band $\Delta f$ of interest. Once the energy matrix has been solved, the velocity, acceleration and sound pressure are derived using these relationships.

$$E = Mv^2 \qquad (8)$$

$$E = \frac{Ma^2}{4\pi^2 f^2} \qquad (9)$$

$$E = \frac{Vp^2}{\rho c^2} \qquad (10)$$

$M$ is the mass of the associated subsystem,

$V$ is the subsystem volume,

$v$ is the (RMS) mean square vibration velocity,

$a$ is the (RMS) mean square vibration acceleration,

$p$ is the (RMS) mean square sound pressure,

$\rho$ is the fluid density,

$c$ is the acoustic wave speed.

In order to see the nature of SEA equation more clearly, the SEA equations for two subsystems are derived.

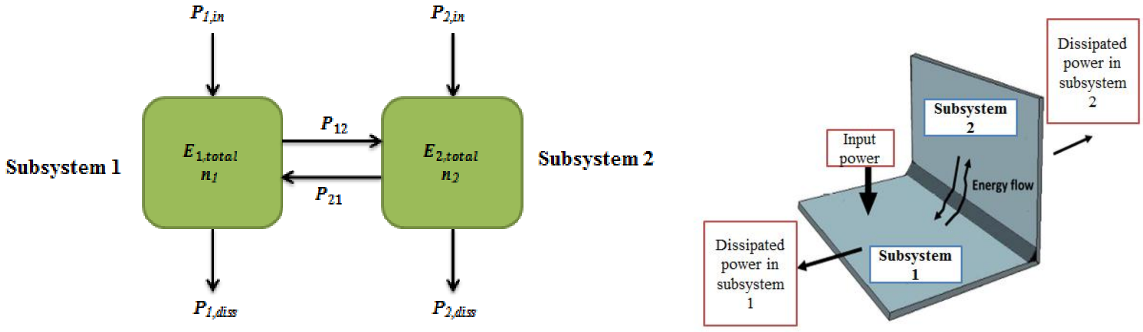


Figure 4: Two subsystems SEA model

By the conservation of energy, for each of these subsystems, the total input power is equal to total output power.

$$P_{in} = P_{out} \tag{11}$$

$$P_{1,in} = P_{1,diss} + P_{12} \; and \; P_{2,in} = P_{2,diss} + P_{21} \tag{12}$$

The dissipated powers due to internal damping are calculated as follows.

$$P_{1,diss} = \omega.\eta_1.E_{1,total} \; and \; P_{2,diss} = \omega.\eta_2.E_{2,total} \tag{13}$$

Because of coupling, subsystems share their vibrational energies, so there is a power flow from subsystem 1 to subsystem 2 and vice versa. From the point of view of subsystem 1, the power flow $P_{12}$ is a power loss and the power flow $P_{21}$ is a power gain. They can be written as follows.

$$P_{12} = \omega.\eta_{12}.E_{1,total} - \omega.\eta_{21}.E_{2,total} \tag{14}$$

$$P_{21} = \omega.\eta_{21}.E_{2,total} - \omega.\eta_{12}.E_{1,total} \tag{15}$$

$$P_{1,in} = \omega.(\eta_1 + \eta_{12}).E_{1,total} - \omega.\eta_{21}.E_{2,total} \tag{16}$$

$$P_{2,in} = -\omega.\eta_{12}.E_{1,total} + \omega.(\eta_2 + \eta_{21}).E_{2,total} \tag{17}$$

The above equations (16) and (17) can be written in the matrix form.

$$\begin{pmatrix} P_{1,in} \\ P_{2,in} \end{pmatrix} = \omega \begin{pmatrix} (\eta_1 + \eta_{12}) & -\eta_{21} \\ -\eta_{12} & (\eta_2 + \eta_{21}) \end{pmatrix} \begin{pmatrix} E_{1,total} \\ E_{2,total} \end{pmatrix} \tag{18}$$

$$\begin{pmatrix} (\eta_1 + \eta_{12}) & -\eta_{21} \\ -\eta_{12} & (\eta_2 + \eta_{21}) \end{pmatrix} \begin{pmatrix} E_{1,total} \\ E_{2,total} \end{pmatrix} = \begin{pmatrix} \frac{P_{1,in}}{\omega} \\ \frac{P_{2,in}}{\omega} \end{pmatrix} \tag{19}$$

If the determinant of the coefficient matrix C is denoted by $D$, then

$$D = \eta_1\eta_2 + \eta_2\eta_{12} + \eta_1\eta_{21} \tag{20}$$

Therefore, the expression for $E_{1,total}$ is

$$E_{1,total} = \frac{\left[\frac{P_{1,in}}{\omega}(\eta_2+\eta_{21}) + \frac{P_{2,in}}{\omega}\eta_{21}\right]}{D} \tag{21}$$

And the expression for $E_{2,total}$ is

$$E_{2,total} = \frac{\left[\frac{P_{1,in}}{\omega}\eta_{12} + \frac{P_{2,in}}{\omega}(\eta_1 + \eta_{12})\right]}{D} \tag{22}$$

In order to make some simplification, it is supposed that only subsystem 1 has external excitation. Then $P_{2,in}$ is zero and therefore,

$$E_{1,total} = \frac{\left[\frac{P_{1,in}}{\omega}(\eta_2 + \eta_{21})\right]}{\eta_1\eta_2 + \eta_2\eta_{12} + \eta_1\eta_{21}} \tag{23}$$

$$E_{2,total} = E_{1,total}\frac{\eta_{12}}{\eta_2 + \eta_{21}} \tag{24}$$

This relation allows us to make quick estimate for $E_{2,total}$ if $E_{1,total}$ is known. On the side of coupling loss factor, only one CLF needs to be known since the consistency relation allows the other to be calculated if the modes in band (or modal densities of subsystems) are known.

Considering now three element subsystems which usually arise when a resonant element such as wall intervenes between two resonant systems of interest, the general equations for this case are written in matrix form as follows.

$$\begin{bmatrix} \eta_1 + \eta_{12} + \eta_{13} & -\eta_{21} & -\eta_{31} \\ -\eta_{12} & \eta_2 + \eta_{21} + \eta_{23} & -\eta_{32} \\ -\eta_{13} & -\eta_{23} & \eta_3 + \eta_{31} + \eta_{32} \end{bmatrix} \times \begin{Bmatrix} E_{1,total} \\ E_{2,total} \\ E_{3total} \end{Bmatrix} = \begin{Bmatrix} \frac{P_{1,in}}{\omega} \\ \frac{P_{2,in}}{\omega} \\ \frac{P_{3,in}}{\omega} \end{Bmatrix} ------(25)$$

Here, the determinant $D$ of the coefficient matrix C is quite complicated and will not be written out. The inverse matrix to the coefficient matrix C is written as follows.

$$[\mathrm{C}]^{-1} = \frac{\begin{pmatrix} \eta_{2t}\eta_{3t} - \eta_{23}\eta_{32} & \eta_{21}\eta_{3t} + \eta_{23}\eta_{31} & \eta_{21}\eta_{32} + \eta_{31}\eta_{2t} \\ \eta_{12}\eta_{3t} + \eta_{13}\eta_{32} & \eta_{1t}\eta_{3t} - \eta_{13}\eta_{31} & \eta_{1t}\eta_{32} + \eta_{31}\eta_{12} \\ \eta_{12}\eta_{23} + \eta_{2t}\eta_{13} & \eta_{1t}\eta_{23} + \eta_{21}\eta_{13} & \eta_{1t}\eta_{2t} - \eta_{12}\eta_{21} \end{pmatrix}}{D} \tag{26}$$

In the above inverse matrix equation (26),$\eta_{1t} = \eta_1 + \eta_{12} + \eta_{13}$, etc. Considering in the same way as in the case of two element subsystems stated previously, in order to obtain a simple result that illustrates the procedure, but that is not representative of many situations of interest, it is firstly assumed that only the subsystem 1 is externally excited so that $P_{2,in} = P_{3,in} = 0$. Secondly, it is assumed that subsystems 1 and 3 are not coupled i.e. $\eta_{13} = \eta_{31} = 0$ so that the three subsystems form a chain (1) → (2) → (3). With these assumptions, the stored energies in each subsystem can be estimated as follows.

$$E_{1,total} = P_{1,in} \frac{(\eta_{2t}\eta_{3t} - \eta_{23}\eta_{32})}{\omega \times D} \quad (27)$$

$$E_{2,total} = P_{1,in} \frac{(\eta_{12}\eta_{3t} + \eta_{13}\eta_{32})}{\omega \times D} = E_{1,tot} \frac{\eta_{12}\eta_{3t}}{\eta_{2t}\eta_{3t} - \eta_{23}\eta_{32}} \quad (28)$$

$$E_{3,total} = P_{1,in} \frac{(\eta_{12}\eta_{23} + \eta_{2t}\eta_{13})}{\omega \times D} = E_{2,tot} \frac{\eta_{23}}{\eta_{3t}} = E_{1,tot} \frac{\eta_{12}\eta_{23}}{\eta_{2t}\eta_{3t} - \eta_{23}\eta_{32}} \quad (29)$$

This three element subsystem is explained together with the example as follows. In the yacht model, when one wants to examine a system which includes two rooms separated by a common wall, such system here is divided into three subsystems such as 1-source room, 2-wall and 3-receiving room. In this system, there are two mechanisms of transmission from room 1 to room 3 if they are coupled. The pressure fluctuations in room 1 will cause to vibrate which in turn causes a pressure to be generated on the other side of the wall. This wall can vibrate in two ways by free bending waves and forced bending waves. Free bending waves interact to cause resonances, the amplitudes of which are dependent on the damping of the wall. The wall then radiates sound into the receiving room. This mechanism of sound transmission is called resonant transmission and it is the dominant mechanism of transmission at and above the critical coincidence frequency. Another way of transmitting sound is non-resonant transmission or forced transmission where the pressure fluctuations force the wall to move in such a way that free bending waves are not generated and so resonances do not occur. In this case, the level of vibration of the wall will be small and its amplitude is not determined by the damping of the wall. This type of mechanism is dominant only under the situation below the critical coincidence frequency where the wall is a poor radiator. This transmission is determined by the mass of the wall.

## 7.2. Critical Coincidence Frequency, Radiation Efficiency and Sound Transmission Loss

The critical coincidence frequency denoted by $f_c$ is the frequency at which the speed of bending wave traveling into the material equals to the speed of sound in the air. In other words, the coincidence occurs when acoustic wavelength equals to the structural flexural wavelength. This can be simply identified by the following expressions.

$$\lambda_x = \lambda_0, k_x = k_0, c_x = c_0$$

$\lambda_x$ is structural flexural wavelength,

$\lambda_0$ is acoustic wavelength,

$k_x$ is the structural flexural wave number,

$k_0$ is the acoustic wave number,

$c_x$ is the structural flexural wave speed,

$c_0$ is the acoustic wave speed (speed of sound in acoustic cavity)

Since the performance of sound reduction is dramatically decreased around this frequency, the consideration of $f_c$ is important in determining the radiation from a panel and transmission through the panel. Moreover, around this frequency, the sound transmission loss *TL* of the panel decreases significantly. The following figure (5) (extracted from the analyzed yacht model) visualizes the location of the critical coincidence frequency over the frequency band of interest where in this figure, cavity 60 represents the right aft peak tank of the yacht and F Plate 1456 means the transverse bulkhead between right aft diesel oil tank and right aft peak tank. In the figure, the critical coincidence frequency occurs between 250 and 315Hz.

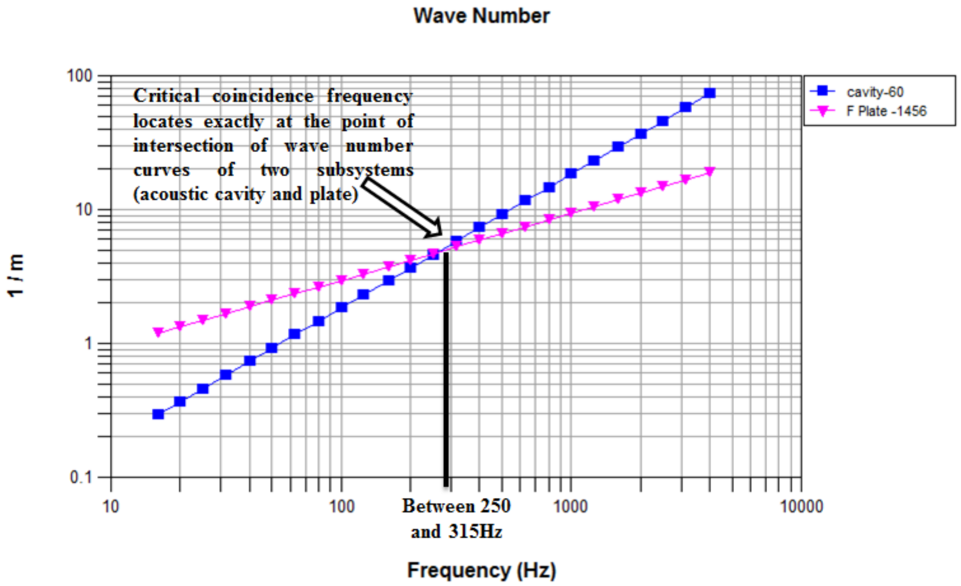


Figure 5: Location of critical coincidence frequency

The radiation efficiency is defined as the ratio of the actual power radiated by the panel to the theoretical power radiated by baffled piston of the same area moving with the same panel average velocity. The radiation efficiency controls the resonant path in SEA area junction. In other words, it controls how much energy gets transmitted into the connected subsystems (SIF or acoustic cavity). To determine the radiation efficiency in VA One, an area junction is required. The radiated power into the subsystem can be expressed in terms of the radiation efficiency as in the following relation.

$$P_{radiated} = \sigma \cdot \rho \cdot c \cdot A \cdot v^2 \qquad (30)$$

$P_{radiated}$ = radiated power to subsystem

$\sigma$ = radiation efficiency

$\rho$ = density of fluid in the acoustic cavity

$c$ = speed of sound in the acoustic cavity

$A$ = area of connection

$v^2$ = average panel velocity

The radiation efficiency is high when the acoustic wavelength (wave speed) is less than the structural wavelength (wave speed) meaning when the acoustic wave number is greater than the structural wave number. Therefore, the left hand side of critical coincidence frequency in the graph in figure (6) represents poor radiator and the right hand side becomes good radiator. The figure (6) shows the general nature of radiation efficiency based on the location of critical coincidence frequency.

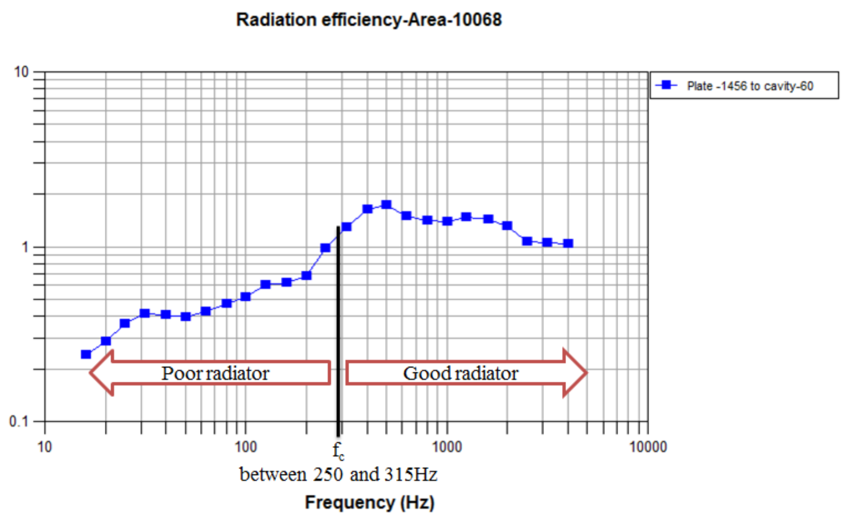


Figure 6: General nature of radiation efficiency with respect to critical coincidence frequency

This paragraph will explain the sound transmission loss *TL* or *STL*. A typical noise control application involves a combination of absorption of sound and transmission of sound energy by a variety of airborne and structure-borne paths. This is illustrated in the figure (7).

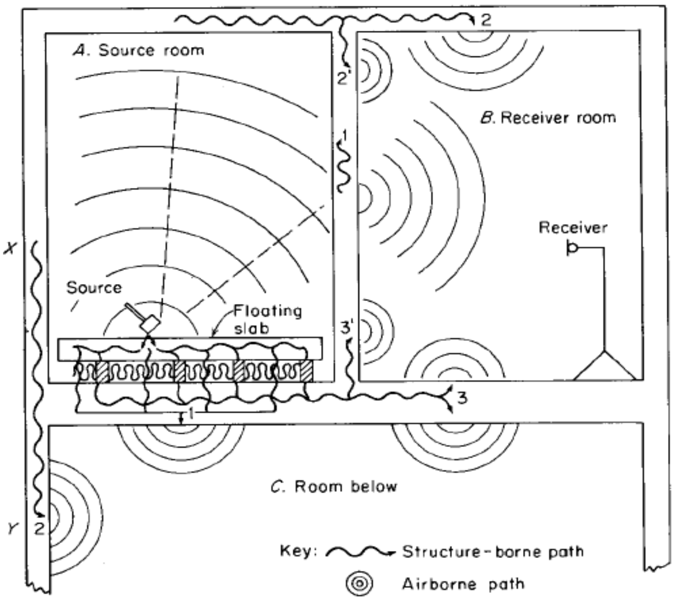


Figure 7: Sound transmission paths between a room containing a noise source and adjacent rooms

When an infinite barrier interrupts a propagating sound pressure wave, the incident sound pressure wave can be reflected back toward the source, allowed to pass through the barrier (wall) and absorbed inside this barrier as illustrated in the figure (8).

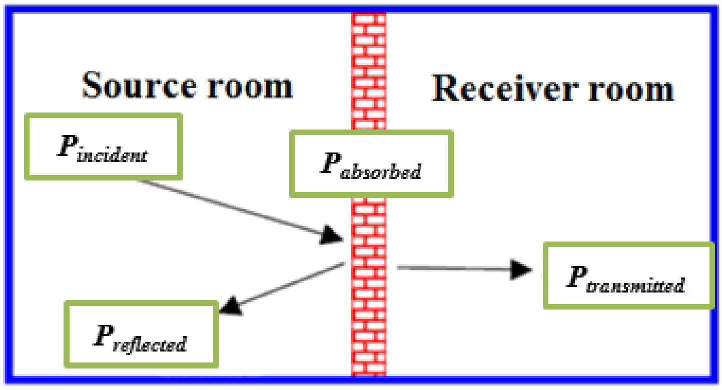


Figure 8: Incident sound power split into reflected, absorbed and transmitted power

Defining $P_{incident}$, $P_{absorbed}$, $P_{reflected}$ and $P_{transmitted}$ as the incident, absorbed, reflected and transmitted sound power respectively, one can write as follows.

$$P_{incident} = P_{absorbed} + P_{reflected} + P_{transmitted} \tag{31}$$

Dividing each term by the incidence sound power $P_{incident}$, the following dimensionless equation (32) is obtained.

$$1 = \alpha + \gamma + \tau \tag{32}$$

$\alpha = \frac{P_{absorbed}}{P_{incident}}$ is the absorption coefficient,

$\gamma = \frac{P_{reflected}}{P_{incident}}$ is the reflection coefficient,

$\tau = \frac{P_{transmitted}}{P_{incident}}$ is the transmission coefficient and this parameter is a frequency-dependent physical property of the material. The sound transmission loss is defined as ten times log ratio of the incident sound power to the transmitted sound power. Therefore, it is written in the equation as below.

$$STL\ or\ TL = 10\ log(\frac{P_{incident}}{P_{transmitted}}) \tag{33}$$

$$STL\ or\ TL = 10\,log\left(\frac{1}{\tau}\right) \tag{34}$$

The incident power can be obtained by the relation: $P_{incident} = \frac{p^2 A}{4\rho c}$

$A$ is the total area of the partition (wall or plate between two acoustic cavities or between a cavity and semi-infinite fluid),

$P$ is the cavity pressure,

$\rho$ and $c$ are the air property

In VA One software, the transmission loss of the panel is normally expressed as effective transmission loss which can be estimated and visualized with a very simple SEA system containing two acoustic cavities separated by a panel or wall similar to the figure (8) illustrated previously. One cavity is excited by a power source. Here, one can calculate the ratio between the amount of acoustic incident power and the portion of power that is transmitted through the panel in the receiving cavity by the following formula.

$$STL\ or\ TL = 10\,log_{10}(\frac{A\omega}{8\pi^2\ c_1^2 n_1 \eta_2}(\frac{E_1}{E_2} - \frac{n_1}{n_2})) \tag{35}$$

$A$ = effective transmission area of the junction (coupling area)

$c_1$ = acoustic wave speed in the source cavity

$\omega$ = center frequency of the band (rad/sec)

$\eta_2$ =damping loss factor of the receiving cavity

$E$ = cavity subsystem energy

$n$ = cavity subsystem modal density (in modes/ (rad/s))

In order to observe the nature of sound transmission loss around the critical coincidence frequency, the results corresponding to the figure (5) is generated and presented in the figure (9).

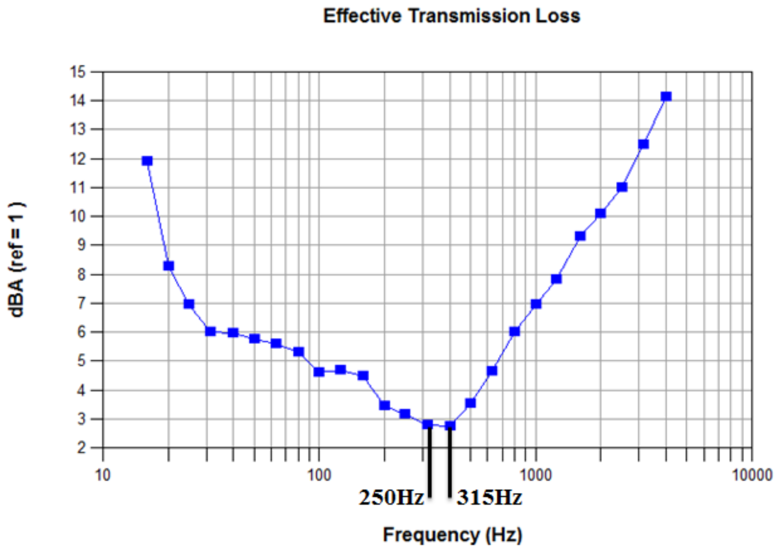


Figure 9: Dramatic decrease in effective transmission loss around critical coincidence frequency

As we can see obviously above, the graph of sound transmission loss has an evident dip about the critical coincidence frequency (between 250 and 315Hz).

A perfectly reflecting material has a transmission coefficient of 0 while the transmission coefficient of an opening is 1. It should be noted that typical materials tend to be better at blocking especially at higher frequencies. The transmission loss *TL* can be measured directly (but not easily) by mounting a test panel between two reverberation rooms and measuring the sound pressure levels on each side. The sound transmitted from an area to another due to the presence of a panel is a frequency dependent amount and is illustrated in the following figure (10).

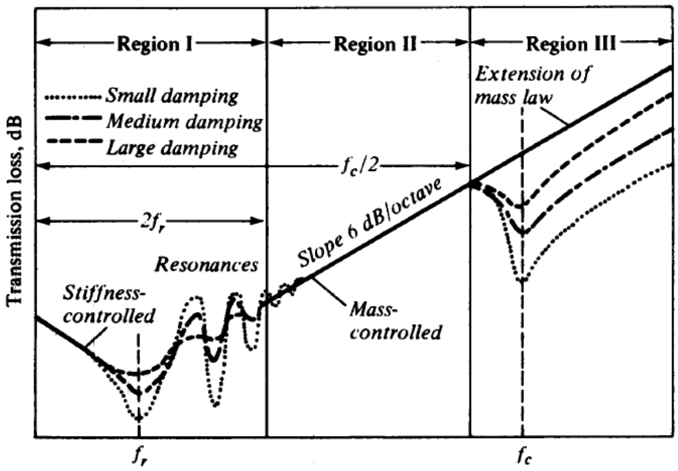


Figure 10: Theoretical Transmission Loss for an infinite homogeneous panel

The *STL* behavior can be divided into three basic regions. In Region I, at the lower frequencies, the response is determined by the panel's static stiffness. Depending on the internal damping in the panel, resonances can also occur which dramatically decrease the *STL*. Just above the stiffness region exists the resonance region where various panel resonances cause large variation in sound transmission.

In Region II (mass-controlled region), the response is dictated by the mass of the panel and the curve follows a 6dB/octave slope. Doubling the mass or doubling the frequency results in a 6 dB increase in transmission loss.

In Region III, the coincidence between the sound wavelength and the structural flexural wavelength again decrease the *STL*. The most effective way to increase energy losses of the panel is to use a viscous interlayer that has high damping in order to transform panels' bending waves into heat energy. This could also have some good effect in the resonance region. The coincidence dip may also be shifted in the frequency range by altering stiffness, boundary conditions and changing thickness of the material. After the coincidence region, the sound transmission loss still increases by 9dB per doubling of frequency.

## 7.3. Modes in Band and Modal Density

The modal count (modes in band) $N_i$ of a subsystem is the number of modes of that subsystem that resonate in the frequency band $\Delta f$ under consideration. In some systems, the number may be of the order of unity and in others (particularly acoustical subsystems at higher frequencies), the number may be in the thousands. Basically, the modal count is a measure of the number of modes available to accept and store energy. In SEA, the modal count is often expressed in terms of a modal density $n_i$ so that $N_i(f) = n_i(f) \cdot \Delta f$. Since the modal count will vary from one frequency band to another, the modal density will also vary with respect to frequency which is the center frequency of the band usually written as $f_c$. Most subsystems have modal densities that vary with frequency.

The reciprocal of modal density $n_i(f)$ is called the average frequency separation between resonant modes within the frequency band $\Delta f$. This average frequency separation is also called modal spacing $\delta f_i$. This modal spacing can also be expressed in terms of radian frequency $\delta\omega_i = \frac{1}{n_i(\omega)} = 2\pi\delta f_i = \frac{2\pi}{n_i(f)}$ and therefore $n_i(\omega) = n_i(f)/2\pi$.

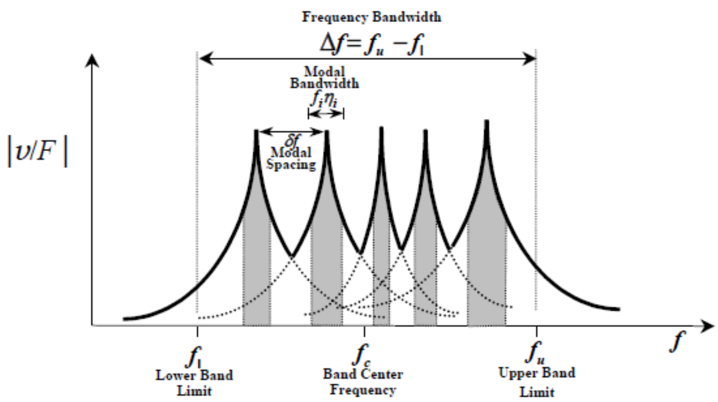


Figure 11: Modal count and modal density in one frequency band of interest

According to the above figure (11), the modal density represents the number of modes for each frequency unit (band). It is one of the most important parameters in SEA because it returns how many resonating modes are available to store or to share energy. This parameter is dependent upon the system dimensions and physical properties but not from the boundary conditions (constraints). There are some general expressions that can be applied to calculate the modal density for simple subsystem dimensions and shapes. These are shown in the following table (1).

Table 1: Modal density (in modes per hertz) formulae for subsystems with simple shapes

| | |
|---|---|
| Beam | $n(f) = \frac{L}{\sqrt{2\pi f}} \sqrt[4]{\frac{\rho A}{EI}}$ |
| Thin flat plate | $n(f) = \frac{A}{2} \sqrt{\frac{12\rho\ 1-\upsilon^2)}{Eh^2}}$ |
| Acoustic cavity | $n(f) = \frac{4\pi V}{c^3} f^2$ |

The modal count may be found by both experimental and computational procedures. Normally in the preliminary design process, the most appropriate way of determining the modal count is to excite the subsystem with a pure tone and observe the response at a second location. The frequency is then swept slowly over the band $\Delta f$ and the response peaks are counted. Only modes that are non-vanishing at the excitation and observation points will show up in the response. For this reason, one should select those locations carefully, either at a corner location for acoustical systems or along a free edge of a structure.

Sometimes when counting the number of modes, they can be missed if their average modal spacing $\delta f_i$ becomes of the same order as their modal bandwidth (resonance bandwidth) $f_i \eta_i$. The equality $\delta f_i = f_i \eta_i$ is the condition of modal overlap and marks the frequency range in which one will begin missing modes because they are too close together to be resolved. It is this limitation that the method called point conductance method is not convenient to be applied in this kind of situation. This method relies on the result that a mean square force $f^2$ in the band $\Delta f$ applied at an average point on the subsystem will result in an injected power such that $P_{in} = f^2/4M_i\delta f_i$ and since the mass $M_i$ is known and presumably $f^2$ and $P_{in}$ can be measured, $\delta f_i$ can be found.

The modal overlap factor is a dimensionless quantity that gives an indication of the dynamic behavior of each subsystem. It provides an indication of when a statistical description of the dynamics of a subsystem is appropriate. It depends on the forcing frequency, the modal density and damping loss factor of subsystem. It is obtainable multiplying the modal density by frequency and the damping loss factor. This relation is as shown in the following equation where the modal density is expressed in radian frequency.

$$m.o.f = \omega \cdot \eta(\omega) \cdot n(\omega) \tag{36}$$

There have been many theoretical studies of modal density for both acoustical and structural systems. In general, the experimentally tested modal density calculations are said to be fairly reliable. Modal density is one of the easier parameters to calculate and it is quite sensible to calculate it if at all possible. There is a partial list of system elements for which calculations of modal density exist. They are as follows.

1. Flat plates with various boundary constraints.
2. Flat plates of complex construction including layered plates.
3. Shells and shell segments, including spheres, cones and cylinders.
4. Acoustic spaces of most shapes, including rectangular, spherical, cylindrical, etc.
5. Various beam and girder shapes including flexural and torsional formations.

## 7.4. Input Power Prediction

The input power is one of the quantities that is presumed to be known in the SEA calculation. Nevertheless, it is only in rare circumstances that the input power will be known directly. Here in this thesis, the user defined power characterized by the power spectrum extracted from RINA measurements for the yachts ranging from 40 to 50m in length is directly applied for airborne noise generation.

The input power can be calculated when the structure is excited with a shaker. Using the force gauge between the structure and the shaker, the mean square force on the structure can be measured. Here in this situation, the excitation may be thought of as highly localized and taken to occur at a point in the system. The mean square force is known instead of mean square pressure and the equation used to calculate the power input is as follows.

$$P_{in} = F^2 \cdot Re(Y_Z(\omega)) \quad (37)$$

$F$ is the point force and $Y_Z$ is the mobility.

The input power can be known if there is the excitation of diffuse acoustic field (DAF) which represents reverberant acoustic load acting over the surface area of a subsystem (face of acoustic cavity or plate). Such DAF is characterized by the mean square (RMS) pressure spectrum that defines the blocked surface pressure across the panel subsystem. The blocked surface pressure is 3dB higher than the pressure within the interior of the chamber (far field). Here in this case, since the DAF pressure is known, the input power can be calculated by the different equations based on where the DAF is excited. If the DAF is applied on the surface of a plate, the equation is as follow.

$$P_{in} = \frac{A \cdot \pi^2 \cdot n \cdot p^2 \cdot \sigma}{m_p \cdot k_a^2} \quad (38)$$

$A$ is the area of the plate,
$n$ is the modal density of the plate (in flexure mode),
$\sigma$ is the radiation efficiency,
$m_p$ is the plate mass,
$k_a$ is the acoustic wave number,
$p$ is the DAF pressure.
If the DAF is applied on one of the surfaces of acoustic cavity, the equation is written as follow.

$$P_{in} = \frac{p^2 A}{4\rho c} \quad (39)$$

In addition to the diffuse acoustic field, another acoustic noise source characterized by mean square turbulent pressure excited only on the panel (not on the face of acoustic cavity) can be applied where the most important determinant of the power injection by the noise field is the ratio of convection speed of the pressure variations to the bending wave speed. In this case, the input power to the structure (panel) in the frequency band $\Delta f$ can be calculated as follow.

$$P_{in} = \frac{p_{\Delta f}^2 A_p^2}{R_{in}} \cdot \frac{\lambda_p \delta_1}{A_p} \tag{40}$$

$p_{\Delta f}^2$ is mean square turbulent pressure measured on the panel in the frequency band

$A_p$ is the area of the panel

$R_{in} = 4 \cdot M \cdot \delta f$ is the input point resistance of the panel

$\lambda_p$ = bending wavelength of the plate

$\delta_1$ = displacement thickness of the turbulent boundary layer profile

The input power can also be calculated when it is possible to measure the vibration or acoustic response of the subsystem acted directly by the source. In this case, three parameters can be constrained such as energy (*E*), velocity (*v*) and acceleration (*a*) giving three spectra, only one of which is necessarily utilized to define the structural constraint noise source acting on the surface of the panel (plate). The corresponding equations to calculate the power input are written as follows where *M* is the total mass of the panel, $\omega$ is the radian center frequency of each band and $\eta$ is the damping loss factor of the panel. In this thesis, such structural constraint noise sources characterized by acceleration spectra from RINA measurements are assigned to the panels for structure borne noise generation in the yacht model.

$$P_{in} = \omega\eta E = \omega\eta M v^2 = \frac{\eta M}{\omega} a^2 \tag{41}$$

In VA One, there are different command icons used to define the corresponding noise generating sources in the yacht model. They are illustrated below.

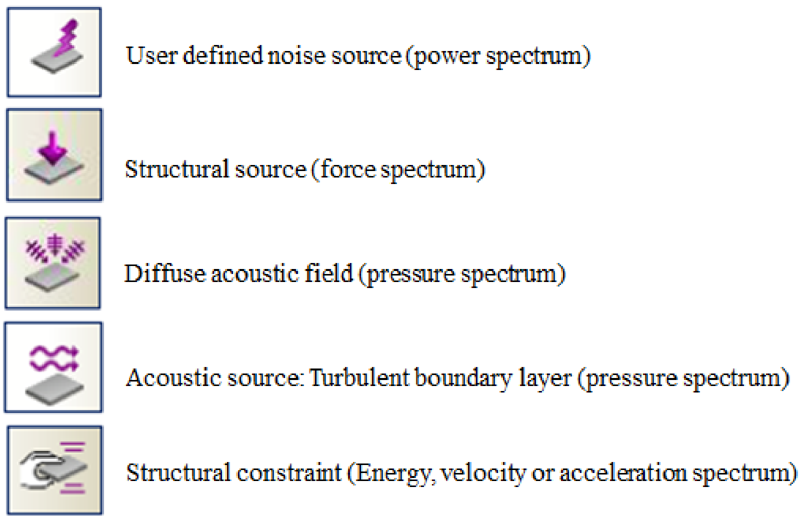


Figure 12: Different VA One command icons for different noise generating sources

## 7.5. Damping Loss Factor (DLF)

The dissipation of stored energy in each subsystem is measured by the parameter $\eta_i$ which is called loss factor (damping loss factor). The damping loss factor is a measure of the ratio of the energy dissipated per unit time to average energy stored. This is presented by the following equation.

$$\eta = \frac{P_{diss}\,(power\ or\ energy\ dissipated\ per\ cycle\ of\ vibration)}{2\pi f E_{stored}} \tag{42}$$

Although there is a good deal of tabular and theoretical information available regarding the damping of various structures, the most commonly used method of determining the damping is simply creating the particular specimen and performing the damping test. Fortunately here in statistical energy analysis, the accuracy to which the damping is required to be known is not too much.

Nevertheless there are some ways which can be applied to estimate the damping loss factor of a system, the experimental methods mostly used to measure the damping of a system include modal analysis curve fitting methods, time domain decay-rate methods and the power injection method (PIM). Each method has its own advantages and drawbacks. The power injection or power input method (PIM) is one of the main methods but this method may display some problems when estimating the DLF of structures with non-uniform distribution of mass. On the other side, decay-rate methods are usually limited to the structure with small damping. The brief descriptions of each method are discussed in the following paragraphs.

### 7.5.1. *Power injection method (PIM)*

The power injection method is a method utilized to estimate the DLF of a system which can be defined as the ratio of the dissipated energy and the total energy per radians of motion.

$$\eta(\omega) = \frac{P_{diss}}{\omega E} \tag{43}$$

Assuming a stationary force excitation applied to the structure, there will be a stationary vibration response field in the structure, meaning that an equal amount of energy must be input from the excitation source to compensate for the dissipation energy from damping. Therefore, it may be assumed that the power input to the structure is equal to the dissipated energy in the steady state conditions. This power input can be measured from the mobility of the system location where the excitation is applied. A measurement of force and acceleration at the driving point allows one to determine $P_{in}$. Measuring the root mean square acceleration of the structure allows the determination of root mean square velocity by the following relation.

$$v^2 = \frac{a^2}{4\pi^2 f^2} \tag{44}$$

Therefore the equation (43) becomes as below.

$$\eta(\omega) = \frac{P_{in}}{\omega E} = \frac{P_{in}}{\omega M v^2} \tag{45}$$

This method has a strong dependency on the amount of response points throughout the system where the response energy can be measured. The greater the number of response points, the greater is the accuracy.

### 7.5.2. *Decay-rate method*

The Decay-Rate Method also known as Impulse Response Decay Method (IRDM) is based on the measurement of the system's decay rate when it is subjected to an impulse or an interrupted stationary excitation. The system's response amplitude measured by an oscilloscope when plotted versus time will have a slope proportional to $e^{\pi f \eta t}$ where *f* is the frequency, $\eta$ is the damping loss factor and t is the time. The decay slope between two instants in time $t_1$ and $t_2$ with the corresponding amplitudes $X_1$ and $X_2$ in decibels is given by the equation below followed by the graphical representation at the particular frequency.

$$20\, log\left(\frac{X_1}{X_2}\right) = 27.3 f \eta (t_2 - t_1) \tag{46}$$

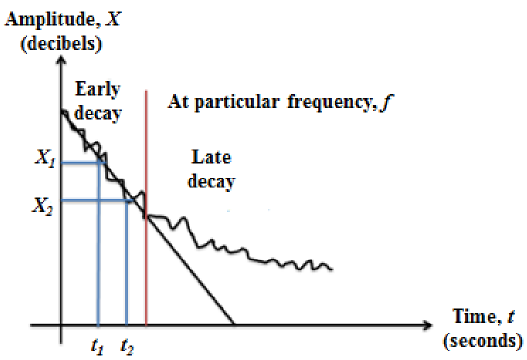


Figure 13: Decay slope shown at particular frequency *f*

Also, defining the decay rate DR as the rate of decrease of the structural vibration level with time in decibels per second, the damping loss factor can be calculated by using the following relation.

$$\eta = \frac{DR}{27.3f} \tag{47}$$

Such measurements of DLF in both methods are performed for each frequency band of interest and the resulting spectra generally plotted in terms of fully octave or one-third octave frequency bands are directly input for each material in VA One when building the yacht model.

## 7.6. Coupling Loss Factor (CLF)

The coupling loss factor is assumed to be independent of the levels of excitation of the individual subsystems. It represents the portion of whole energy in the subsystem i transferred through a junction from subsystem i to j. The power flow between subsystems can be described either in terms of the actual energies of vibration or in terms of the energy of vibration that they would have in the absence of coupling. This power transferred between subsystems i and j can be described using the coupling loss factors as follows.

$$P_{ij} = \omega\eta_{ij}E_{i,total} - \omega\eta_{ji}E_{j,total} \text{ and } P_{ji} = \omega\eta_{ji}E_{j,total} - \omega\eta_{ij}E_{i,total} \tag{48}$$

$\eta_{ij}$ and $\eta_{ji}$ are coupling loss factors between subsystems i and j.

The theoretical calculation of coupling loss factor can be complicated for the following reasons.

(a) Neither of the subsystem is dense, which means that only a few modes of each of the two subsystems resonate in the frequency band of interest.

(b) The junction is not just a point but extends along a line or over an area.

The calculation of coupling loss factor is different based on the type of SEA junctions by which the subsystems are connected.

### 7.6.1. *Calculation of CLF for SEA area junction*

There are mainly two paths of sound transmission between subsystems through the SEA area junction, namely resonant transmission and non-resonant transmission paths illustrated in the figure (14).

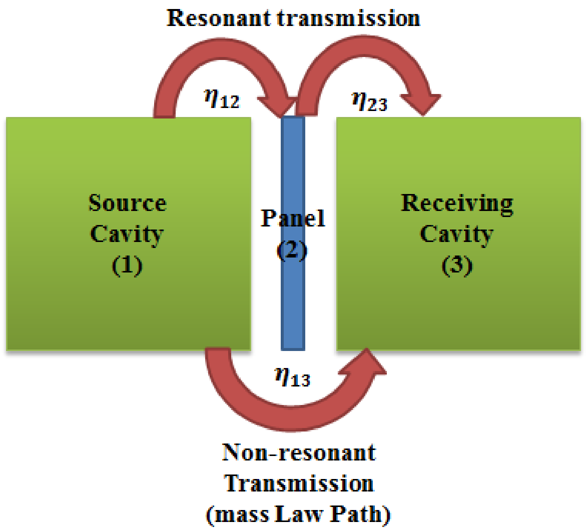


Figure 14: Sound transmission paths through SEA area junction

To calculate the CLF from resonant path, it is necessary to compute the radiation efficiency of resonant modes of panel subsystem. In an SEA model, what is interested about the radiation efficiency is the ensemble average radiation efficiency when there is a reverberant field in the panel (i.e. the resonant radiation efficiency of the panel). Then the CLF is calculated by the following equations for particular subsystem coupling.

$$\eta_{12} = \frac{\rho_1 c_1 A_2}{\omega m_2}\sigma_{12} \text{ and } \eta_{23} = \frac{\rho_3 c_3 A_2}{\omega m_2}\sigma_{23} \tag{49}$$

$\eta_{12}$ is the CLF between subsystems 1 and 2,

$\eta_{23}$ is the CLF between subsystems 2 and 3,

$\sigma_{12}$ and $\sigma_{23}$ are the radiation efficiencies,

$\rho$ is the fluid density in each acoustic cavity,

$c$ is the fluid speed in each acoustic cavity,

$\omega$ is the radian frequency (center frequency of each band),

$A$ and $m$ are the area and mass of panel between two cavities.

The coupling loss factor between two acoustic cavities (two connecting rooms with an open door or no panel) is identical to the coupling loss factor for non-resonant sound transmission through a panel. It depends on the angle of incidence and the panel mass and is normally considered as additional CLF to those calculated from resonant path in SEA general equations. The SEA area junction assumes field incidence angle θ from 0 to 78 degrees. The relation (Mass law) applied to calculate such CLF is expressed in terms of transmission coefficient $\tau$ derived from acoustic impedance $Z$.

$$\mathcal{T}_{13}(\theta) = \mathcal{T}_{31}(\theta) = \frac{4Re(Z_1)Re(Z_2)}{|Z_1+Z_2+Z_3|^2} \qquad (50)$$

$$\text{Where, } Z_1(\theta) = \frac{\rho_1 c_1}{cos(\theta)} \text{ and } Z_2 = i\omega m_2 \text{and } Z_3(\theta) = \frac{\rho_3 c_3}{cos(\theta)}$$

$$\eta_{13} \propto \frac{\mathcal{T}_{13}(\theta)}{n_1\,\omega} \text{ and } \eta_{31} \propto \frac{\mathcal{T}_{31}(\theta)}{n_3\omega} \Rightarrow \eta_{13}n_1 = \eta_{31}n_3$$

$\eta_{13}$ and $\eta_{31}$ are the CLF between subsystem 1 and 3,

$Z$ is explained in the next section.

### 7.6.2. *Calculation of CLF for SEA point and line junctions*

The SEA point and line junctions are used to connect two or more SEA plate (panel) subsystems. Here, the coupling loss factor is expressed as the function of transmission coefficient $\tau$ derived from acoustic impedance mismatch $Z$ in the same way as to calculate the CLF of area junction for non-resonant transmission but with slight difference. The CLF for point and line junction is calculated from the integration of all possible angles of incidence on particular junction.

$$\mathcal{T}_{12} = \frac{P_{transmitted}}{P_{incident}} = \frac{4Re(Z_1)Re(Z_2)}{|Z_1+Z_2+\cdots+Z_N|^2} \qquad (51)$$

$$\text{Where, } \eta_{12} \propto \frac{\mathcal{T}_{12}}{n_1\,\omega}$$

$Re(Z)$ means real part of $Z$ which is complex number,

$Z$ is the infinite acoustic impedance,

$n$ is the modal density.

The example of subsystems coupled by line junction is illustrated in the figure (15). Since the nature of point junction is the same as that of line junction, the example showing the subsystems coupled by the point junction will not be illustrated.

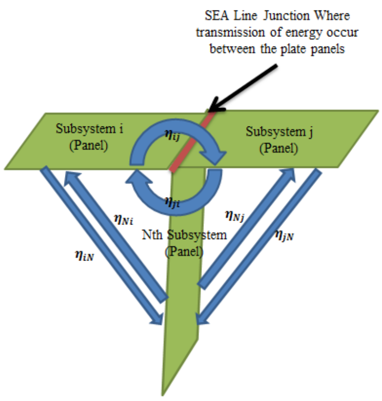


Figure 15: Subsystems coupled by line junction

The infinite acoustic impedance $Z$ (in complex number form) is the ratio of sound pressure $P$ (unit in Pascal (Pa)) and volume flow rate $U$ (unit in cubic meter per second) of the fluid which are also in complex number forms.

$$Z = \frac{P}{U} \tag{52}$$

Where, $P = Pe^{i(wt+\theta(P))}$ and $U = Ue^{i(wt+\theta(U))}$

The calculation of CLF for all SEA junctions (point, line and area) obeys the law of reciprocity stated by the following equation.

$$\eta_{ij} n_i = \eta_{ji} n_j \tag{53}$$

$n_i$ and $n_j$ are modal densities of subsystem i and j.

## 7.7. Description of Full Octave and Third Octave Frequency Bands

In general, the engineering analyses by frequency basis are not performed at all frequencies throughout the whole frequency range of interest. In order to avoid time consuming, the whole frequency range is divided into sets of frequencies called bands. Each band covers a specific range of frequencies. Although there are many scales defining the octave bands in engineering, the two standardized frequency bands which are mostly applied are octave bands (full octave bands) and one-third octave bands. A band is said to be full octave when the upper limit frequency is twice the lower limit frequency and said to be one-third octave when the upper limit frequency is cube root of two times the lower limit frequency. Whichever way the frequency band is defined, the general form defining the particular bands can be written as follows.

$$f_{upper} = f_{centre} \cdot f_d \tag{54}$$

$$f_{lower} = f_{centre} \div f_d \tag{55}$$

$$f_d = 2^{\frac{1}{2N}} \; and \; r = \frac{f_d^2 - 1}{f_d} \tag{56}$$

If the band is full octave, $N$ is 1 and if it is third octave, $N$ is 3. If it is tenth octave, then $N$ is 10 and so on. The results of calculations are usually presented in terms of constant percentage bandwidths. For this, the nominal center frequency of the band $f_{centre}$ is normally used which is generally the geometric mean of the upper limit and lower limit frequencies. This relation derived from equations (54) and (55) can be shown as the following equation.

$$f_{centre} = \sqrt{f_{upper} \cdot f_{lower}} \tag{57}$$

And the bandwidth $\Delta f = f_{upper} - f_{lower}$ is always a constant fraction $r$ of the center frequency ($\Delta f = r \cdot f_{centre}$). Here in this thesis, the SEA analysis is performed on the one-third octave frequency bands.

## 7.8. Different Representations of Energy, Velocity, Acceleration, Power and Sound Pressure in Acoustic Theory

In VA One software, the spectra (plotted versus frequency) of energy, velocity, acceleration, power and sound pressure can be expressed in terms of their original units as well as in power spectral density. In engineering usage, the power spectral density of the energy of vibration may be denoted by $psd(E(f))$ and the energy of vibration associated with a frequency band $\Delta f$ in the range $f_{lower} < f < f_{upper}$ is simply mentioned by the following relation.

$$E_{\Delta f} = \int_{f_{lower}}^{f_{upper}} psd(E(f))\, df \tag{58}$$

This integration can be shown graphically as the hatched area in the following figure (16).

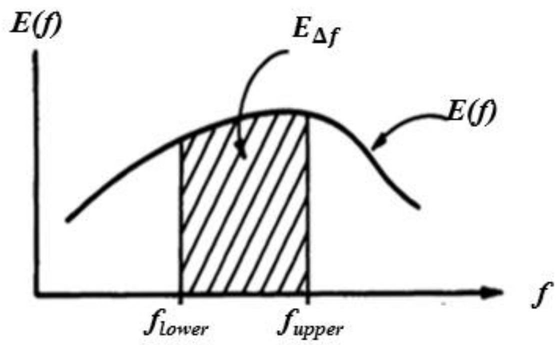


Figure 16: Integration of power spectral density of energy in frequency band of interest

The SI unit for the energy is the joule (J) or watt-second which is the amount of work involved when a force of 1N acts along a distance of 1m. The unit for the power spectral density of energy $psd(E(f))$ is joule per hertz (joule second) because the unit of frequency is cycles per second or hertz (Hz). The following table (2) shows the summary of the relations between energy, velocity, acceleration, power and sound pressure and their corresponding power spectral densities as follows.

Table 2: Equations of power spectral density for each parameter

| Parameter | Unit | Power spectral density (*psd*) | Unit | Relation between these parameters |
|---|---|---|---|---|
| Energy | J or Nm | $psd(E(f)) = \frac{E}{\Delta f}$ | J/Hz | |
| Velocity | m/s | $psd(v(f)) = \frac{v_{rms}^2}{\Delta f}$ | $(m/s)^2/Hz$ | $v_{rms}^2 = \frac{E}{M}$ |
| Acceleration | $m/s^2$ | $psd(a(f)) = \frac{a_{rms}^2}{\Delta f}$ | $(m/s^2)^2/Hz$ | $a_{rms}^2 = 4\pi^2 f^2 v_{rms}^2$ |
| Power | W | $psd(P(f)) = \frac{P}{\Delta f}$ | W/Hz | $P = \omega\eta E$ |
| Sound Pressure | Pa | $psd(p(f)) = \frac{p_{rms}^2}{\Delta f}$ | $Pa^2/Hz$ | $p_{rms}^2 = \frac{E\,\rho\,c^2}{V}$ |

In addition to the power spectral density, these parameters can also be expressed in terms of the level (dB) where each of these parameters has its own reference value. The following table (3) summarizes the calculation of the level (dB) value of each parameter.

Table 3: Equations of the level (dB) values for each parameter

| Parameter | Equation | Reference value | Relation between their level (dB) |
|---|---|---|---|
| Energy level | $L_E = 10\,log(\frac{E}{E_{ref}})$, dB | $E_{ref} = 10^{-12}$ J | - |
| Velocity level | $L_v = 20\,log\left(\frac{v_{rms}}{v_{ref}}\right)$, dB | $v_{ref} = 1$ m/s | $L_v = L_E - 10\,log\,M - 120$, dB |
| Acceleration level | $L_a = 20\,log\left(\frac{a_{rms}}{a_{ref}}\right)$, dB | $a_{ref} = 1\ m/s^2$ | $L_a = L_v + 20\,log\,f - 4$, dB |
| Power level | $L_P = 10\,log(\frac{P}{P_{ref}})$, dB | $P_{ref} = 10^{-12}$ W | $L_P = L_E + 10\,log(f\eta) + 8$, dB |
| Sound Pressure level | $L_p = 20\,log\left(\frac{p_{rms}}{p_{ref}}\right)$, dB | $p_{ref} = 2 \times 10^{-5}$ Pa | $L_p = L_E - 10\,log\left(\frac{V}{\rho c^2}\right) - 26$, dB |

The sound pressure and sound pressure level stated in the tables (2) and (3) represent the total sound pressure and its level contributed from both airborne and structure borne noises. The structure borne sound pressure $p_s$ and pressure level $L_{p_s}$ in a room having the equivalent overall surface area *A*, filled with the fluid density $\rho$ where the fluid speed is *c*, induced by one vibrating surface with the area $S$, velocity $v$ and radiation efficiency $\sigma$ can be written as in the equations (59) and (60).

$$p_s^2 = \frac{4\,\rho^2\,c^2\,v_{rms}^2\,S\,\sigma}{A} \tag{59}$$

$$L_{p_s} = L_v + 10\,log(\frac{4S\sigma\rho^2c^2}{A}) + 94, \text{dB} \tag{60}$$

The total structure borne sound pressure level $L_{p_s}$(total) in an accommodation space caused by all the surrounding radiating surfaces is determined through the following relation.

$$L_{p_s}(total) = 10\,log\left[\sum_{i=1}^{N} 10^{\frac{L_{p_s,i}}{10}}\right], \text{dB} \tag{61}$$

The summation is made over all the surfaces. In every accommodation space, the airborne noise contributions from various noise sources are added logarithmically to the total structure borne noise for each of the considered octave bands and consequently A-weighted sound level dB(A) can be calculated as the results.

A-weighting is commonly used as the international standards in various engineering analyses relating to the measurement of sound pressure level. A-weighting is applied to instrument-measured sound pressure levels in an effort to account for the relative loudness perceived by the human ear because the ear is less sensitive to low audio frequencies. It is employed by arithmetically adding a table of values (in both octave and third octave) to the measured sound pressure levels in dB. In order to account for such A-weighing, the A-weighing function $R_A(f)$ is defined which is then used to calculate the loss or gain in dB values $A(f)$. Their expressions are shown in the equations (62) and (63) and the results of calculation for A-weighing values are presented in the figure (17).

$$R_A(f) = \frac{12194^2 f^4}{(f^2+20.6^2)(f^2+12194^2)\sqrt{(f^2+107.7^2)(f^2+737.9^2)}} \tag{62}$$

$$A(f) = 20\,log(R_A(f)) + 2, dB \tag{63}$$

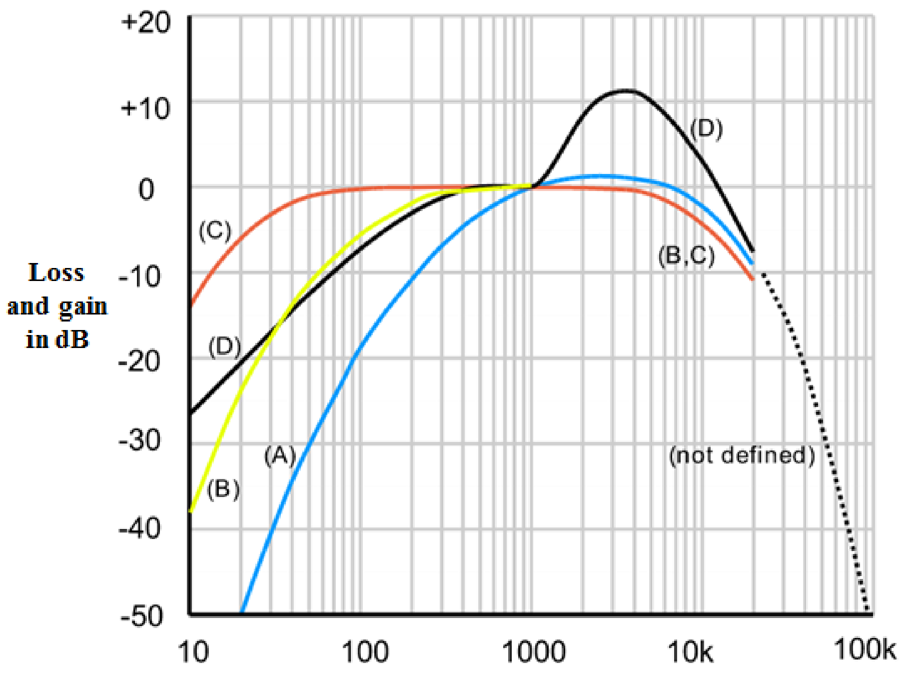


Figure 17: Loss and gain in dB when changing from dB to dB(A) (Blue line) and other scales

The required dB(A) values of sound pressure level are obtained by adding or subtracting the $A(f)$ values from the initial dB values at the particular frequency.

# 8. STATISTICAL ENERGY ANALYSIS OF 40m MOTOR YACHT

## 8.1. Case Study

The statistical energy analysis is applied to the 40m ice class motor yacht whose principal dimensions are as shown in the following table.

Table 4: Yacht's principal dimensions

| | | |
|---|---|---|
| Length overall | LOA | 40.86m |
| Length on waterline | LWL | 39.26m |
| Maximum beam | B | 9.4m |
| Beam on waterline | BWL | 8.9m |
| Depth molded | D | 6.1m |
| Draft | T | 2.75m |
| Maximum draft | $T_{max}$ | 2.79m |

In order to identify the acoustic problems that may arise in the analysis of this yacht, the interior plans of the yacht should be known. Therefore, the general arrangement plan of the yacht is studied and this is as shown in the following figure (18).

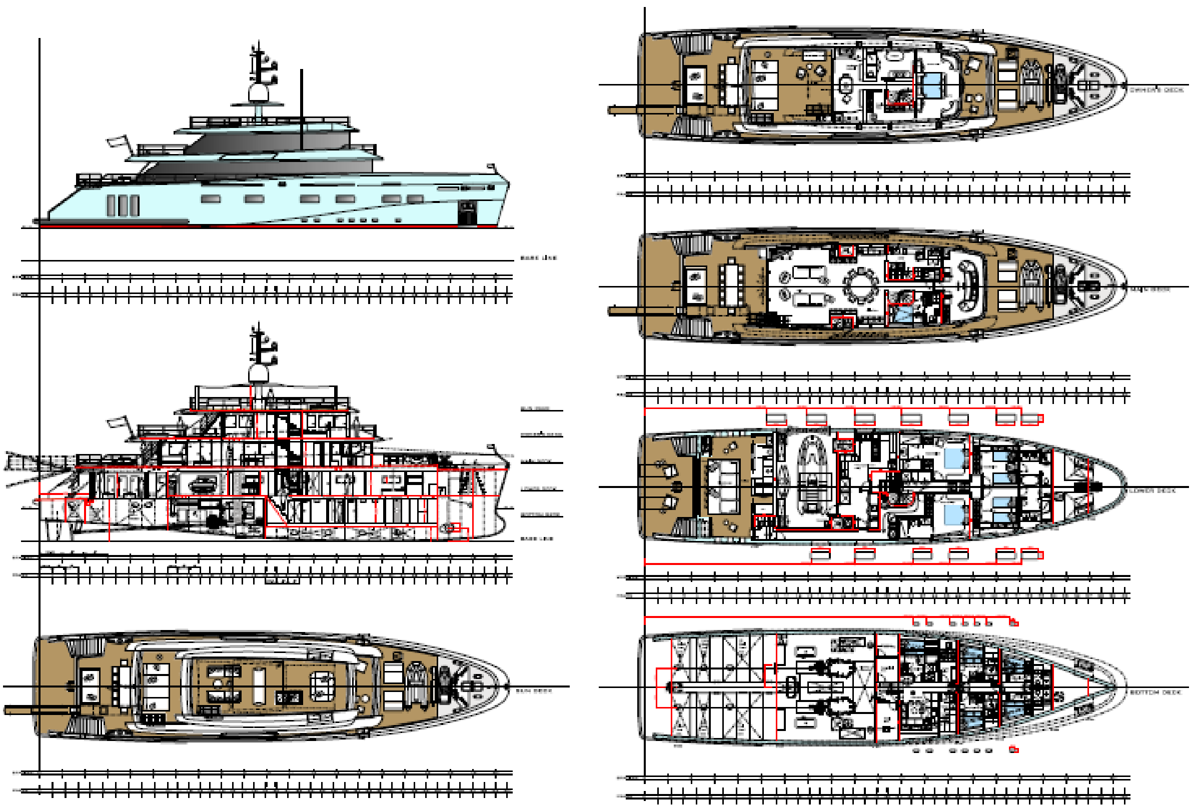

Figure 18: General arrangement plan of the yacht

In the GA plan, the characteristics of the main engines that will be the main noise generating sources are presented below.

Table 5: Characteristics of the main engine

| | |
|---|---|
| Main engine type | CAT C32 ACERT |
| Maximum continuous rating power | 1081kW |
| Nominal revolution | 2300rpm |

And the characteristics of the propellers which are another main noise generating sources are presented as below.

Table 6: Characteristics of propeller

| | |
|---|---|
| Diameter | 1.4 m |
| Number of blades | 5 |

The vibroacoustic system is described in terms of a source path-receiver model. Sources inject the energy into a vibroacoustic system. This energy propagates along various transmission paths, before arriving at the various receiving locations of interest. In general, the transmission paths in the vibroacoustic system involve transmission through many different structural and acoustic components. The transmission of noise and vibration within a vibroacoustic system therefore depends on the way in which the system components are joined together and the dynamic properties of the individual components. In order to let the energy propagate throughout the yacht model, this yacht model consists of three main objects:

1. Subsystems that are used to model the various structural and acoustic components that transmit energy through the vibroacoustic system.
2. Junctions that are used to model the connections between the various subsystems in a system. They are also used to describe the way in which the energy is transmitted between the different subsystems in a system.
3. Sources that are used to model the various sources that inject energy into the subsystems in a vibroacoustic system.

## 8.2. Creating SEA 3D Model

The steps to create the SEA 3D model are presented as follows.

- Assigning body and floor acoustic lines to form SEA 3D plate model
- Assigning beam and plate physical properties
- Assigning noise control treatment (NCT)
- Assigning damping of the panels and insulations
- Creation of SEA acoustic cavities
- Applying fluid loading and underwater SIF
- Creation of corresponding SEA subsystem junctions
- Assigning noise generating sources onboard the yacht

### 8.2.1. *Assigning body and floor acoustic lines to form SEA 3D plate model*

There are two ways to construct the model in the vibroacoustic one software. One is manual creation of the model and the other is using the scripts of the marine modeler module. Obviously, the latter way is easier to create the yacht model. In order to apply the scripts of marine modeler module, three different files (xml file, dxf file and excel file) must be prepared. Three fundamental drawings such as the lines plan, the general arrangement and the structural drawings of the yacht are necessary. By using the lines plan, the description of the hull shape is drawn in the software and save the file as xml file. Then by using the GA plan, the internal partition of each floor is defined and save it as dxf file and therefore the SEA subsystems such as plates and acoustic cavities can be built. Finally, the excel file highlighting the primary supporting members of the bottom such as bottom girders, transverse frames, the position of bulkheads and the heights of each deck must be entered in the script. Then, by using these three files defining each part, the software builds a preliminary 3D model composed by nodes, acoustic ducts and plates. Then the model is furnished to include more details by some corrections corresponding to the insulation plan and general arrangement plan.

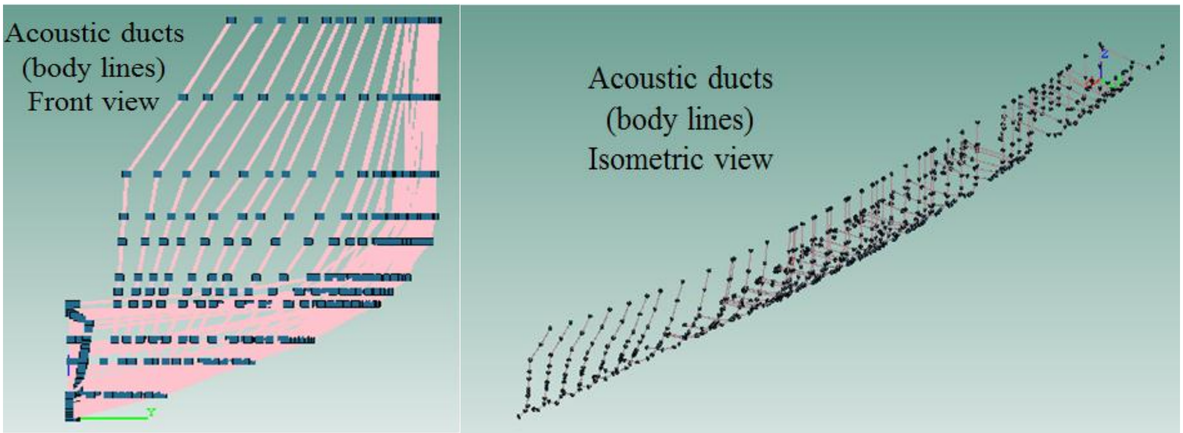


Figure 19: Body lines input to form 3D plate model

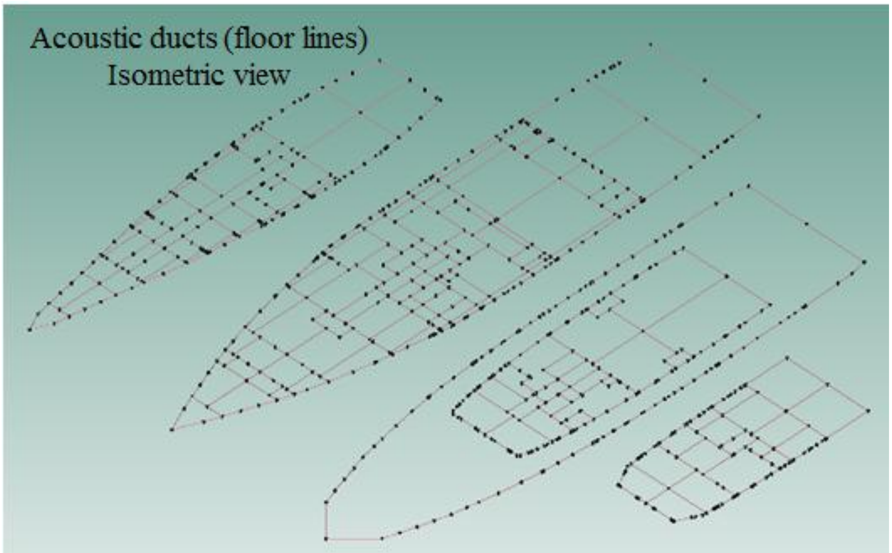


Figure 20: Floor lines input to form 3D plate model

### 8.2.2. *Assigning beam and plate physical properties*

When the plate model is finished with furnishing, then the physical properties of each plate are defined such as the type of plate, material, thickness and so on. There are different types of plate which can be defined in the VA One software. They are as follows:

1. Uniform construction
2. Sandwich construction
3. Composite construction
4. General laminate construction
5. Ribbed construction

The following figure (21) illustrates the nature of these different types of plate.

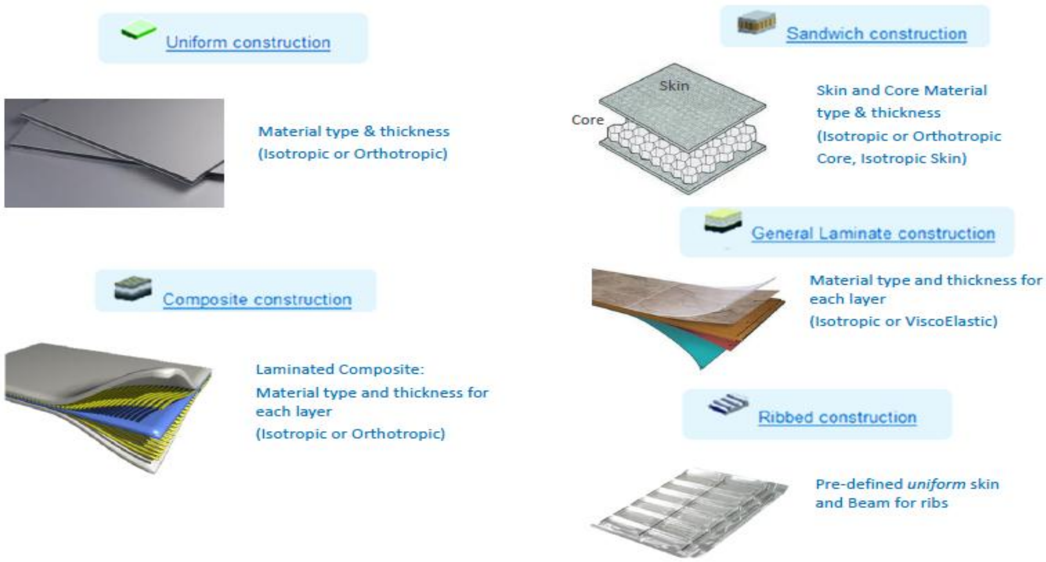


Figure 21: Different forms of plates which can be defined in VA One

In the creation of beam property, different beam profiles are used in the construction of this yacht such as bulb profile, I beam, T beam, Holland profile, L profile and so on. Regardless of different beam profiles, as it is explained previously, only the moment of inertia (second moment of area), area, perimeter and corresponding material of the beam should be defined in this software. An example is shown in the following figure (22).

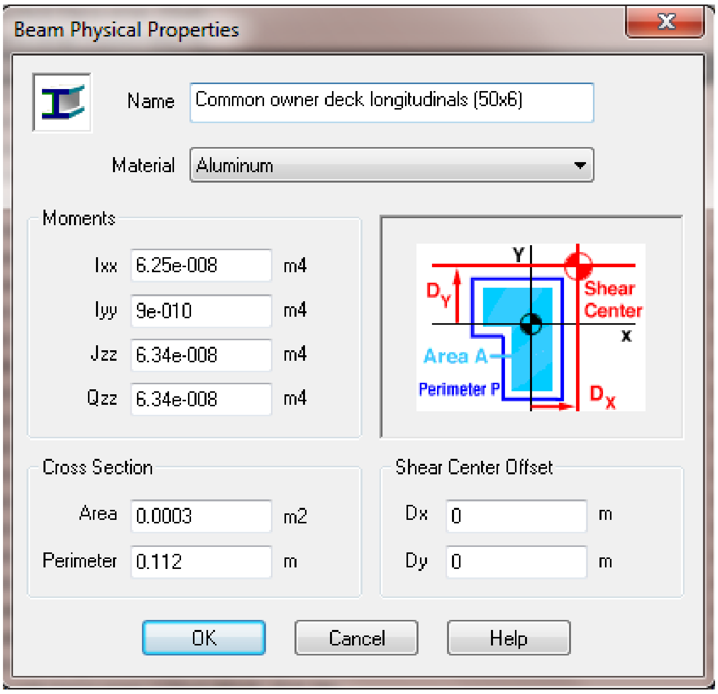


Figure 22: Example of beam element property

*A* is the area of the section,

*P* is the perimeter of the section,

*Dx* and *Dy* are the coordinates representing the shear center offsets,

*Ixx* is the second moment of area of the section about the beam's local x-axis,

*Iyy* is the second moment of area of the section about the beam's local y-axis,

*Jzz* is the polar moment of area of the section about the beam's local z-axis,

*Qzz* is the torsion constant of the beam section.

The different types of beam (stiffeners) used in various parts of this yacht are presented with the table in the Appendix III.

If the plate has stiffeners in the local longitudinal and transverse directions on it, it is distinguished as ribbed plate. A ribbed plate consists of two separately specified sets of uniformly spaced ribs in two orthogonal directions applied to an SEA plate. In this way, it is possible to take into consideration of secondary stiffeners for bottom, and primary and secondary stiffeners for the side, deck and bulkheads. When defining the ribbed plates, if the stiffeners on the plate are not of the same profile, the new stiffeners with the same profile which in total give the same moment of inertia as the total one given by the summation of moments of inertia of different ribs. A modal formulation is used to compute the vibroacoustic properties of a ribbed plate or shell such as modal density, radiation efficiency and so on. A rectangle is fitted to the subsystem geometry by preserving area and perimeter. By solving the equation that includes the effects of the ribs, the natural frequencies of the simply supported modes of the rectangular ribbed panels are calculated in this software. Presence of ribs induces complex modal behaviors such as smeared modes where half wavelength is larger than spacing, sub-panel modes where half wavelength is smaller than spacing, combination of both in the same frequency band possible, in mid-frequency, sub panel modes grouped in certain bands, modal formulation used to compute the number of modes in band and the effect of ribs decreases with frequency (asymptotes to un-ribbed plate). When the bending wavelength in the base plate or shell is larger than the ribs spacing, the rib dynamics are included by smearing the rib's mass and stiffness into the base panel properties, which results in an equivalent orthotropic panel. When the bending wavelength in the base plate or shell is smaller than the ribs spacing, the rib dynamics are included as rigid boundaries between identical sub-panels with the base plate or shell properties. The local modes in all sub-panels tend to have the same wavelength and same natural frequency resulting in groups of modes typical of periodic structures.

In the creation of ribbed property of a plate, the skin plate (base material) is defined at first. Then the corresponding beam profile, the mean spacing of beams, the standard deviation of beam spacing if the spacing is not constant and their centroid offsets which mean the distance between the center of the beam and the center of the plate in the corresponding local x and y directions are defined. In this software, local x direction is denoted by Ribs – 1 direction and local y direction is denoted by Ribs – 2 direction. An example of defining the ribbed plate is shown in the following figure (23).

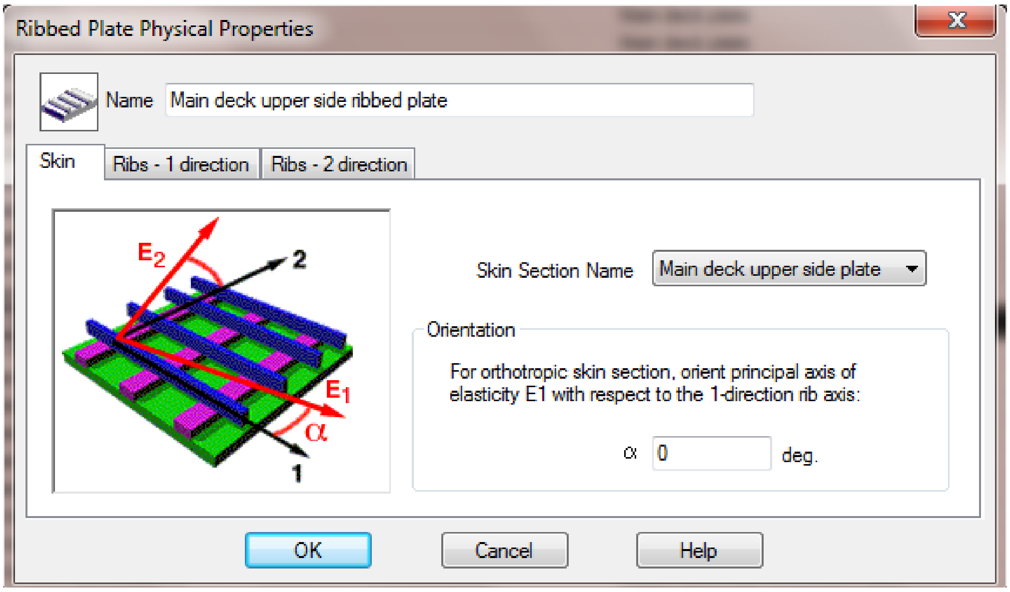


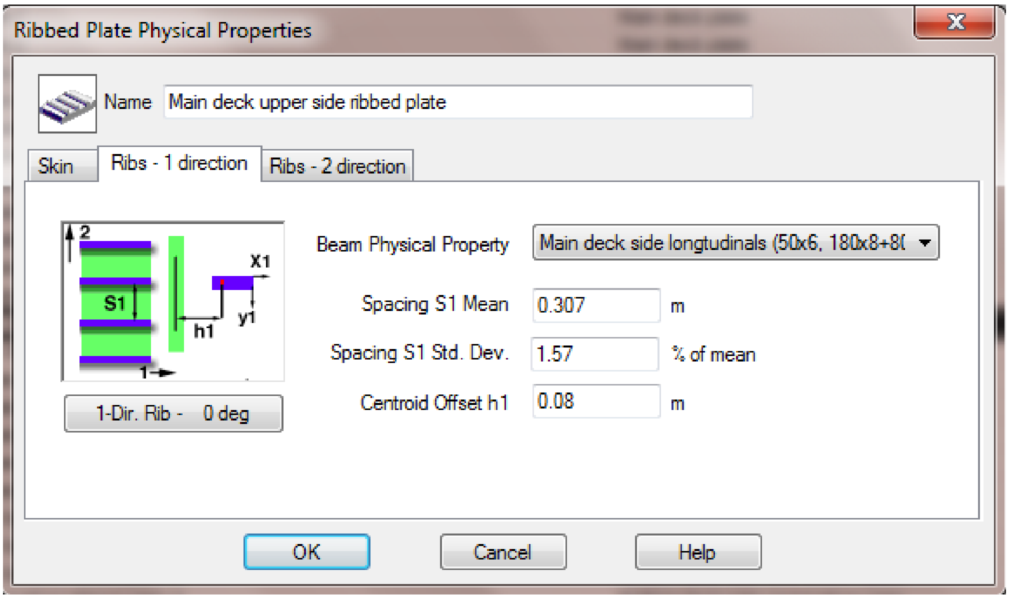

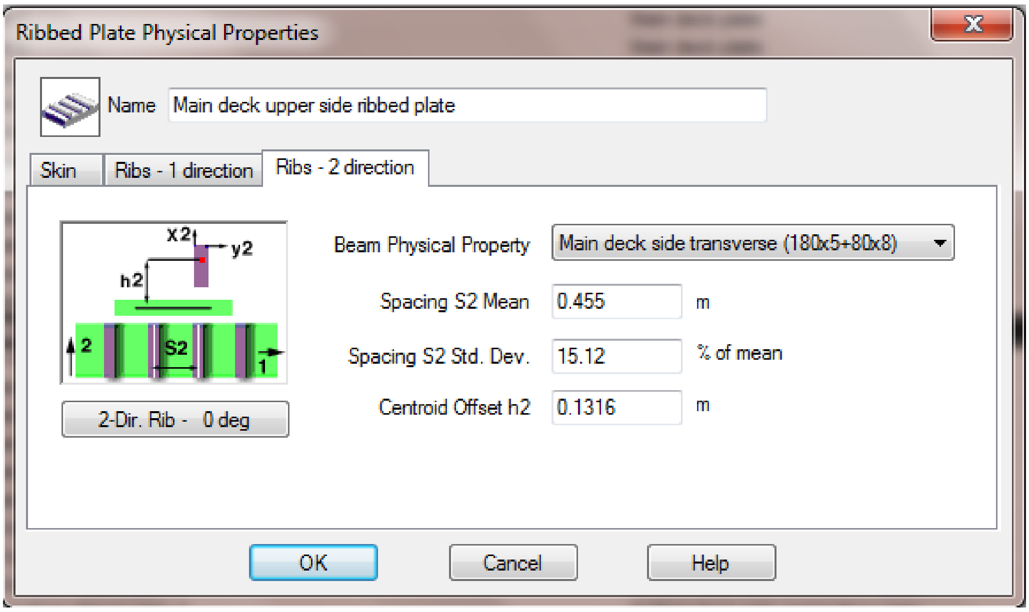


Figure 23: Example of defining ribbed plate property

If all the ribbed plates are added in the model, the reorient panel performance is done prior to the next step. This means setting the orientation of all panels with respect to the convention (global coordinate system). This is presented in the figure (24).

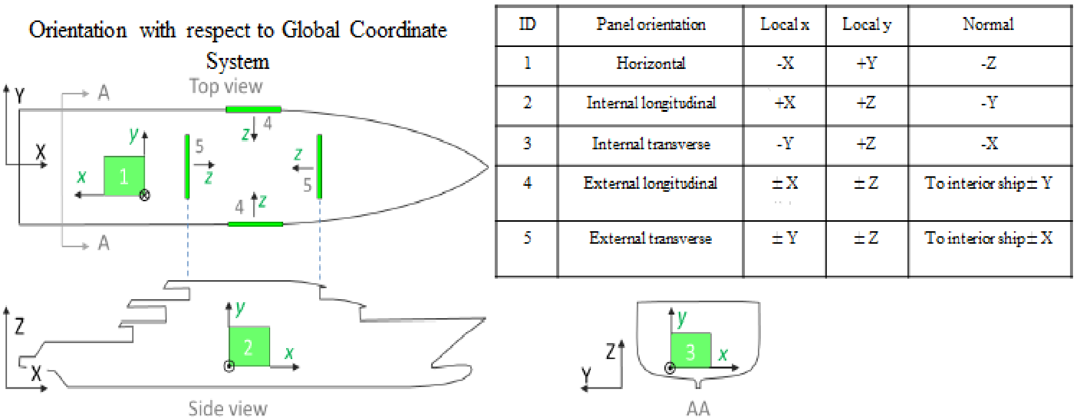


| ID | Panel orientation | Local x | Local y | Normal |
|---|---|---|---|---|
| 1 | Horizontal | -X | +Y | -Z |
| 2 | Internal longitudinal | +X | +Z | -Y |
| 3 | Internal transverse | -Y | +Z | -X |
| 4 | External longitudinal | ±X | ±Z | To interior ship±Y |
| 5 | External transverse | ±Y | ±Z | To interior ship±X |

Figure 24: Reorientation of panels with respect to the global coordinate system

The different types of plates and ribbed plates used in this yacht model are presented with the tables in the Appendices I, II, IV(a) and IV(b) respectively.

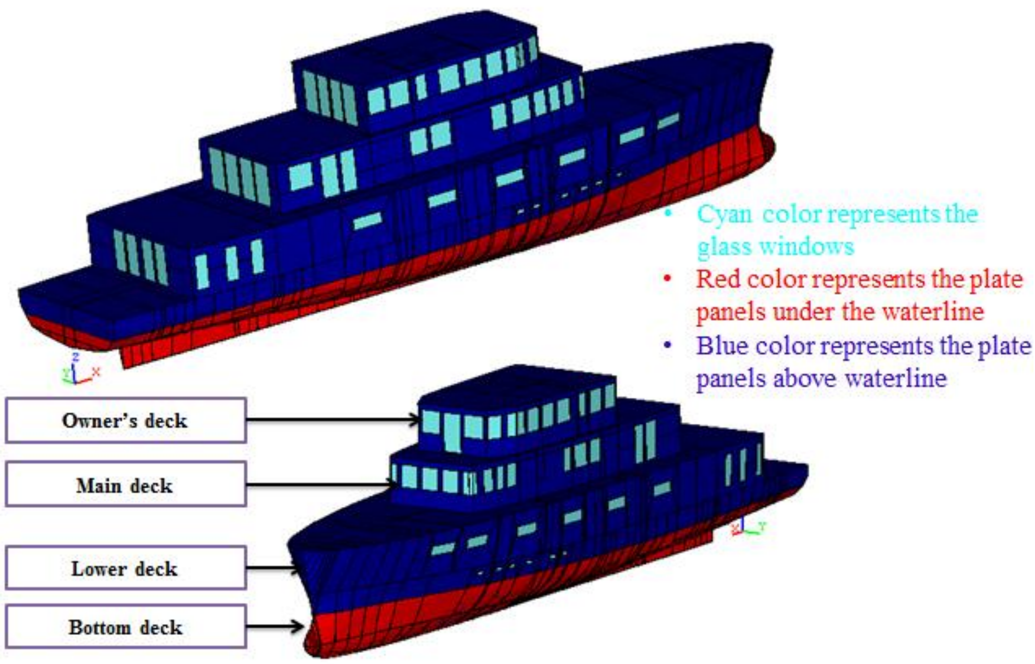


Figure 25: 3D plate model with the physical properties

In the above 3D plate model, each plate should have its own not only physical property (meaning type of plate and material) but also acoustic insulation and damping property. In order to make each plate have all characteristics, the followings shown in figure (26) should be assigned particularly.

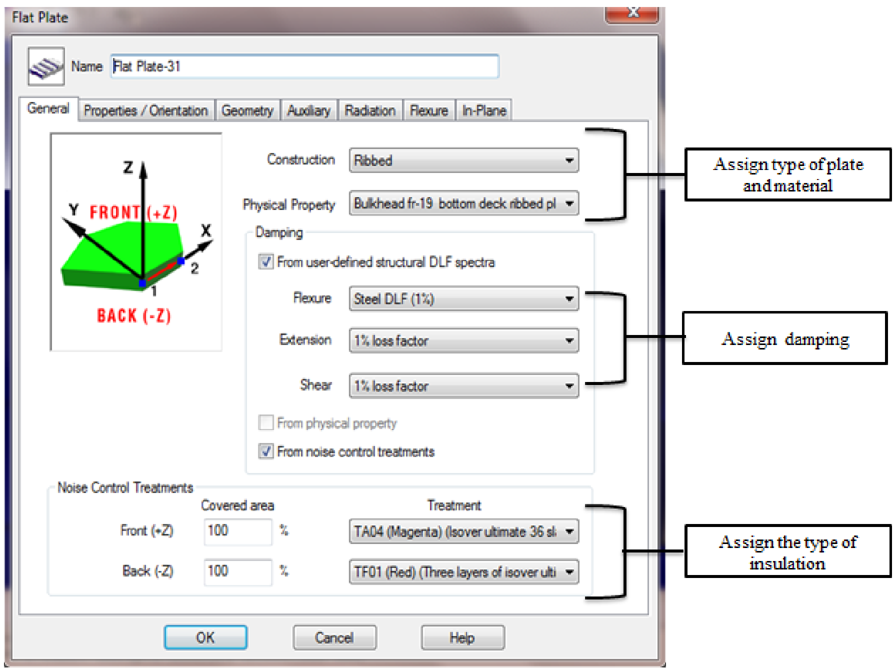


Figure 26: Example of defining all properties for each SEA plate subsystem

### 8.2.3. *Assigning noise control treatment (NCT)*

After assigning the physical properties (type of plate and material) to each plate panel, the completion of the properties of the plates are done by assigning the noise control treatments (NCT). The noise control treatment applied to the SEA plates can affect the energy flows that occur between the plates and any adjacent acoustic cavity subsystems and the mass and the stiffness of the panel. The resonant path coupling loss factor describes the energy flow between the panel and the cavity. The non-resonant path coupling loss factor describes the energy flow between the two acoustic cavities. The software initially calculates the coupling loss factor for an untrimmed panel and then accounts for the effects of the noise control treatment by applying an insertion loss to this coupling loss factor. Such an approach assumes that any energy not transmitted into the acoustic cavity remains in the panel. However, in many instances some of the energy that leaves the panel is dissipated within the noise control treatment and does not get radiated into the cavity. Therefore, adding or increasing the thickness of noise control treatment reduces the sound pressure level in the acoustic room of interest.

There are several ways of defining noise control treatment in this software utilizing foam and/or fibre materials or user-defined acoustic parameters (insertion loss, absorption, mass, damping). Moreover, it is possible to create layered materials or to collect different layers in a multiple noise control treatment. The following figure (27) illustrates the different ways of defining noise control treatment (NCT) in VA One.

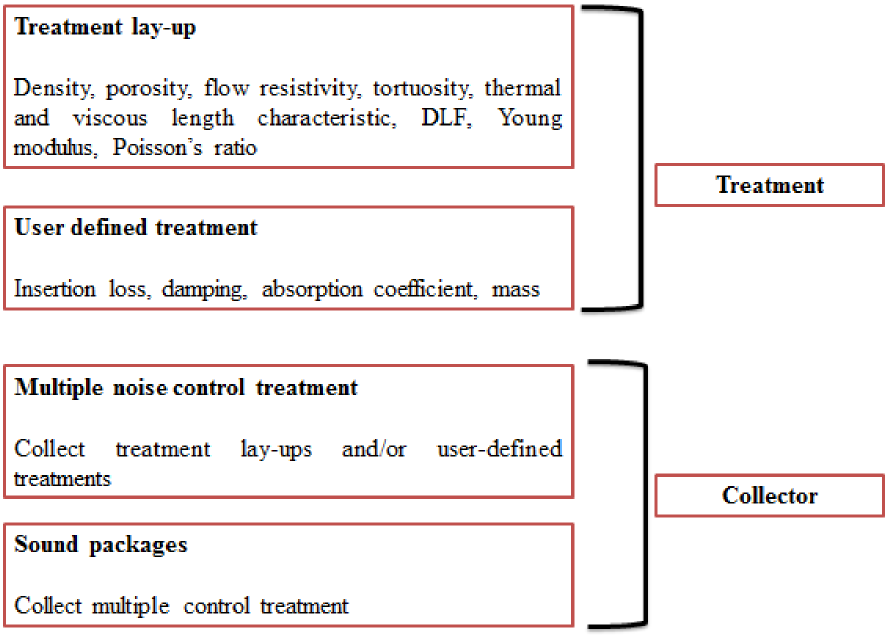


Figure 27: Different ways of defining noise control treatments

For the present model, the treatment lay-up option is applied, i.e. an explicit mathematical model of a lay-up based on the behavior of individual layers according to the insulation plans which are described with the table in the Appendix V. Depending on the type of insulation and corresponding colors, the 3D model can be visualized as in the figure (28) where the yacht model is shrunk for the purpose of clearly viewing the interior insulation.

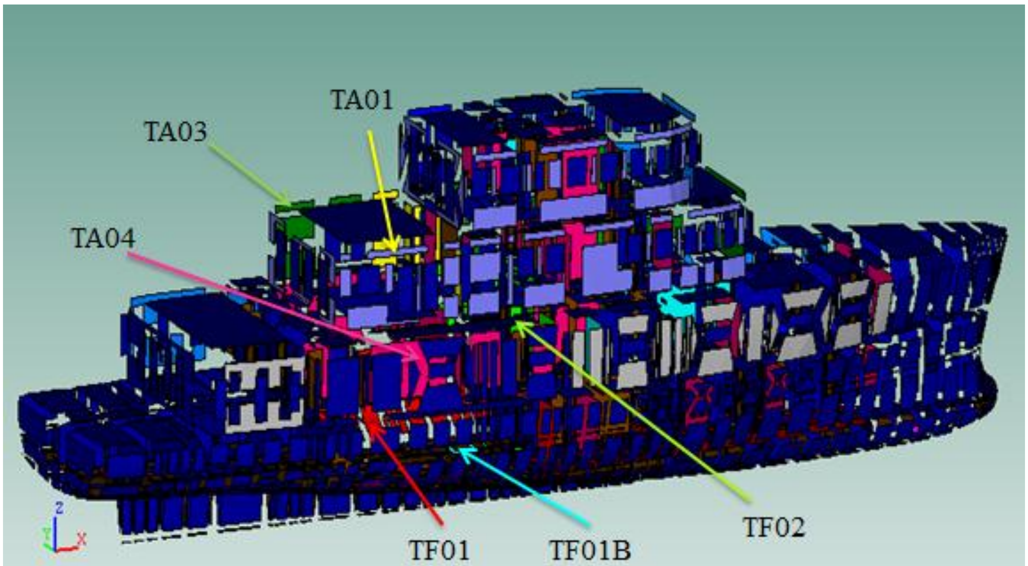


Figure 28: 3D plate model with insulation

In VA One, when defining the insulation by treatment lay-up option, the insulation is defined layer by layer. These layers can be of foam, fiber, gap (fluid), panel (solid), septum (limp), perforated plate or resistive layer types. Then the sound absorption behavior can be visualized for each insulated plate. The following figure (29) shows an example of adding insulation to one of the plates in the yacht model together with the plot of sound absorption spectrum in air.

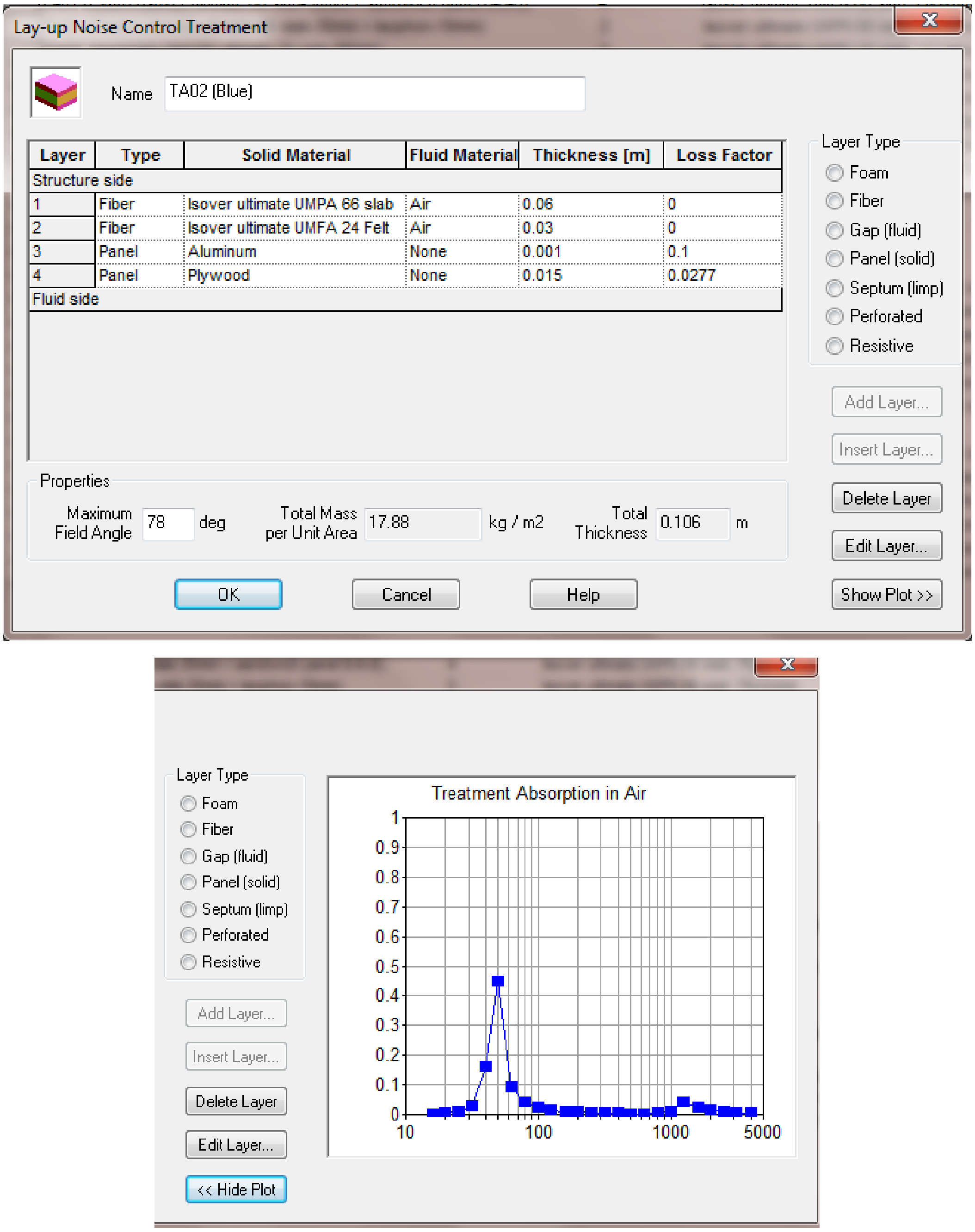


Figure 29: Example of defining insulation layers for one of the plates together with sound absorption spectrum in air due to the corresponding insulation treatments

### 8.2.4. *Assigning damping of the panels and insulations*

After assigning all the physical properties including the insulations, the damping in SEA panels is defined. In this software, there are three ways to define the damping loss factor (DLF) of the SEA plate subsystems. It can be assigned user-defined or from physical properties if the panel is of general laminate type or from noise control treatment. Actually the DLF should be defined for three wave types such as flexural, extensional and shear. But here, what we are interested in is that of flexural. Therefore, we simply put the default value which is one percentage for extensional and shear mode. For flexural, we assign the damping loss factor spectra (DLF versus frequency) for each material which are used in the yacht. These damping loss factor spectra are extracted directly from the particular damping test for each material and some are shown below.

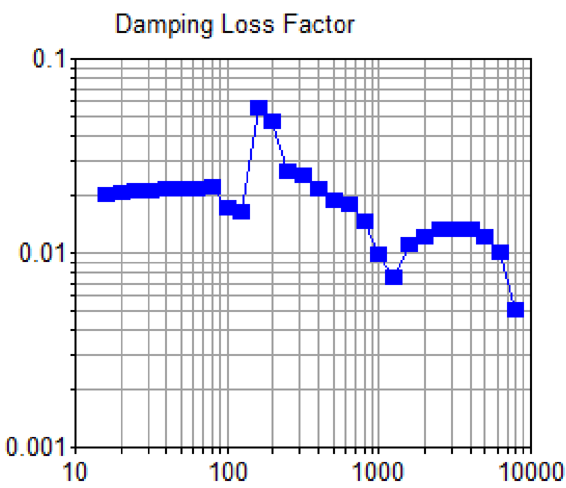


Figure 30: Damping loss factor (DLF spectrum) for Mascoat paint

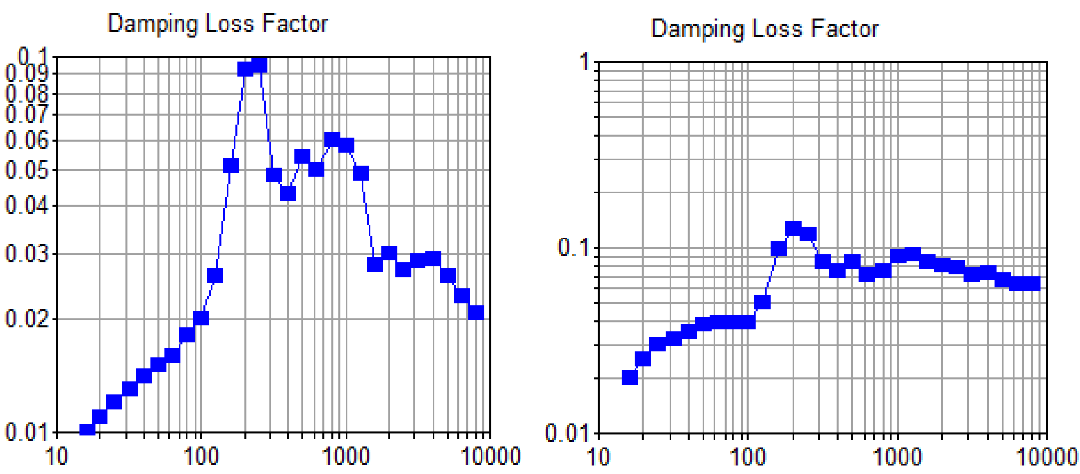


Figure 31: Damping loss factor (DLF spectrum) for tempered glass and laminated glass

### 8.2.5. *Creation of SEA acoustic cavities*

Before the creation of SEA acoustic cavities, the physical properties of particular fluid which will be filled in each cavity has to be defined. According to the capacity plan of this yacht, there are altogether five types of fluid filled throughout the whole yacht such as air, fresh water, sea water, diesel oil and lube oil. The required data when defining the fluid physical properties are shown in the following figure (32) where the speed of sound, density, kinematic viscosity and ratio of specific heats can be obtained from the literature. The molecular mass is calculated based on the molecular formula of particular fluid. The Prandtl number of fluid is defined as the ratio of momentum diffusivity to the thermal conductivity and written as follows.

$$\text{Prandtl no} = \frac{c_p \rho \upsilon}{\kappa}$$

$c_p$ is the specific heat at constant pressure,

$\kappa$ is the thermal conductivity of the fluid

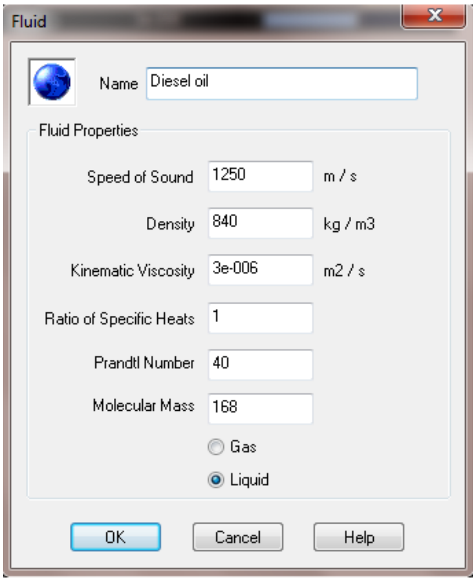


Figure 32: Example of defining fluid physical properties

The next step in the model construction is the creation of the SEA acoustic cavities which are volume subsystems used to predict the sound pressure level in a model and they consist of a set of faces that form a valid enclosed volume of acoustic fluid. A single (scalar) pressure wave field model is used to describe the statistics of the cavity's acoustic resonances (or standing waves) in each frequency band. VA One will calculate the reverberant energy level spectrum and the reverberant sound pressure level spectrum (which is equivalent to the volume average of several microphone pressure measurements). While creating the acoustic cavities, the corresponding fluid is filled in each cavity together with defining the damping of each SEA cavity by one of three ways such as assigning the damping loss factor spectra, absorption calculated from noise control treatments and assigning absorption spectra. Here in this thesis, since the noise control treatments have already been assigned throughout the yacht model by the time being, the damping for SEA cavity is defined from absorption from noise control treatments and this is illustrated in the figure (33).

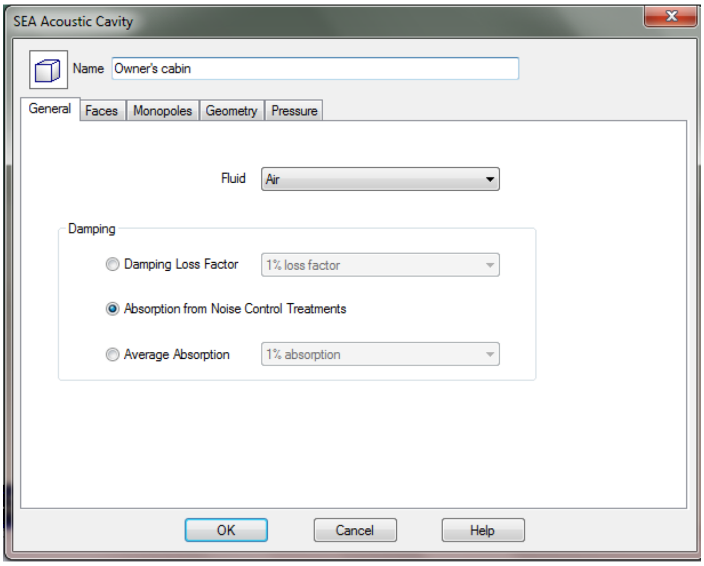


Figure 33: Example of defining SEA acoustic cavity

The SEA 3D model after the creation of such acoustic cavities is shown in the following figure (34).

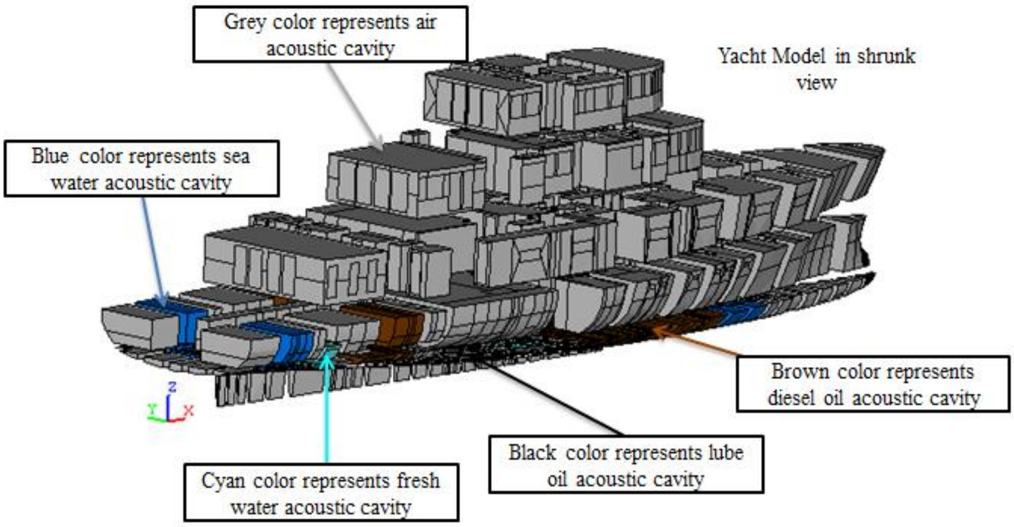


Figure 34: 3D model showing acoustic cavities

### 8.2.6. *Applying fluid loading and underwater SIF*

The fluid loading is applied to the panels which are under the waterlines of 2.79m which is the maximum draft of the yacht. Due to this fluid loading (sea water loading), the mass of the plates of ship hull under the waterline increases, the number of modes in band and wave number increases and the effect (response) decreases as the frequency increases. In order to apply this fluid loading, the orientation of all panels must be checked with the global coordinate system at first. Then, the loading is applied in each negative z-direction of all plates under the waterline. This is represented in the figure (35).

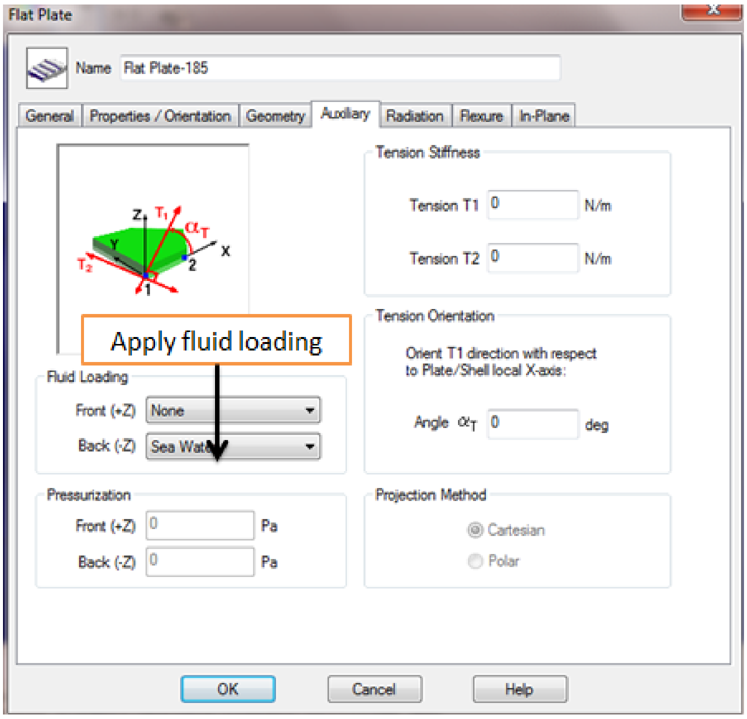


Figure 35: Example of applying fluid loading to the submerged SEA plate subsystem

This fluid loading application is followed by the last SEA subsystem that must be included in the yacht model: Semi-infinite fluid (SIF) to take into consideration the presence of sea water around the hull. An SIF in VA One represents an unbounded exterior acoustic space. The acoustic waves radiated by a subsystem connected to a semi-infinite fluid are not reflected back on the subsystem. This purpose is to model the exterior acoustic radiation impedance on SEA subsystems, i.e. to add the radiation damping to them; therefore the SIF can be considered as an energy dissipating sink. It is defined by an acoustic fluid and a single 3D node location at which the radiated sound pressure level could be evaluated. Here in this thesis, the underwater SIF is defined at Z = -100m. This SIF is shown in the figure (36).

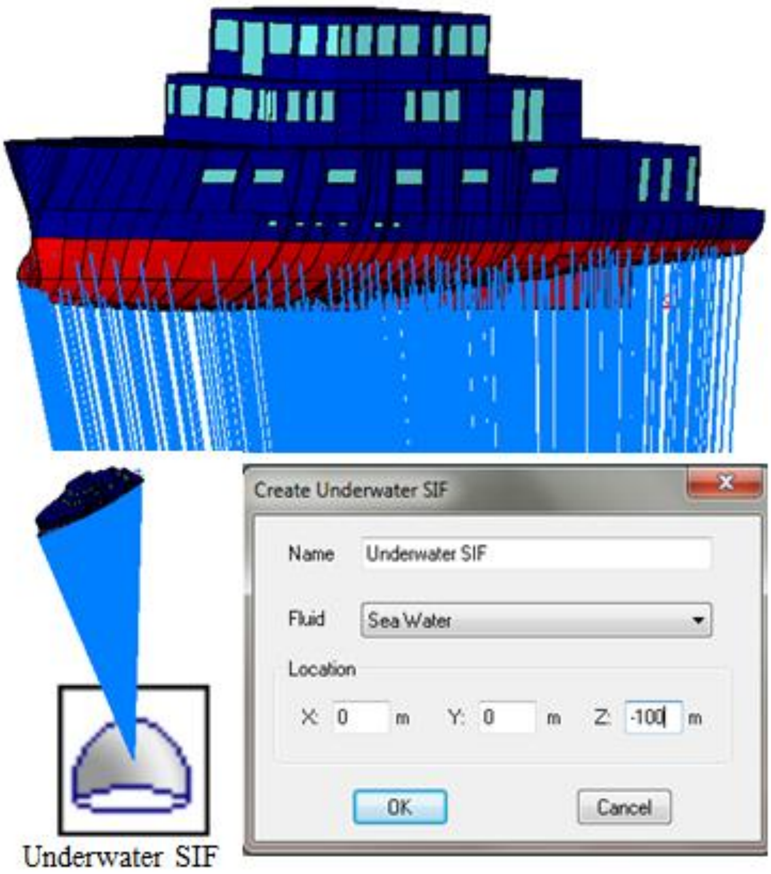


Figure 36: 3D model with underwater SIF

### 8.2.7. *Creation of corresponding SEA subsystem junctions*

All the subsystems of the model should be connected to each other by pressing auto-connect button in the software. There are three types of subsystem junctions in this software such as point junction, line junction and area junction. Point junction shows the transmission of vibration energy between two or more subsystems coupled at a discrete point and connections between subsystems that are small compared with a wavelength. Line junction shows the transmission of vibration energy between two or more subsystems coupled along a line and connections between subsystems that are continuous and large compared with a wavelength. Area junction shows the transmission of vibration energy between an SEA acoustic plate and one or two SEA acoustic cavities that share a common bounding area or face. The following diagrams (37), (38), (39) show the visualization of the corresponding junctions formed in this yacht model.

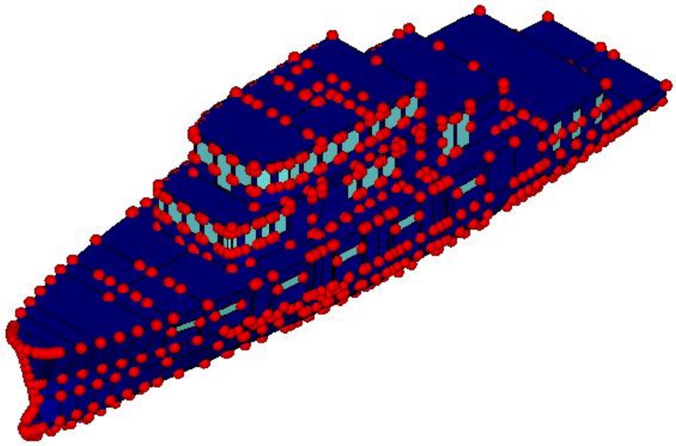

Figure 37: 3D model showing point junctions of subsystems

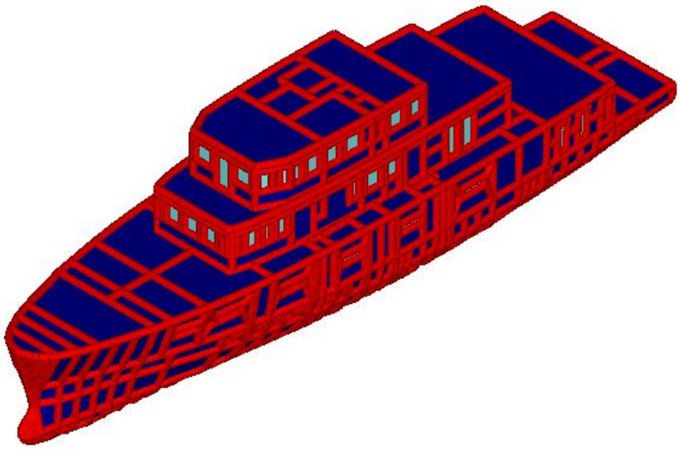

Figure 38: 3D model showing line junctions of subsystems

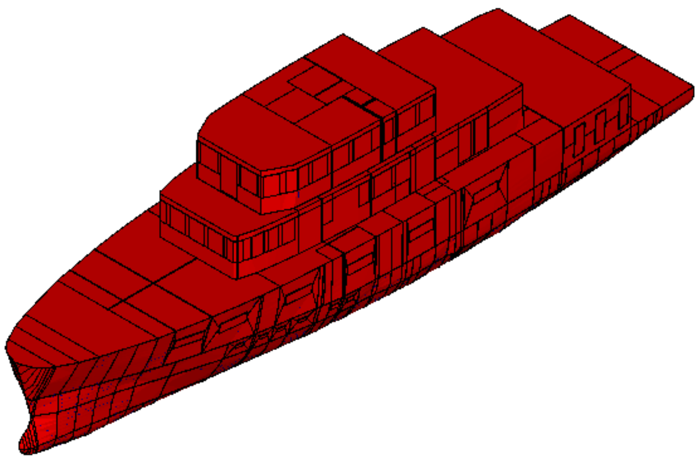

Figure 39: 3D model showing area junctions of subsystems

### 8.2.8. *Assigning noise generating sources on board the yacht*

The final step in the yacht model creation is the application of particular noise generating sources on the yacht. Noise spectra have been taken into consideration in accordance with the manufacturer data or estimated on the basis of RINA database and on board measurements of similar machineries. As explained previously, the noise is of two kinds: airborne noise and structure borne noise. Therefore, the noise sources considered in this SEA analysis are in terms of airborne and structure borne noise sources. The main noise generating sources defined in this analysis are main engines (RINA onboard measurements) and propellers (statistics data based on RINA measurement).

The noise propagation analysis is performed in accordance with the condition proposed by the shipyard. This is navigation at cruise speed and this condition has its own corresponding noise spectra.

Noise generating sources can be applied to the model in different ways. For the airborne noise, since the yacht contains two engines, a power spectrum consisting of power inputs from both engines are assigned to the cavity of the engine room. A power source in VA One is a direct model of the power that a mechanism or environment applies to a wave field of any subsystem. In this case, it means the acoustic power (i.e. sound pressure power) that a vibrating engine injects into the reverberant field of the room. This spectrum is shown in the following figure (40) where the horizontal axis represents the center frequency (Hz) of particular one-third octave frequency bands.

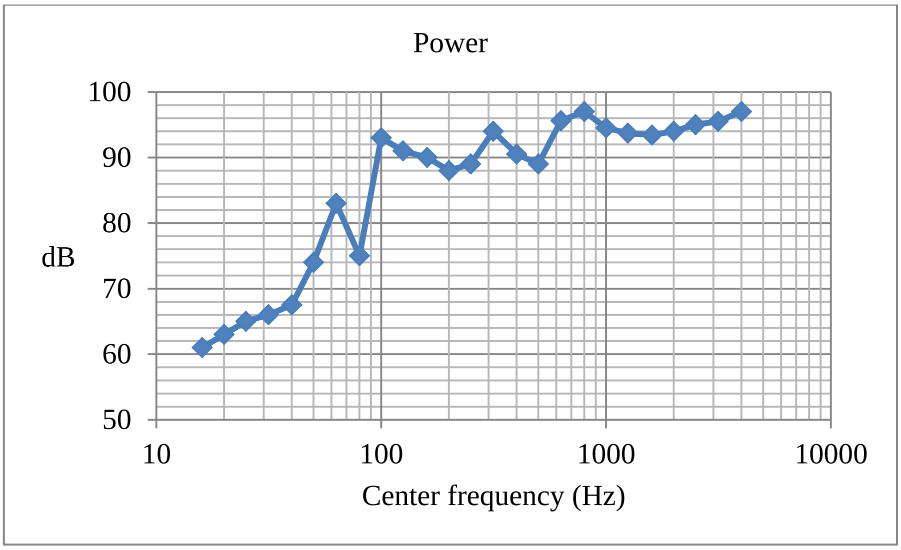


Figure 40: Power spectrum applied to engine room acoustic cavity from two engines (Navigation condition at cruise speed)

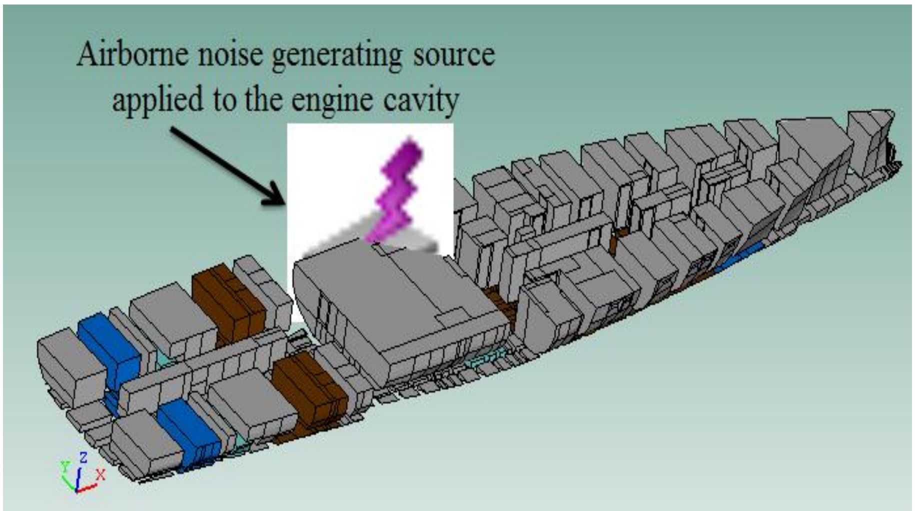


Figure 41: Power spectrum applied to the engine room cavity for airborne noise generation

For structure borne noise, some energy constraints are applied on plates. SEA constraints fix the response of a SEA subsystem to a known level. For example, when it is not convenient to measure the loads or power inputs directly for some source environments, it is often possible to measure the vibration or acoustic response of subsystems that are directly acted upon by the source. The variable being constrained in this SEA equations is the energy level of a given wave field. The input power that must be supplied to the subsystem in order to satisfy the constraint becomes the unknown in the SEA equations. In this sense, the acceleration due to propellers and main engines are applied on plates representing the shell of the bottom and the beams of the engine block and on plates which are close to the operating propeller respectively. The acceleration spectra due to the engine and propeller are shown in the figures (42) and (43) respectively.

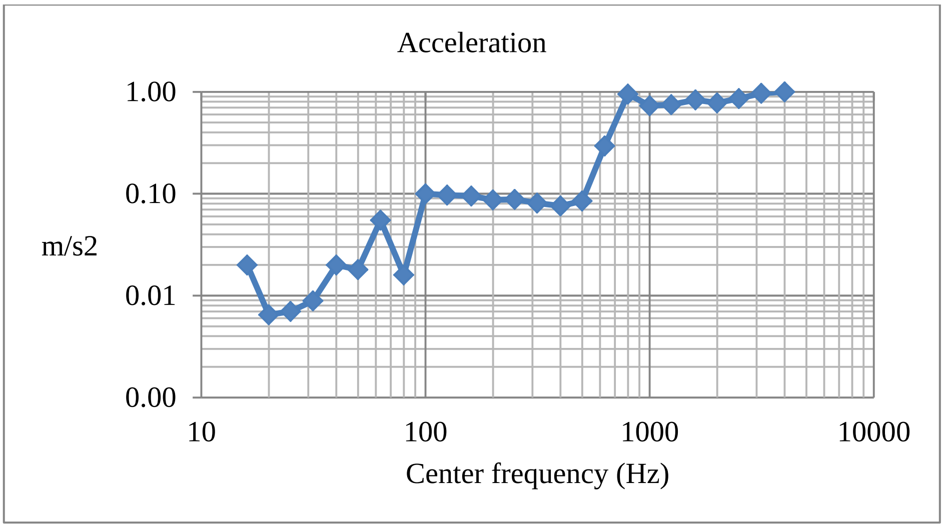


Figure 42: Acceleration spectrum due to main engine (Navigation condition at cruise speed)

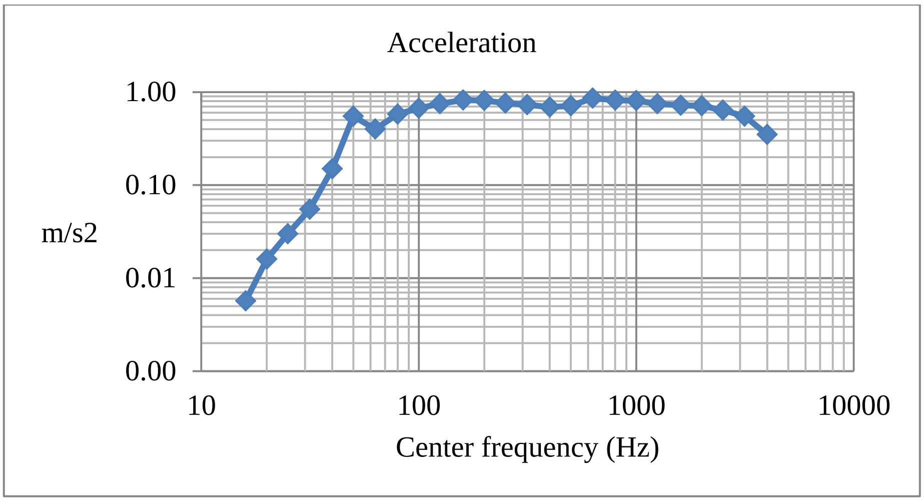


Figure 43: Acceleration spectrum due to propeller (Navigation condition at cruise speed)

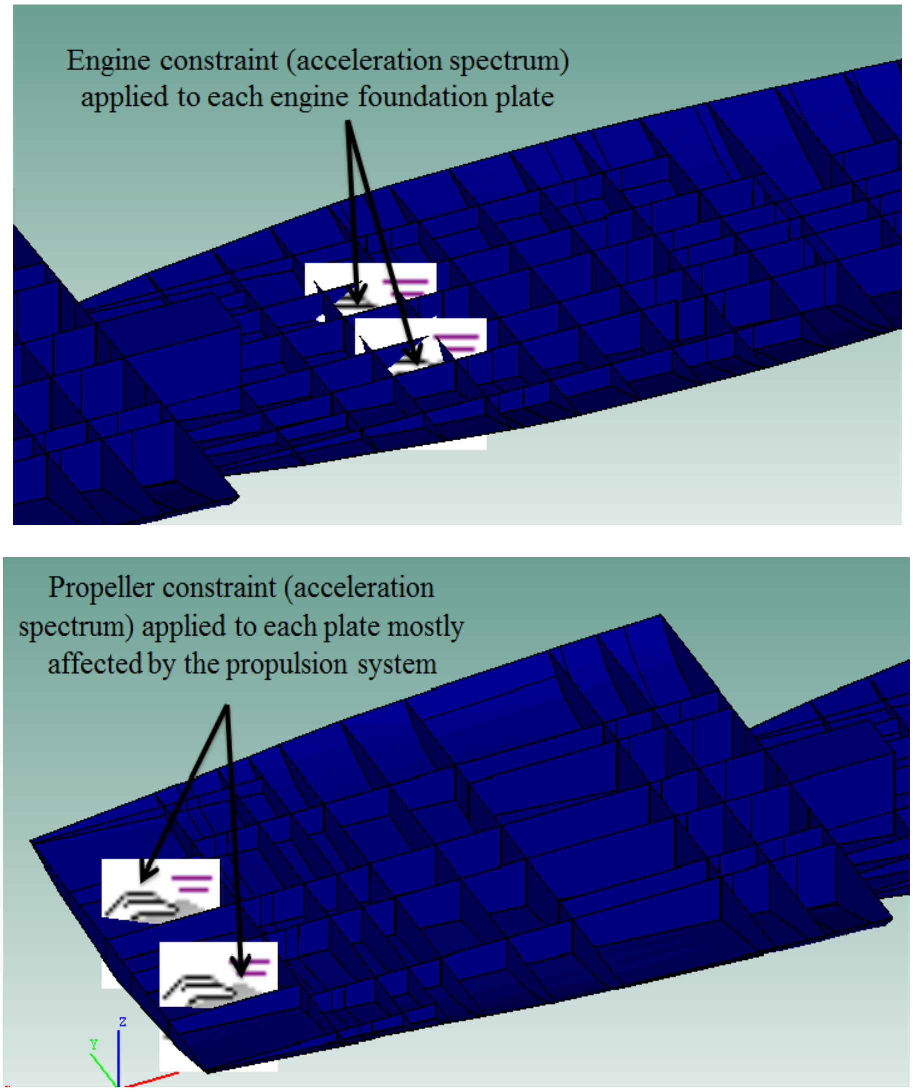


Figure 44: Acceleration spectrum applied to the corresponding plates for structure borne noise generation

## 8.3. Results of the SEA Analysis

The SEA analysis for noise propagation prediction is carried out in the one-third octave frequency bands starting from 16Hz to 4000Hz center frequency. The following table (7) shows each frequency band including upper limit frequency, lower limit frequency, center frequency and bandwidth in which VA One software works.

Table 7: Frequency domain through which the SEA analysis is performed

| Lower limit frequency (Hz) | Upper limit frequency (Hz) | Center frequency (Hz) | Bandwidth (Hz) |
|---|---|---|---|
| 14.3 | 18 | 16 | 3.7 |
| 18 | 22.4 | 20 | 4.4 |
| 22.4 | 28 | 25 | 5.6 |
| 28 | 35.5 | 31.5 | 7.5 |
| 35.5 | 45 | 40 | 9.5 |
| 45 | 56 | 50 | 11 |
| 56 | 71 | 63 | 15 |
| 71 | 90 | 80 | 19 |
| 90 | 112 | 100 | 22 |
| 112 | 140 | 125 | 28 |
| 140 | 180 | 160 | 40 |
| 180 | 224 | 200 | 44 |
| 224 | 280 | 250 | 56 |
| 280 | 355 | 315 | 75 |
| 355 | 450 | 400 | 95 |
| 450 | 560 | 500 | 110 |
| 560 | 710 | 630 | 150 |
| 710 | 900 | 800 | 190 |
| 900 | 1120 | 1000 | 220 |
| 1120 | 1400 | 1250 | 280 |
| 1400 | 1800 | 1600 | 400 |
| 1800 | 2240 | 2000 | 440 |
| 2240 | 2800 | 2500 | 560 |
| 2800 | 3550 | 3150 | 750 |
| 3550 | 4500 | 4000 | 950 |

The noise distribution prediction model allows to determine the noise level in the selected frequency ranging from 16 to 4000Hz in the band of interest at the given region of the yacht model. The following diagrams in the figure (45) represent the final result of an analysis in the form of distribution of the overall sound pressure level for all acoustic cavities composing the yacht volume for the selected one-third octave frequency bands. These figures let us understand how the energy propagates into the structure and it shows the regions which are most affected by the high noise levels. It could be visualized through the contour plot that displays the spatial distribution of sound pressure level in each cavities in dB(A). As it is explained in the theoretical part, the A-weighing is really common in noise measurements. It is used in order to account for the relative loudness perceived by the human ears which are less sensitive to low and high audio frequencies. In the figure (45), the contour plot is scaled in dB(A) and the dB reference is $2 \times 10^{-5}$ Pa.

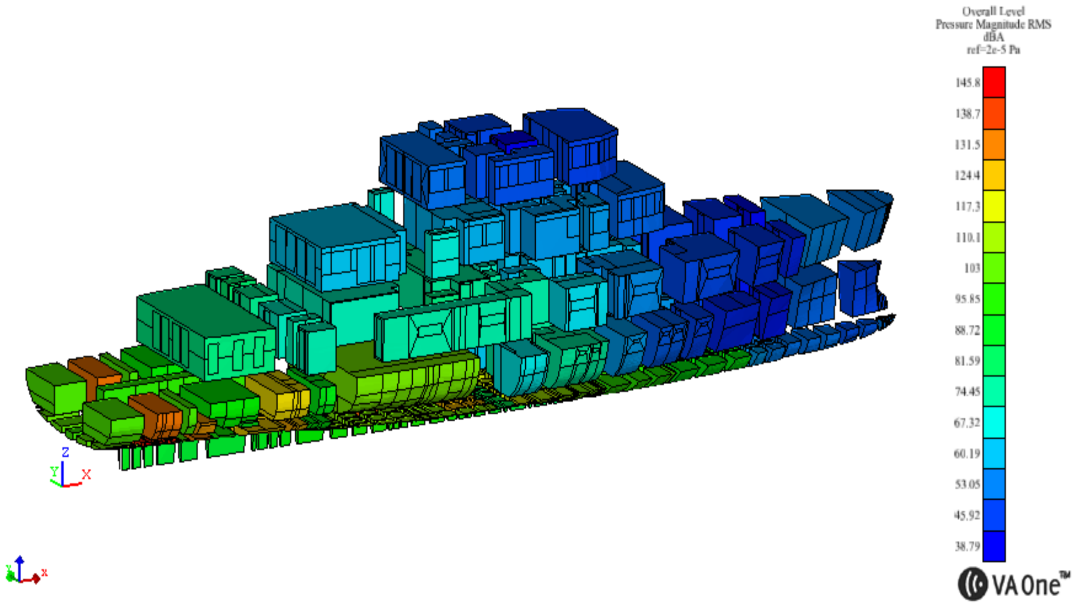


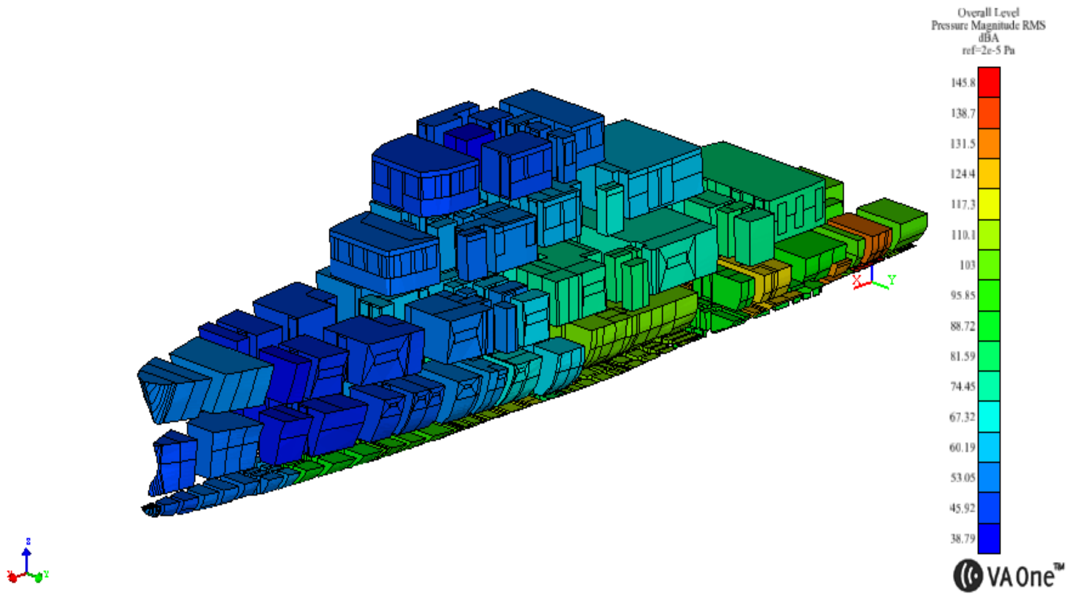

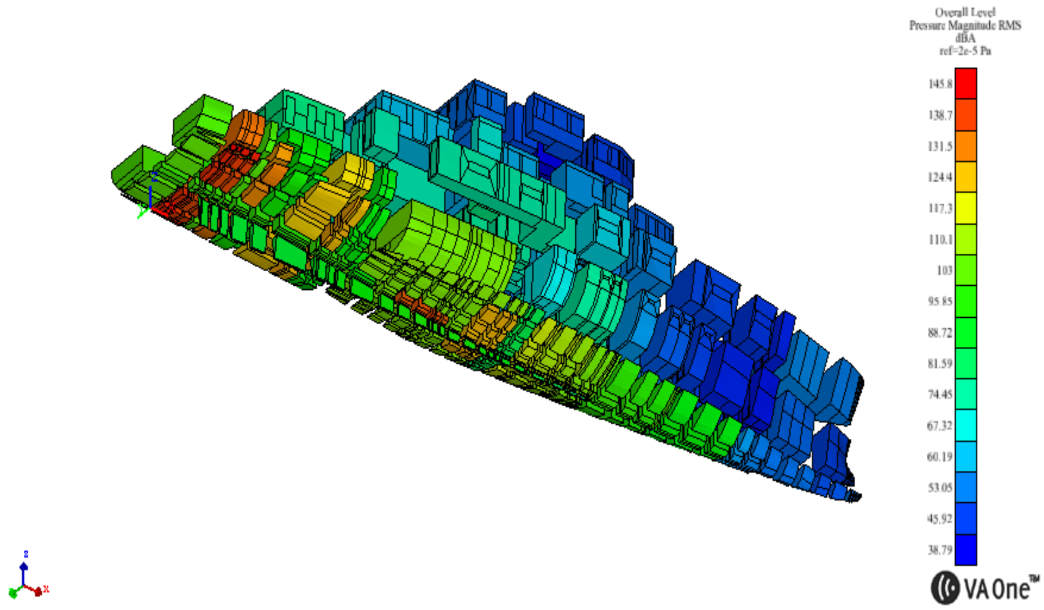


Figure 45: Overall sound pressure level dB(A) contour plot

In this thesis, since the experimental noise measurement data on board the yacht are not available, the generated results of sound pressure level in dB(A) from SEA analysis are checked with RINA's class notations for comfort on board. Such notations can be assigned depending on the type of vessels as follows.

- COMF-NOISE to assess the noise levels on all types of ships
- COMF-VIB to assess the vibration levels on all types of ships
- COMF Yacht to assess the noise and vibration levels on pleasure or charter yachts
- COMF (LY) to assess the noise and vibration levels on large yachts (LPP>60m)
- DOLPHIN to set the limit for the underwater radiated noise for commercial vessels, pleasure yachts and yachts above 24m.

Among the above RINA's class notations for comfort, the notation COMF Yacht is developed with the intention to obtain the best compromise between the limit levels and the performance of luxury pleasure yachts taking into account the wellness of the crew as well. Therefore, this notation is used to check the comfort and wellness of passengers and crew in this thesis. In the table (8), the limit levels for noise comfort on the pleasure yachts are shown.

Table 8: Noise limit levels for pleasure yachts at navigation condition

| Type of space | Navigation | |
|---|---|---|
| | $L_A$ | $L_B$ |
| Passenger spaces | | |
| Passenger cabins - superior | 50 | 55 |
| Passenger cabins - standard | 53 | 60 |
| Public spaces - lounges | 55 | 60 |
| Open main deck recreation areas, aft | 65 | 70 |
| Open deck recreation areas above, aft | 60 | 75 |
| Crew accommodations | | |
| Crew cabins | 55 | 60 |
| Senior officer cabins | 52 | 55 |
| Navigation spaces/ radar room | 65 | 65 |
| Radio room | 60 | 60 |
| Look-out, incl. Navigation wings and windows | 70 | 70 |
| Hospital | 55 | 60 |
| Public crew spaces | 60 | 65 |
| Work spaces without equipment operating | 70 | 75 |
| Workshop other those forming part of machinery | 85 | 85 |
| Galley | 70 | 75 |
| Offices | 60 | 65 |
| Mess room/ recreation room | 60 | 65 |
| Engine control room | 75 | 75 |
| Crew open deck | 75 | 75 |

The notation is differentiate by a letter A or B which represents the merit level achieved for the assignment of the notation, the merit A corresponding to the lowest level of noise and vibration. If the calculated sound pressure level is lower than the first value, it means that it satisfies the noise level limit of merit A and if the calculated sound pressure level is lower than the second value, it satisfies that of merit B. The following table (9) shows the predicted dB(A) sound pressure level through the analyzed frequency bands at navigation condition at cruise speed in each acoustic cavity throughout the whole yacht model according to the general arrangement plan and the highest (peak) sound pressure level is checked if it passes the noise criteria stated in the table (8).

Table 9: Predicted sound pressure level dB(A) in each room

| Deck | Center frequency (Hz) / Compartment name | Acceptable limit in dB(A), Merit A-B | Peak value | 16 | 20 | 25 | 31.5 |
|---|---|---|---|---|---|---|---|
| Owner deck | Owner's cabin | 50-55 | 38.63 | 2.68 | -3.93 | 2.12 | 6.83 |
| | Bathroom | 50-55 | 40.46 | 2.20 | -5.24 | 1.83 | 7.43 |
| | Toilet | 50-55 | 42.67 | 6.76 | 2.44 | 8.02 | 11.50 |
| | Dressing room | 50-55 | 41.33 | 0.76 | 0.29 | 6.67 | 9.28 |
| | Living room | 55-60 | 44.51 | -0.23 | -1.02 | 5.23 | 8.59 |
| Main deck | Navigation space/radar room | 65-65 | 43.49 | 7.27 | -0.91 | 9.61 | 12.26 |
| | Captain's cabin | 52-55 | 51.88 | 7.05 | 0.96 | 7.72 | 11.88 |
| | Toilet in Captain's cabin | 52-55 | 51.90 | 7.07 | -0.36 | 8.90 | 10.65 |
| | Day Head | 60-65 | 53.24 | 5.26 | 0.19 | 5.68 | 8.43 |
| | Pantry | 55-60 | 49.68 | 3.93 | 0.40 | 6.44 | 10.31 |
| | Dining room | 55-60 | 51.67 | 11.02 | 7.56 | 11.97 | 17.00 |
| | Salon | 55-60 | 54.83 | 16.32 | 12.68 | 19.63 | 21.31 |
| Lower deck | Guest cabin 1 | 53-60 | 38.62 | 7.71 | 3.11 | 8.85 | 9.68 |
| | Guest cabin 2 | 53-60 | 39.90 | 6.41 | 1.76 | 8.14 | 8.99 |
| | Guest cabin 3 | 53-60 | 46.84 | 10.53 | 5.91 | 10.25 | 13.79 |
| | Guest cabin 4 | 53-60 | 49.00 | 10.62 | 6.38 | 10.59 | 15.13 |
| | Bathroom (Guest cabin 1) | 53-60 | 38.44 | 3.24 | -1.49 | 3.69 | 6.47 |
| | Bathroom (Guest cabin 2) | 53-60 | 39.71 | 2.34 | -2.58 | 2.61 | 5.48 |
| | Bathroom (Guest cabin 3) | 53-60 | 47.63 | 11.69 | 7.76 | 12.73 | 16.04 |
| | Bathroom (Guest cabin 4) | 53-60 | 55.82 | 11.03 | 6.61 | 11.95 | 15.02 |
| | Food preparation area/ galley | 70-75 | 72.64 | 17.59 | 13.77 | 18.24 | 21.34 |
| | Life boat store room | 70-75 | 66.47 | 19.34 | 16.38 | 20.44 | 25.16 |
| | Corridor beside galley | 70-75 | 71.11 | 16.42 | 12.86 | 19.15 | 22.01 |
| | Cinema/Lounge | 55-60 | 59.49 | 17.91 | 20.30 | 28.50 | 32.32 |
| | Bar | 55-60 | 59.44 | 18.84 | 17.73 | 24.89 | 28.97 |
| Bottom deck | Crew cabin 1 | 55-60 | 36.60 | 6.60 | 1.74 | 6.14 | 8.19 |
| | Crew cabin 2 | 55-60 | 36.76 | 7.19 | 1.86 | 6.14 | 8.23 |
| | Crew cabin 3 | 55-60 | 42.92 | 10.32 | 5.46 | 9.87 | 11.33 |
| | Crew cabin 4 | 55-60 | 43.47 | 10.38 | 5.56 | 10.04 | 11.51 |
| | Crew cabin 5 | 55-60 | 59.64 | 12.30 | 7.71 | 13.29 | 16.60 |
| | Bathroom (Crew cabin 1) | 55-60 | 35.79 | 8.63 | 0.62 | 5.07 | 7.40 |
| | Bathroom (Crew cabin 2) | 55-60 | 34.95 | 16.41 | -1.42 | 2.91 | 5.44 |
| | Bathroom (Crew cabin 3) | 55-60 | 40.83 | 7.39 | 3.37 | 8.00 | 9.71 |
| | Bathroom (Crew cabin 4) | 55-60 | 41.23 | 7.41 | 3.41 | 8.08 | 9.90 |
| | Bathroom (Crew cabin 5) | 55-60 | 52.27 | 3.77 | -0.70 | 4.62 | 7.62 |

| | | | | | | | |
|---|---|---|---|---|---|---|---|
| | Laundry/Ironing room | 70-75 | 47.80 | 10.08 | 5.65 | 10.96 | 14.06 |
| | Storage | 70-75 | 49.94 | 10.96 | 6.49 | 11.88 | 14.43 |
| | Crew mess room | 60-65 | 64.16 | 12.97 | 8.47 | 14.93 | 14.11 |
| | Control room | 75-75 | 60.71 | 19.06 | 14.09 | 17.48 | 16.89 |
| | Pump-manifold room | 85-85 | 56.16 | 16.14 | 12.04 | 17.37 | 19.34 |
| | Battery room | 85-85 | 57.05 | 19.07 | 14.61 | 19.31 | 19.35 |
| | Engine room | | 99.81 | 17.92 | 15.03 | 20.28 | 19.73 |

| Deck | Center frequency (Hz) / Compartment name | 40 | 50 | 63 | 80 | 100 | 125 | 160 |
|---|---|---|---|---|---|---|---|---|
| Owner deck | Owner's cabin | 17.76 | 21.71 | 17.91 | 30.92 | 38.63 | 34.73 | 35.93 |
| | Bathroom | 15.48 | 22.99 | 15.55 | 36.76 | 37.91 | 29.12 | 35.36 |
| | Toilet | 21.28 | 28.48 | 21.17 | 39.24 | 42.12 | 35.63 | 38.10 |
| | Dressing room | 18.51 | 24.54 | 23.31 | 32.56 | 37.87 | 33.43 | 35.51 |
| | Living room | 18.04 | 26.36 | 17.73 | 38.46 | 44.42 | 36.93 | 38.83 |
| Main deck | Navigation space/radar room | 23.29 | 27.65 | 22.14 | 31.84 | 40.66 | 38.28 | 39.26 |
| | Captain's cabin | 23.77 | 31.29 | 34.43 | 37.81 | 43.02 | 40.73 | 40.71 |
| | Toilet in Captain's cabin | 23.52 | 29.47 | 28.11 | 37.20 | 41.16 | 35.53 | 40.85 |
| | Day Head | 19.51 | 27.75 | 20.99 | 34.26 | 40.01 | 36.65 | 38.56 |
| | Pantry | 22.46 | 31.26 | 29.97 | 36.60 | 41.67 | 36.66 | 37.73 |
| | Dining room | 29.34 | 39.82 | 33.06 | 38.83 | 51.67 | 51.49 | 45.10 |
| | Salon | 34.04 | 43.49 | 38.67 | 50.38 | 54.83 | 54.28 | 48.23 |
| Lower deck | Guest cabin 1 | 21.18 | 24.97 | 23.97 | 33.64 | 35.26 | 36.17 | 35.05 |
| | Guest cabin 2 | 20.73 | 25.19 | 25.01 | 34.86 | 37.39 | 36.63 | 34.60 |
| | Guest cabin 3 | 25.30 | 31.12 | 28.41 | 37.98 | 36.06 | 39.79 | 40.15 |
| | Guest cabin 4 | 26.67 | 32.00 | 29.92 | 40.45 | 37.34 | 41.61 | 42.76 |
| | Bathroom (Guest cabin 1) | 16.80 | 20.28 | 21.62 | 28.48 | 31.19 | 30.15 | 32.02 |
| | Bathroom (Guest cabin 2) | 15.80 | 19.71 | 21.62 | 29.36 | 33.85 | 30.38 | 31.78 |
| | Bathroom (Guest cabin 3) | 28.04 | 37.62 | 30.54 | 40.47 | 40.13 | 41.61 | 40.89 |
| | Bathroom (Guest cabin 4) | 27.45 | 34.15 | 35.18 | 44.61 | 48.17 | 45.96 | 45.29 |
| | Food preparation area/ galley | 33.09 | 43.57 | 37.83 | 41.32 | 48.04 | 52.63 | 55.33 |
| | Life boat store room | 38.37 | 48.89 | 41.50 | 55.48 | 57.29 | 62.77 | 61.73 |
| | Corridor beside galley | 36.70 | 44.82 | 45.76 | 51.41 | 48.11 | 56.23 | 55.34 |
| | Cinema/Lounge | 47.08 | 57.29 | 54.33 | 57.85 | 57.33 | 58.09 | 57.14 |
| | Bar | 41.43 | 47.38 | 48.27 | 59.15 | 59.17 | 59.44 | 58.16 |
| Bottom deck | Crew cabin 1 | 16.64 | 19.97 | 19.15 | 27.42 | 34.85 | 36.60 | 33.75 |
| | Crew cabin 2 | 16.68 | 19.82 | 19.32 | 27.90 | 34.70 | 36.76 | 33.88 |
| | Crew cabin 3 | 21.68 | 25.50 | 22.93 | 30.89 | 38.49 | 41.57 | 39.08 |
| | Crew cabin 4 | 21.94 | 25.91 | 23.47 | 31.25 | 38.76 | 42.04 | 39.73 |
| | Crew cabin 5 | 28.35 | 32.97 | 30.97 | 37.39 | 45.56 | 49.38 | 44.62 |
| | Bathroom (Crew cabin 1) | 15.48 | 18.05 | 16.56 | 27.58 | 35.79 | 33.10 | 31.53 |

| | | | | | | | | |
|---|---|---|---|---|---|---|---|---|
| | Bathroom (Crew cabin 2) | 14.19 | 17.29 | 16.26 | 27.16 | 34.95 | 32.05 | 31.03 |
| | Bathroom (Crew cabin 3) | 19.87 | 23.43 | 19.45 | 29.45 | 38.03 | 35.80 | 34.80 |
| | Bathroom (Crew cabin 4) | 20.31 | 23.91 | 19.82 | 29.24 | 38.12 | 36.03 | 35.13 |
| | Bathroom (Crew cabin 5) | 19.97 | 27.37 | 26.76 | 33.09 | 41.71 | 41.23 | 40.93 |
| | Laundry/Ironing room | 25.34 | 30.49 | 24.62 | 35.06 | 43.12 | 41.75 | 42.25 |
| | Storage | 25.83 | 30.89 | 25.18 | 35.81 | 43.47 | 42.63 | 43.31 |
| | Crew mess room | 27.70 | 34.44 | 33.28 | 39.35 | 45.91 | 49.44 | 50.39 |
| | Control room | 33.02 | 43.01 | 40.87 | 41.69 | 48.75 | 49.94 | 48.88 |
| | Pump-manifold room | 34.28 | 40.61 | 35.69 | 39.05 | 49.17 | 50.40 | 48.69 |
| | Battery room | 33.73 | 44.17 | 39.32 | 43.13 | 55.21 | 55.31 | 54.57 |
| | Engine room | 32.96 | 47.22 | 51.84 | 53.88 | 67.55 | 69.44 | 72.16 |

| Deck | Center frequency (Hz) / Compartment name | 200 | 250 | 315 | 400 | 500 | 630 | 800 |
|---|---|---|---|---|---|---|---|---|
| Owner deck | Owner's cabin | 34.46 | 32.66 | 34.81 | 33.44 | 32.50 | 37.20 | 38.06 |
| | Bathroom | 34.25 | 33.61 | 35.63 | 33.04 | 29.68 | 37.29 | 40.46 |
| | Toilet | 36.89 | 37.34 | 37.50 | 36.86 | 35.88 | 38.49 | 42.67 |
| | Dressing room | 36.67 | 35.08 | 36.45 | 35.99 | 31.48 | 38.14 | 41.33 |
| | Living room | 38.10 | 37.00 | 40.20 | 37.12 | 36.30 | 41.52 | 44.51 |
| Main deck | Navigation space/radar room | 37.26 | 36.87 | 38.42 | 38.55 | 37.04 | 42.90 | 43.49 |
| | Captain's cabin | 43.40 | 40.23 | 41.05 | 41.60 | 39.59 | 46.90 | 51.88 |
| | Toilet in Captain's cabin | 40.24 | 39.60 | 41.16 | 41.03 | 39.17 | 46.96 | 51.90 |
| | Day Head | 40.25 | 38.40 | 38.16 | 38.92 | 38.31 | 45.64 | 53.24 |
| | Pantry | 38.08 | 36.46 | 37.40 | 37.67 | 36.38 | 44.57 | 49.68 |
| | Dining room | 47.06 | 46.26 | 46.12 | 46.51 | 41.12 | 49.29 | 50.50 |
| | Salon | 48.42 | 46.97 | 46.46 | 46.69 | 42.24 | 49.43 | 49.10 |
| Lower deck | Guest cabin 1 | 33.79 | 31.45 | 31.79 | 32.01 | 30.87 | 37.79 | 38.62 |
| | Guest cabin 2 | 33.43 | 31.27 | 31.86 | 32.18 | 31.19 | 38.19 | 39.90 |
| | Guest cabin 3 | 38.07 | 36.68 | 37.41 | 37.92 | 38.24 | 44.33 | 46.84 |
| | Guest cabin 4 | 40.41 | 39.24 | 41.54 | 42.52 | 42.14 | 48.46 | 49.00 |
| | Bathroom (Guest cabin 1) | 29.60 | 28.89 | 30.99 | 31.32 | 29.05 | 37.01 | 38.44 |
| | Bathroom (Guest cabin 2) | 29.66 | 29.01 | 30.87 | 31.33 | 29.51 | 37.25 | 39.71 |
| | Bathroom (Guest cabin 3) | 38.49 | 37.42 | 38.12 | 38.57 | 38.91 | 44.83 | 47.63 |
| | Bathroom (Guest cabin 4) | 44.33 | 43.99 | 45.91 | 46.95 | 47.08 | 54.44 | 55.19 |
| | Food preparation area/ galley | 54.02 | 55.14 | 56.41 | 59.12 | 58.01 | 66.64 | 72.64 |
| | Life boat store room | 59.62 | 57.69 | 57.70 | 56.61 | 56.23 | 60.53 | 66.47 |
| | Corridor beside galley | 53.70 | 52.78 | 55.51 | 57.13 | 57.46 | 65.59 | 71.11 |
| | Cinema/Lounge | 53.58 | 54.47 | 54.79 | 54.89 | 55.93 | 57.22 | 59.49 |
| | Bar | 56.79 | 56.75 | 58.37 | 58.38 | 59.28 | 58.63 | 54.44 |
| Bottom deck | Crew cabin 1 | 30.47 | 27.64 | 26.93 | 24.61 | 22.06 | 28.82 | 34.81 |
| | Crew cabin 2 | 30.64 | 27.74 | 27.04 | 24.80 | 22.40 | 29.09 | 35.14 |

| | | | | | | | | |
|---|---|---|---|---|---|---|---|---|
| | Crew cabin 3 | 36.23 | 33.76 | 33.20 | 31.10 | 29.60 | 36.61 | 42.92 |
| | Crew cabin 4 | 36.84 | 34.08 | 33.58 | 31.53 | 30.03 | 37.11 | 43.47 |
| | Crew cabin 5 | 46.24 | 45.20 | 46.51 | 49.55 | 48.63 | 54.12 | 59.64 |
| | Bathroom (Crew cabin 1) | 27.25 | 26.01 | 27.51 | 26.35 | 23.18 | 29.30 | 32.37 |
| | Bathroom (Crew cabin 2) | 27.60 | 26.36 | 27.58 | 26.91 | 24.41 | 30.00 | 34.08 |
| | Bathroom (Crew cabin 3) | 32.03 | 30.74 | 32.28 | 29.41 | 27.27 | 34.89 | 40.83 |
| | Bathroom (Crew cabin 4) | 32.44 | 30.90 | 32.41 | 29.40 | 27.04 | 35.03 | 41.23 |
| | Bathroom (Crew cabin 5) | 40.69 | 39.55 | 41.65 | 41.28 | 39.51 | 46.40 | 52.27 |
| | Laundry/Ironing room | 46.65 | 41.28 | 41.30 | 38.66 | 36.23 | 43.57 | 47.80 |
| | Storage | 47.32 | 42.51 | 45.44 | 42.73 | 39.35 | 47.54 | 49.94 |
| | Crew mess room | 53.77 | 50.42 | 56.81 | 53.67 | 49.89 | 56.31 | 61.63 |
| | Control room | 50.26 | 46.71 | 51.37 | 47.49 | 47.20 | 54.62 | 60.71 |
| | Pump-manifold room | 46.96 | 44.17 | 49.69 | 43.59 | 43.33 | 51.23 | 56.16 |
| | Battery room | 48.43 | 45.89 | 45.31 | 43.09 | 42.46 | 50.44 | 57.05 |
| | Engine room | 73.79 | 77.72 | 84.91 | 84.54 | 85.28 | 93.75 | 97.00 |

| Deck | Center frequency (Hz) / Compartment name | 1000 | 1250 | 1600 | 2000 | 2500 | 3150 | 4000 |
|---|---|---|---|---|---|---|---|---|
| Owner deck | Owner's cabin | 32.40 | 27.40 | 25.09 | 20.57 | 14.62 | 13.52 | 9.68 |
| | Bathroom | 35.20 | 29.76 | 28.97 | 27.01 | 21.59 | 20.74 | 17.34 |
| | Toilet | 35.96 | 31.29 | 31.46 | 29.14 | 26.69 | 23.79 | 19.47 |
| | Dressing room | 36.04 | 30.58 | 30.23 | 26.03 | 23.99 | 21.21 | 17.04 |
| | Living room | 39.82 | 35.07 | 32.90 | 28.49 | 22.93 | 21.62 | 17.52 |
| Main deck | Navigation space/radar room | 37.95 | 33.25 | 32.05 | 28.28 | 23.46 | 23.17 | 19.84 |
| | Captain's cabin | 45.30 | 41.73 | 43.51 | 39.62 | 37.85 | 36.10 | 32.22 |
| | Toilet in Captain's cabin | 46.34 | 41.70 | 42.02 | 37.58 | 32.97 | 33.32 | 29.39 |
| | Day Head | 48.24 | 45.99 | 43.98 | 39.61 | 36.88 | 33.98 | 30.21 |
| | Pantry | 44.51 | 40.07 | 38.53 | 34.30 | 29.08 | 28.53 | 25.34 |
| | Dining room | 42.97 | 36.04 | 34.99 | 31.44 | 28.22 | 26.74 | 22.68 |
| | Salon | 42.59 | 35.88 | 34.74 | 31.26 | 28.12 | 26.59 | 22.56 |
| Lower deck | Guest cabin 1 | 34.58 | 31.82 | 30.11 | 25.98 | 21.66 | 20.34 | 17.05 |
| | Guest cabin 2 | 36.13 | 34.61 | 32.29 | 27.85 | 23.38 | 21.70 | 18.01 |
| | Guest cabin 3 | 40.58 | 35.96 | 39.58 | 35.84 | 33.94 | 33.90 | 31.14 |
| | Guest cabin 4 | 42.17 | 35.44 | 34.80 | 31.23 | 27.37 | 26.58 | 24.36 |
| | Bathroom (Guest cabin 1) | 32.42 | 27.09 | 27.73 | 23.44 | 18.06 | 17.26 | 12.87 |
| | Bathroom (Guest cabin 2) | 34.92 | 31.65 | 30.03 | 25.41 | 19.99 | 18.59 | 13.92 |
| | Bathroom (Guest cabin 3) | 41.33 | 37.58 | 41.22 | 36.99 | 34.79 | 34.61 | 31.72 |
| | Bathroom (Guest cabin 4) | 55.82 | 54.49 | 52.63 | 48.59 | 45.78 | 43.17 | 39.56 |
| | Food preparation area/ galley | 63.27 | 57.72 | 58.95 | 57.10 | 54.33 | 54.59 | 53.01 |
| | Life boat store room | 57.70 | 52.56 | 57.69 | 55.54 | 52.90 | 51.22 | 48.33 |
| | Corridor beside galley | 61.18 | 53.72 | 54.51 | 51.12 | 47.96 | 47.05 | 44.43 |

| | | | | | | | | |
|---|---|---|---|---|---|---|---|---|
| | Cinema/Lounge | 53.83 | 51.07 | 50.10 | 48.44 | 46.07 | 43.16 | 38.39 |
| | Bar | 46.98 | 47.59 | 53.14 | 44.80 | 45.33 | 46.19 | 39.42 |
| Bottom deck | Crew cabin 1 | 26.71 | 22.14 | 25.17 | 21.35 | 18.60 | 17.67 | 12.79 |
| | Crew cabin 2 | 27.06 | 22.51 | 25.66 | 21.87 | 19.08 | 18.13 | 13.20 |
| | Crew cabin 3 | 35.45 | 30.73 | 33.38 | 30.09 | 28.06 | 28.34 | 23.83 |
| | Crew cabin 4 | 36.00 | 31.11 | 33.66 | 30.39 | 28.34 | 28.57 | 24.02 |
| | Crew cabin 5 | 54.20 | 51.65 | 53.34 | 51.58 | 51.60 | 50.55 | 48.23 |
| | Bathroom (Crew cabin 1) | 19.92 | 15.22 | 20.27 | 9.99 | 10.57 | 11.30 | 3.15 |
| | Bathroom (Crew cabin 2) | 24.26 | 20.41 | 23.54 | 17.93 | 13.56 | 14.27 | 8.16 |
| | Bathroom (Crew cabin 3) | 32.06 | 28.01 | 30.76 | 25.95 | 22.06 | 24.89 | 19.34 |
| | Bathroom (Crew cabin 4) | 32.54 | 28.48 | 31.15 | 26.55 | 22.38 | 25.17 | 19.71 |
| | Bathroom (Crew cabin 5) | 45.26 | 42.22 | 44.60 | 40.55 | 37.29 | 40.78 | 35.09 |
| | Laundry/Ironing room | 39.03 | 33.96 | 37.93 | 32.52 | 33.62 | 39.22 | 31.93 |
| | Storage | 40.53 | 35.54 | 40.43 | 34.31 | 36.73 | 45.91 | 37.11 |
| | Crew mess room | 56.42 | 50.34 | 48.87 | 48.57 | 51.10 | 64.16 | 61.45 |
| | Control room | 52.75 | 48.55 | 53.56 | 52.30 | 58.39 | 54.15 | 51.63 |
| | Pump-manifold room | 47.65 | 43.47 | 47.11 | 40.64 | 42.76 | 44.75 | 42.71 |
| | Battery room | 49.44 | 45.05 | 49.70 | 47.45 | 46.88 | 47.34 | 46.31 |
| | Engine room | 94.29 | 91.24 | 93.25 | 95.09 | 96.99 | 98.00 | 99.81 |

The noise (sound pressure level) dB(A) stated in each room consists of the contribution from both airborne and structure borne noises. In the engine room, both airborne and structure borne noises exist but the most part of sound energy input to the engine room cavity comes from airborne noise source. These airborne noises propagate to the adjacent cavities, one after another throughout the whole yacht starting from the engine cavity and decrease in intensity because of the absorption from insulations in the propagation path. The structure borne noise constraints applied to engine foundations and the plates closed to the propellers inject the vibrational energy. This vibrational energy starting from the places of excitation travels via the plate panels throughout the whole structure of the yacht model and then the vibration is induced in the plate panels, causing them to radiate noise into the acoustic cavities. The structure borne noises decrease in value when traveling through the structure because of structural damping, obstruction or structural discontinuities in the transmission path.

Obviously it can be known that the highest sound pressure level can be found in the engine room where the engine noise sources are located and the cavities near the plates in the aft region which are mostly affected by the propellers. But throughout the model, the highest sound pressure level is found in the acoustic cavities which are filled with fluid other than air.

When comparing the acoustic cavities filled with air, it is obviously seen that the engine room has the highest sound pressure level. Here, the highest SPL is about 99.81 dB(A). Then the energy propagates into the adjacent cavities until the fore areas and the upper deck spaces that are less noisy. The figures (46), (47), (48) and (49) visualize the highest SPL in each room among the analyzed frequency bands with respect to the general arrangement plan of the yacht. The corresponding colors filled in the acoustic cavities are selected based on the contour plot of figure (45).

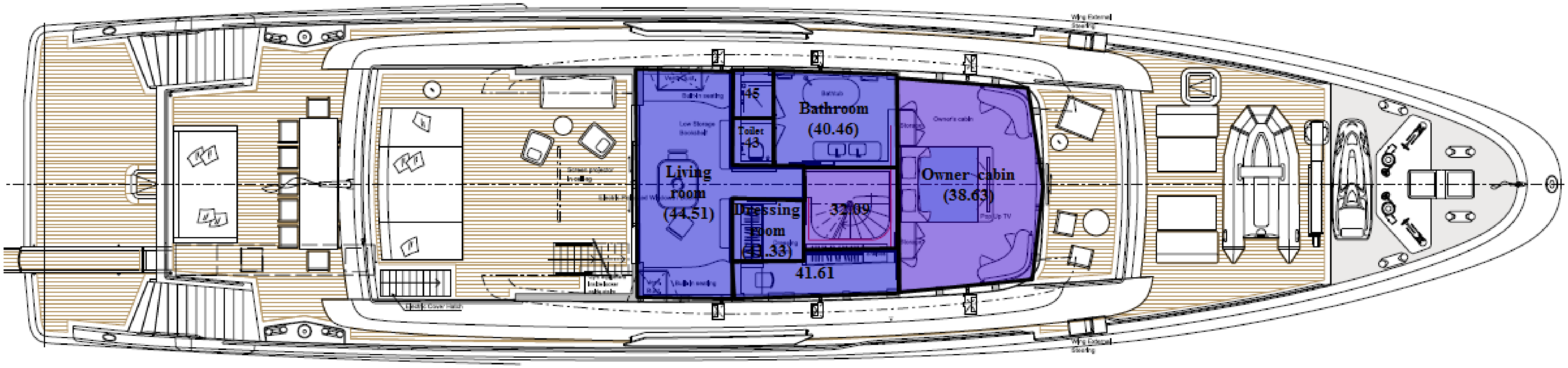


Figure 46: Highest sound pressure level in dB(A) on owner's deck

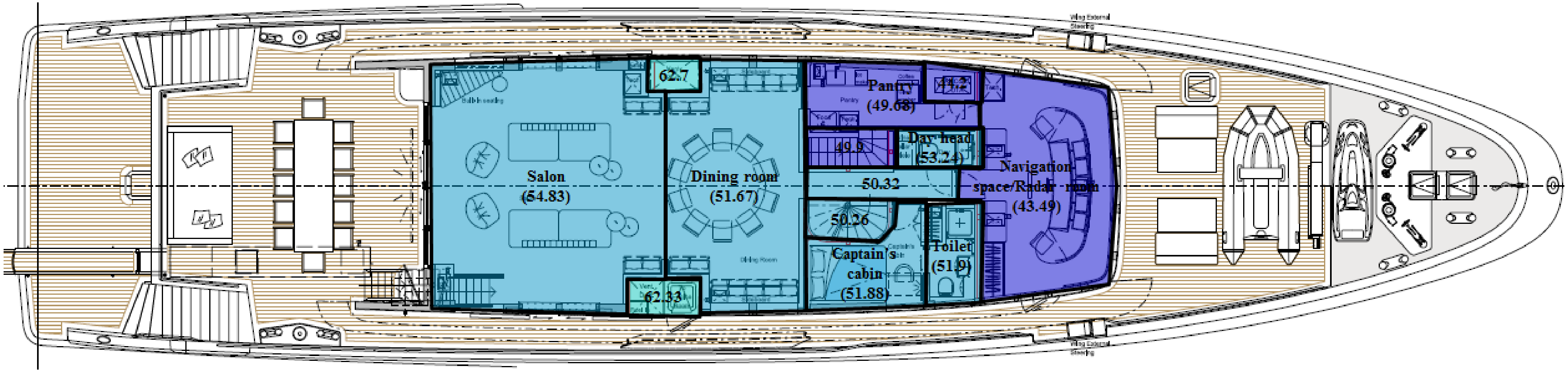


Figure 47: Highest sound pressure level in dB(A) on main deck

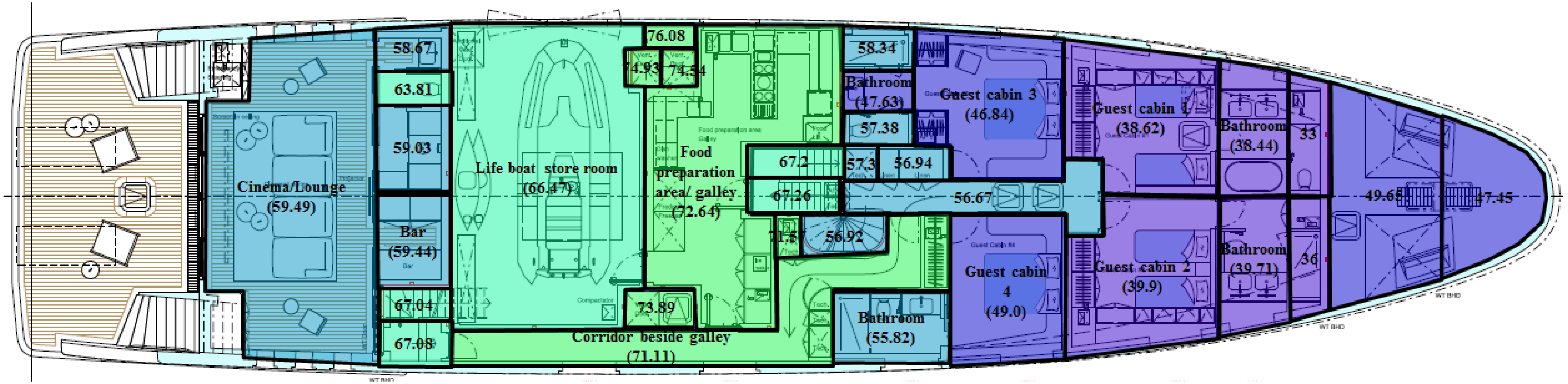


Figure 48: Highest sound pressure level in dB(A) on lower deck

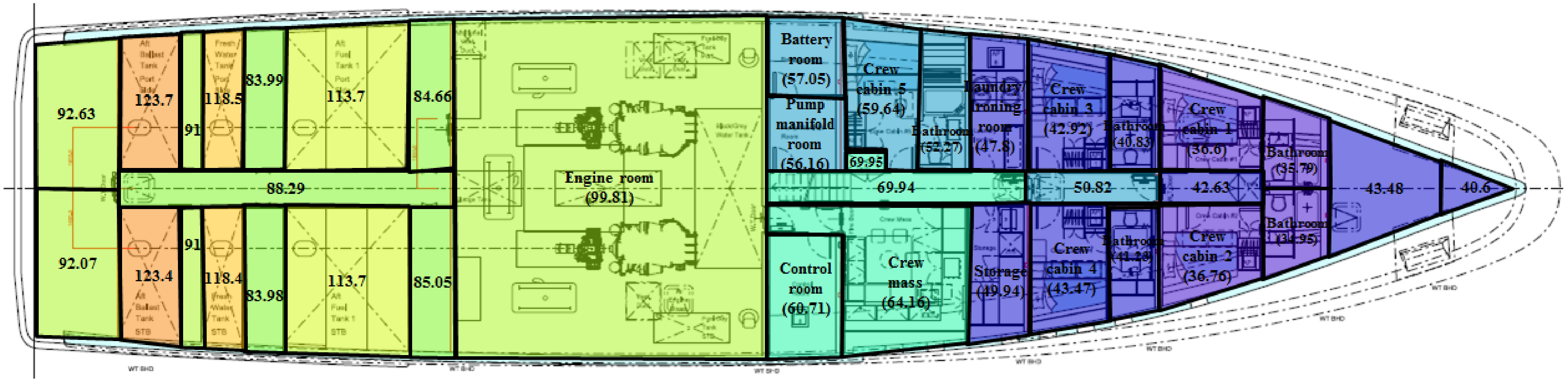


Figure 49: Highest sound pressure level in dB(A) on bottom deck

As it is already known that the volume or intensity of sound is measured in units called decibels (dB), generally on a scale from zero to 120. The higher the number in decibels, the louder is the noise. The louder the noise, the greater is the risk of hearing loss. Hearing loss does not happen immediately after the person has heard the sound pressure level higher than 120 dB. It occurs with regular exposure to noise levels of 120 decibels or more for some periods. In order to inform how loud the particular noise level is, the following noise comparison chart in dB(A) is presented. Therefore, one can imagine how it is like to one's ear staying in the corresponding cavities in the yacht.

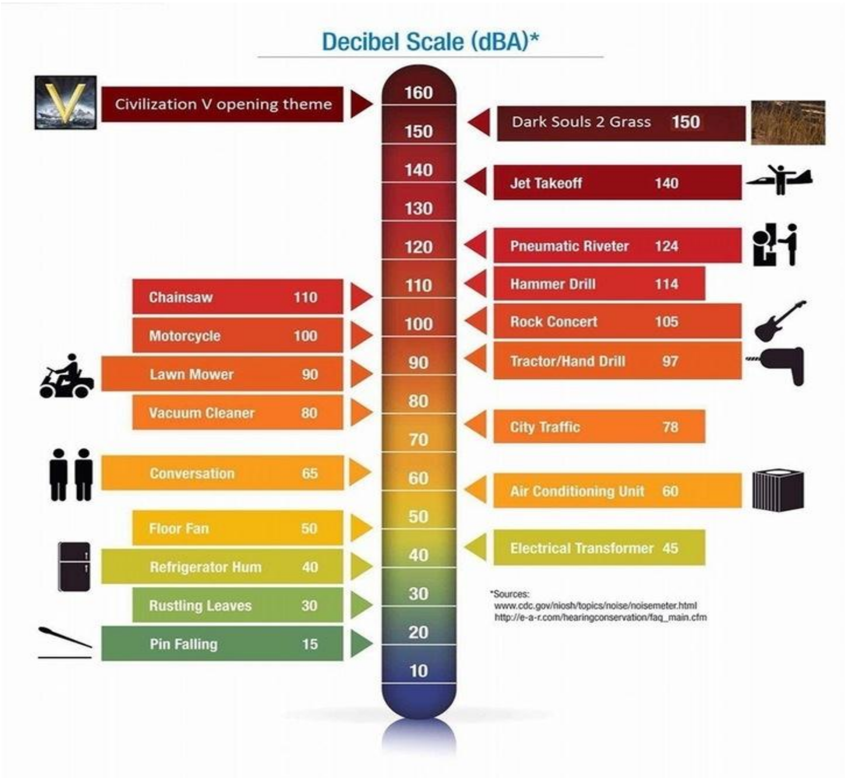


Figure 50: Decibel dB(A) loudness comparison chart

By the time being, the interest is put on the owner's cabin. The owner's cabin locates on the uppermost deck and in the forward region of that deck where the estimated highest sound pressure level is about 38.63 dB(A) and this, according to the chart, represents the noise from humming refrigerator. This satisfies the comfort noise criteria proposed by the RINA measurement. The VA One software allows to show the total energy of vibration induced in the owner's cabin propagated from the noise sources from engines and propellers. This is presented in the figure (51).

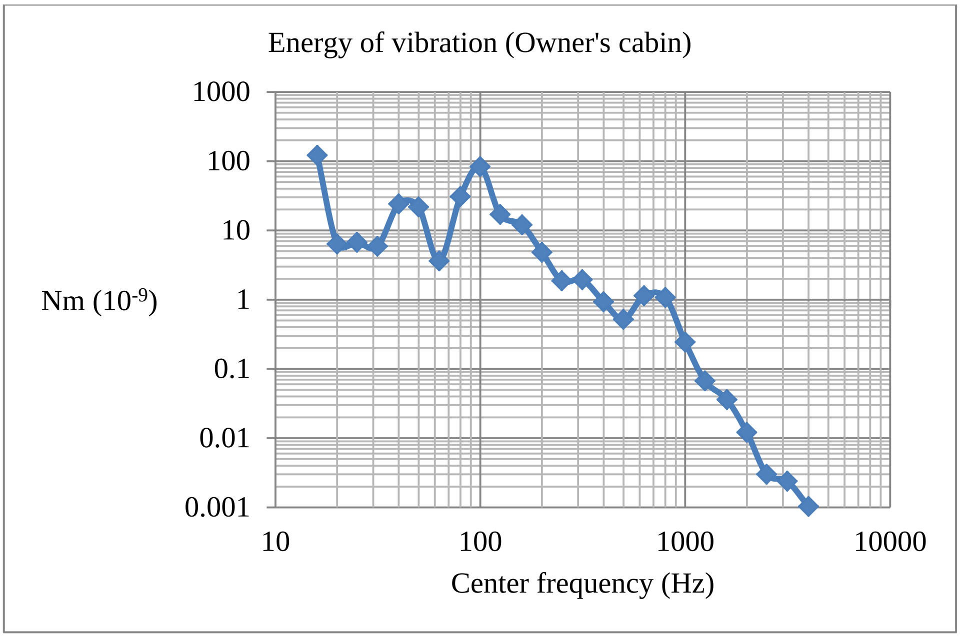


Figure 51: Energy of vibration measured in owner's cabin

Then, the Engineering Unit (Sound pressure level) for the owner's cabin is plotted. The Engineering Units of an SEA subsystem such as cavity are derived from subsystem's resonant energy, which is the primary measure of the amplitude of vibration in SEA. They are related to the total vibrational energy $E$ of the wave field of the subsystem by the following equation, already stated in the theoretical part of this thesis.

$$p_{rms}^2 = \frac{E\,\rho\,c^2}{V} \text{ and } L_p = 20\,log\left(\frac{p_{rms}}{p_{ref}}\right), \text{dB} \qquad (64)$$

$V$ = volume of owner's cabin = 49.77 $m^3$

$\rho$ = density of air in owner's cabin = 1.21 kg/ $m^3$

$c$ = speed of sound in owner's cabin = 343 m/s

By the relations in equation (64), the sound pressure and pressure level in Pa and dB is calculated respectively through the frequency bands and then illustrated in the figures (52) and (53) where the dB reference is $2 \times 10^{-5}$Pa.

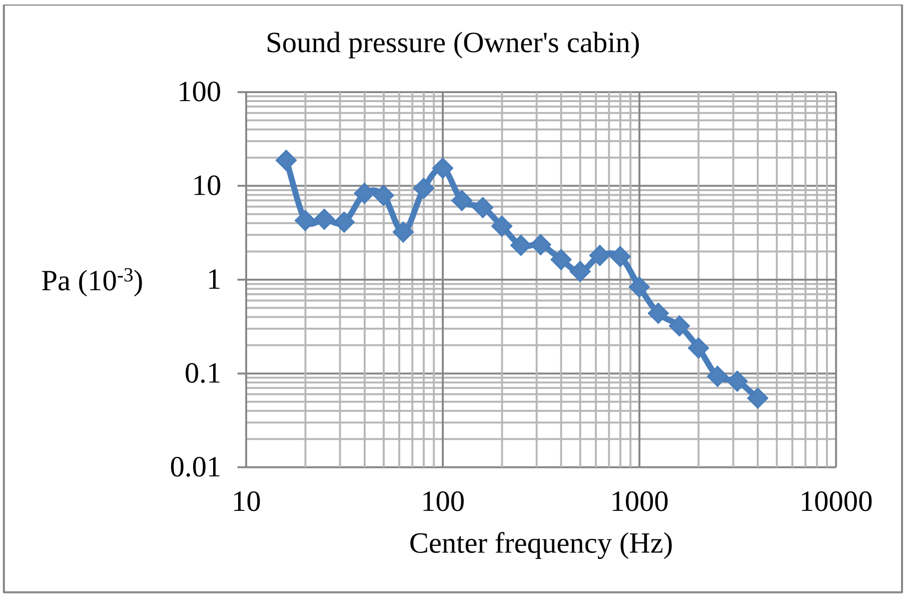


Figure 52: Sound pressure (Pa) in owner's cabin

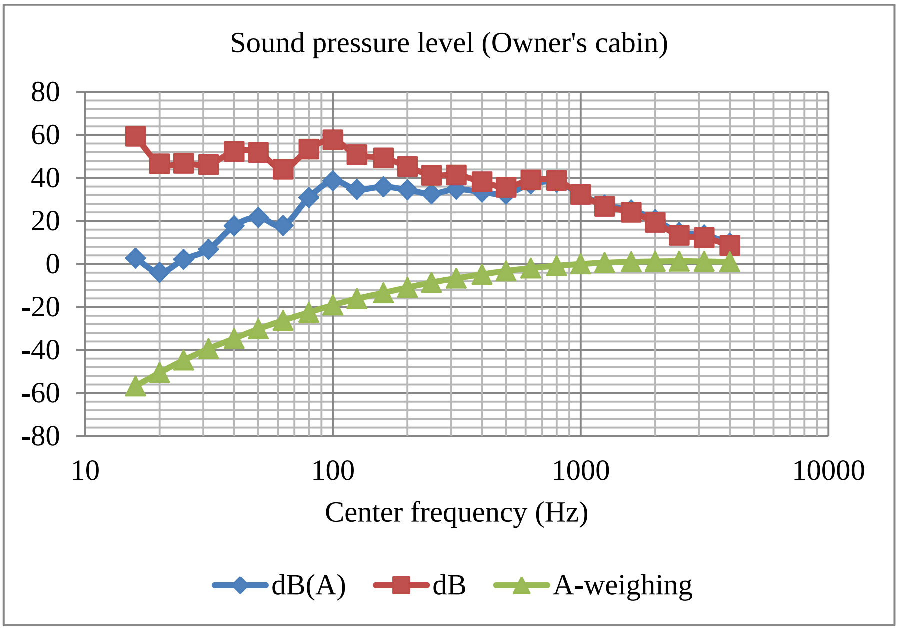


Figure 53: Sound pressure level (in dB and dB(A)) in owner's cabin

The VA One software also allows to display the power inputs for each SEA subsystem in the analysis. Therefore here, the power input to the owner's cabin is visualized and how the plates, especially the glass windows surrounding the owner's cabin contribute to the sound pressure level of the cabin is investigated. In the figure (54), although there are a lot more plates providing the power input to the owner's cabin, in order to see more clearly the results, only those of the windows are shown which are considered the major contribution to the sound pressure level of the cavity. Here, the dB reference is $1 \times 10^{-12}$W.

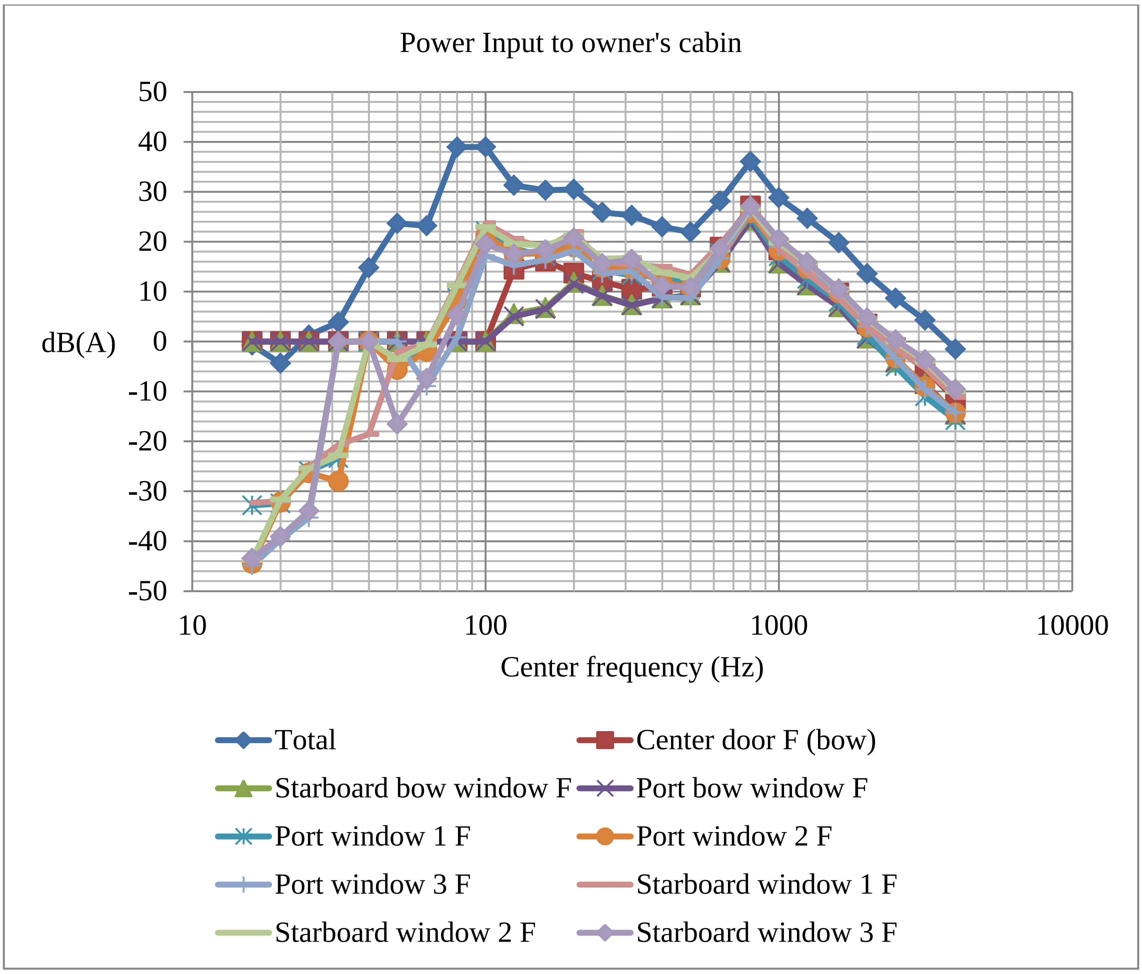


Figure 54: Power inputs to owner’s cabin

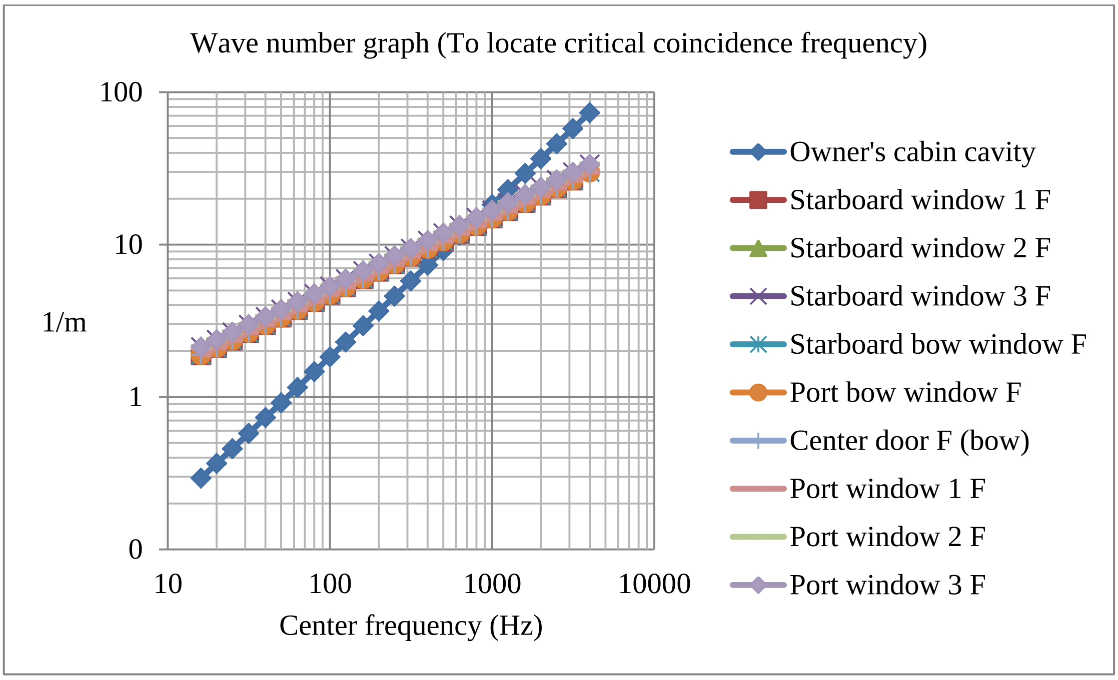


Figure 55: Wave number graphs of owner’s cabin cavity and the glass windows and door

In the figure 54, the contributions from different glass windows of the owner's cabin can be identified. Particularly, we can distinguish between three different frequency ranges. In the lower frequency range which is below 100Hz, there is no major power input from these windows and even the center glass sliding door and port and starboard bow windows do not input any power to the cavity. In the medium frequency range from 100Hz to 800Hz, these glass panels radiate more noise, with the highest values at 800Hz which is the critical coincidence frequency. The location of critical coincidence frequency of these glass panels can be found by the visualization of wave number plot of each panel against the wave number of the acoustic cavity. This is shown in the figure 55. And after the critical coincidence frequency (800Hz), the power input decreases gradually. At the time of the SEA analysis, the designs of these windows are considered such that they are directly connected to the steel and aluminum structures without any damping material at the particular junctions. If these damping effects from junctions are included, the noise radiated from these panels into the cavity could decrease. The glass windows and center glass door of the owner's cabin discussed just now are illustrated in the figure (56).

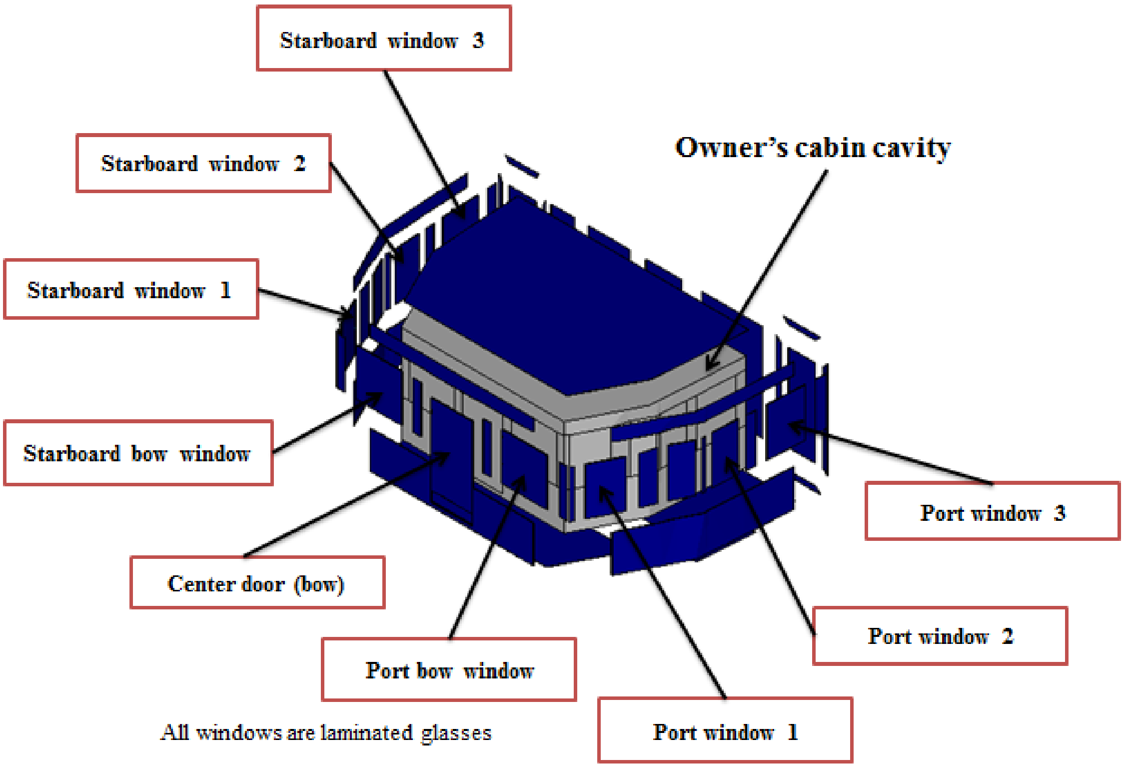


Figure 56: Glass windows and door radiating noise into the owner's cabin

In order to understand how the contribution of windows to the sound pressure level of the owner's cabin changes as a function of the physical properties of the panel, a second SEA analysis on this yacht model has been carried out. In this analysis, the thickness of the glass windows described above is increased by 10%, 20% and 30% respectively and then the nature of sound pressure level drop is investigated. Of course the location of critical coincidence frequency will shift in each condition to somewhere other than 800Hz, since the increase in each panel thickness is considered relatively small, the particular investigation is performed at initial critical coincidence frequency which is 800Hz. Then, the power input from these glass windows to the owner's cabin is plotted at 800Hz for each condition and there one can obviously see how the power contribution from each panel drops. This is presented in the figure (57) and the corresponding decrease in sound pressure level in owner's cabin is shown in figure (58).

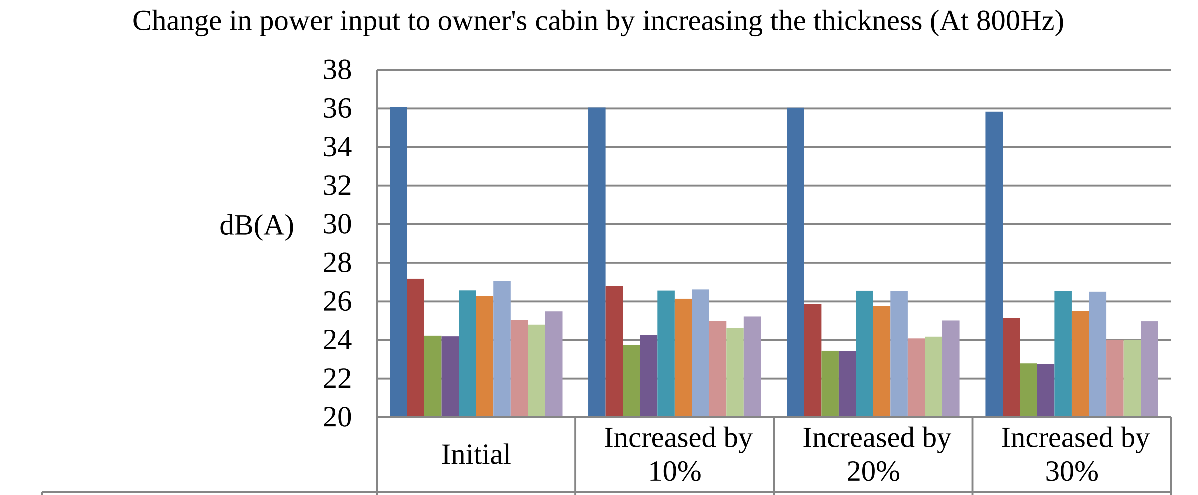


| | Initial | Increased by 10% | Increased by 20% | Increased by 30% |
|---|---|---|---|---|
| Total | 36.06 | 36.05 | 36.04 | 35.84 |
| Center door F (bow) | 27.17 | 26.79 | 25.87 | 25.14 |
| Starboard bow window F | 24.22 | 23.75 | 23.45 | 22.78 |
| Port bow window F | 24.19 | 24.25 | 23.42 | 22.77 |
| Starboard window 1 F | 26.57 | 26.56 | 26.55 | 26.54 |
| Starboard window 2 F | 26.29 | 26.14 | 25.77 | 25.50 |
| Starboard window 3 F | 27.07 | 26.62 | 26.52 | 26.50 |
| Port window 1 F | 25.03 | 24.99 | 24.08 | 24.01 |
| Port window 2 F | 24.79 | 24.63 | 24.17 | 24.01 |
| Port window 3 F | 25.48 | 25.22 | 25.01 | 24.97 |

Figure 57: Decrease in power input from different glass windows and door

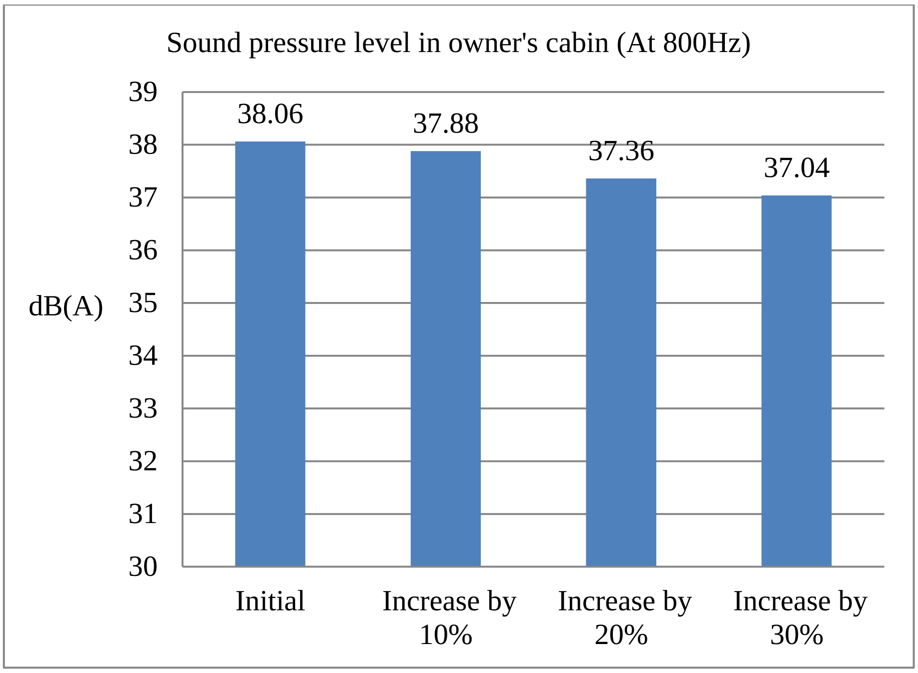


Figure 58: Decrease in sound pressure level in owner's cabin

As it can be obviously observed in the figure (58), the sound pressure level in the owner's cabin is decreased by only 1 dB(A) even when the thickness of the windows are increased up to 30%. Anyway, this is of great value in this kind of analysis. In order to reduce more noise, it is more practical to add the insulation or increase the thickness of existing insulation surrounding the acoustic room of interest rather than increasing the particular structure of the room. Alternatively, when the insulation thickness is intended to be constant, then one can use the insulation material of the same thickness but of having greater air flow resistivity in the purpose for blocking more sound energy traveling from one room to another.

By the time being, the interest is put on the salon which is located on the main deck in the aft region, where the estimated highest sound pressure level is about 54.83 dB(A) and this, according to the chart, represents the noise level between those coming from air conditioning unit and floor fan. The SEA plate subsystems composing the salon cavity is shown in the figure (59) where the plate panels which contribute the highest power input are named accordingly. Based on the SEA analysis, apart from the glass windows surrounding the salon, the highest power input comes from the floor plates.

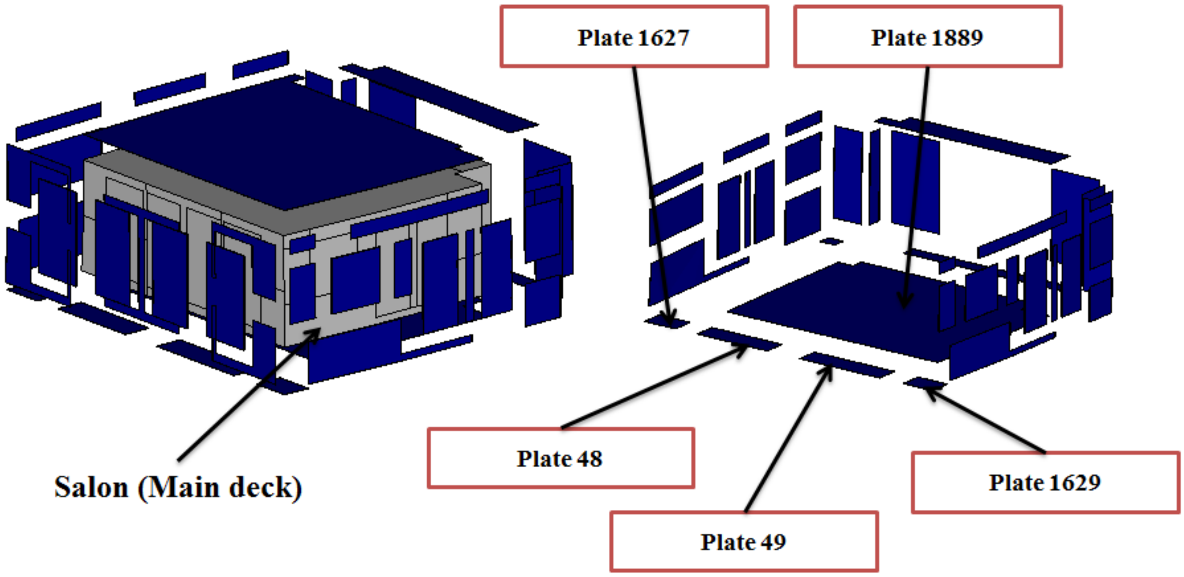


Figure 59: Different floor plates radiating noise into the salon cavity

Then the graphs of sound pressure level, the wave number of floor plates and salon acoustic cavity, and the corresponding power inputs from these plates named in the figure (59) are presented in the same way as the owner's cabin.

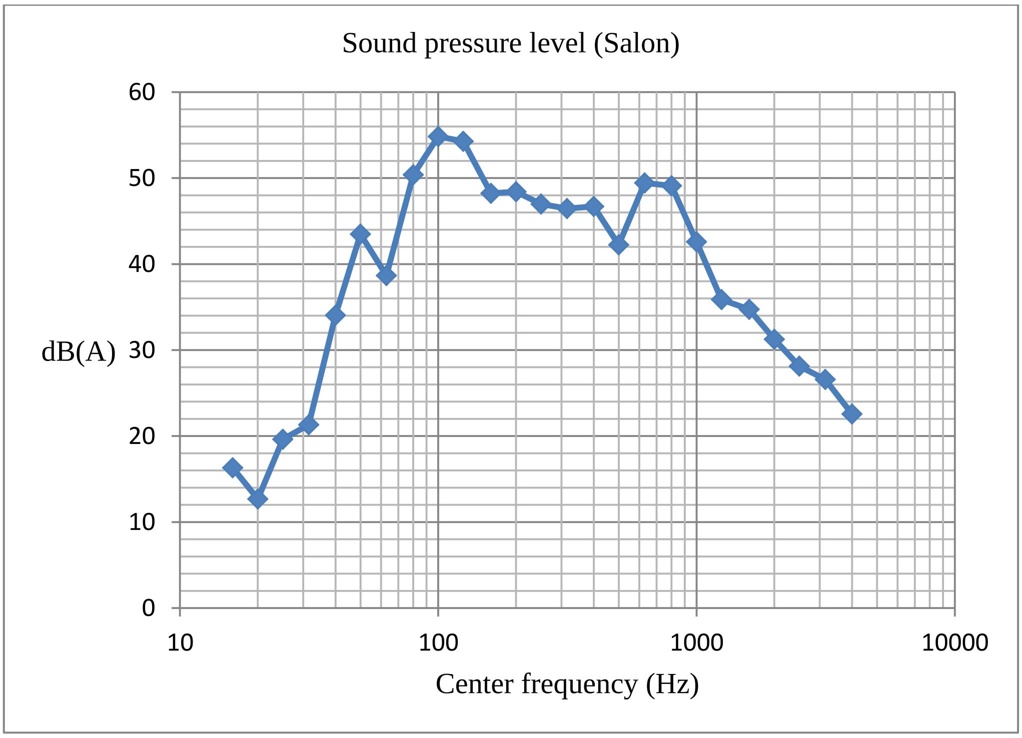


Figure 60: Sound pressure level dB(A) in salon

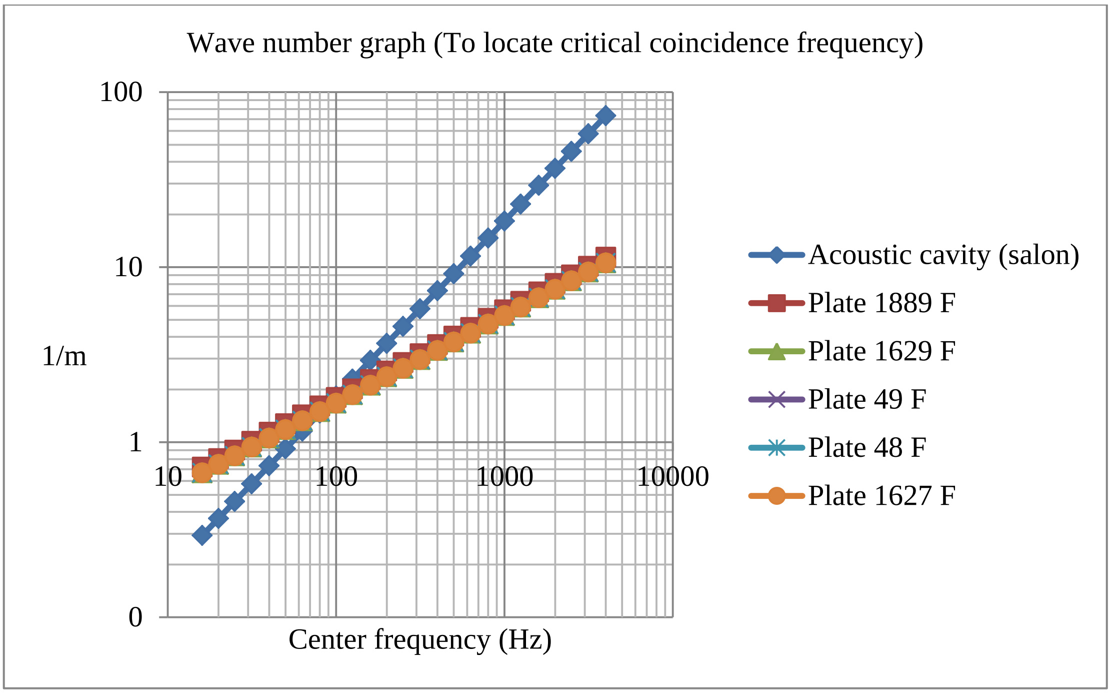


Figure 61: Wave number graphs of salon cavity and the floor plates of interest

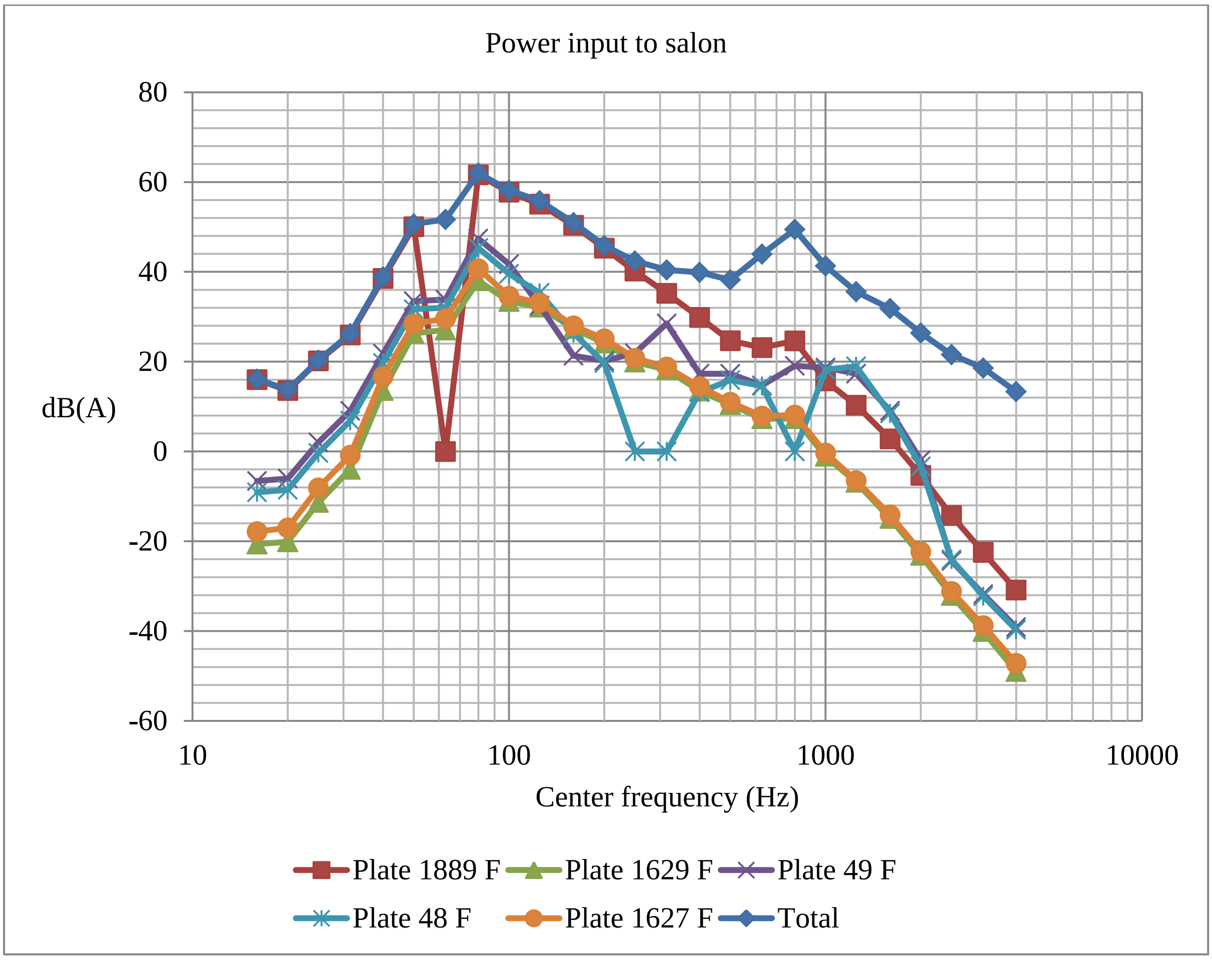


Figure 62: Power inputs to salon

As it can be seen in the figure 61, the critical coincidence frequency occurs around 80Hz and at this frequency, the power inputs from each plate are higher than those at the other frequencies. This can be visualized in the figure 62. At this time, a third SEA analysis is performed at 80Hz in order to see how the changes in insulation thickness of these particular plates contribute to the power input to the salon cavity. In this analysis, the same way of increasing the insulation thickness is applied to the floor plates such as by 10%, 20% and 30% respectively as that of the windows of the owner's cabin. The corresponding decrease in power inputs from these plate panels is presented in the figure 63. And the corresponding decrease in sound pressure level in salon is presented in the figure 64.

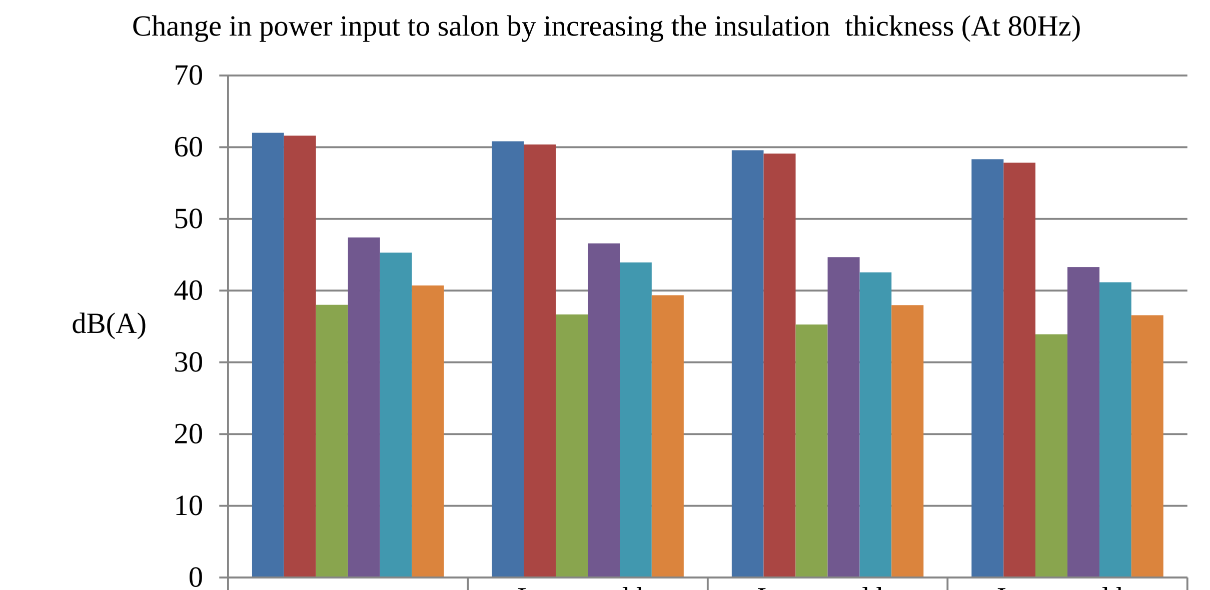


| | Initial | Increased by 10% | Increased by 20% | Increased by 30% |
|---|---|---|---|---|
| Total | 62.01 | 60.82 | 59.58 | 58.33 |
| Plate 1889 F | 61.60 | 60.38 | 59.11 | 57.82 |
| Plate 1629 F | 38.03 | 36.67 | 35.28 | 33.91 |
| Plate 49 F | 47.40 | 46.58 | 44.67 | 43.28 |
| Plate 48 F | 45.30 | 43.94 | 42.55 | 41.16 |
| Plate 1627 F | 40.71 | 39.36 | 37.97 | 36.56 |

Figure 63: Decrease in power input from different floor panels to salon cavity

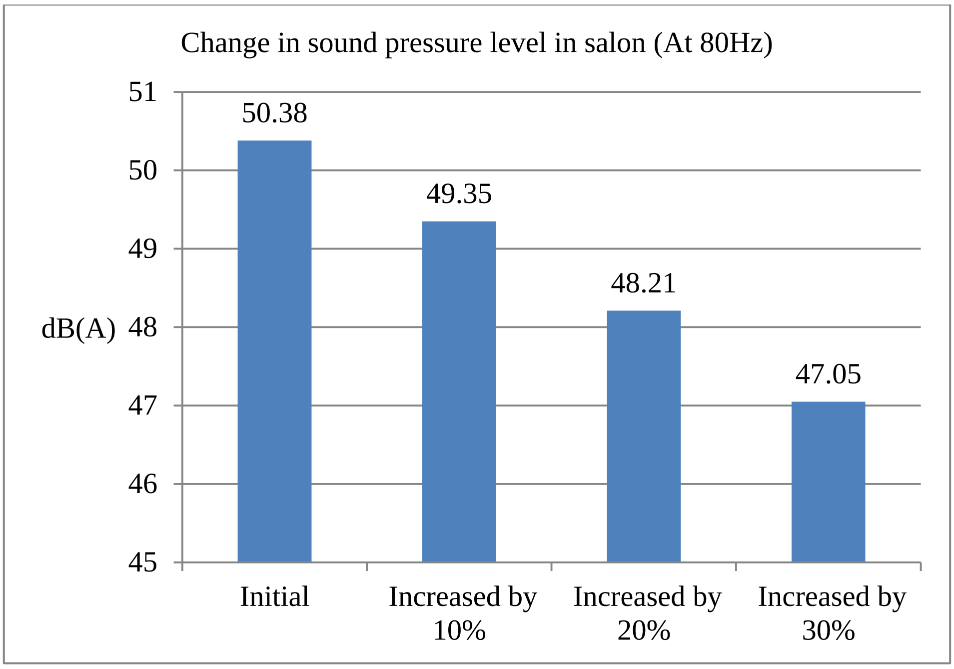


Figure 64: Decrease in sound pressure level in salon

As it can be observed clearly in the figure (64), the sound pressure level of salon decreases by 1 dB(A) every time the insulation thickness of floor plate panels is increased by 10%. When the insulation thickness is increased by 30%, the sound pressure level is dropped by about 6.6% (3.33 dB(A) decreases) which is considered a great decrease of noise in this analysis. The VA One also allows to see the behavior of sound transmission loss of the panels by changing the physical properties. The following sound transmission loss plot (figure 65) is generated for the plate 1889, showing the loss of sound energy throughout the analyzed frequency bands when it travels from life boat store room (lower deck) to salon (main deck) via the floor plate 1889. There one can see, around the critical coincidence frequency (80Hz), the transmission loss dramatically decreases. When increasing the thickness of corresponding insulation, the transmission loss at the particular frequency becomes increased. And this is shown in the figure (66) where one can see that the loss of sound energy is increased by 38.7% when the insulation thickness is increased by 30% and this can be apparently effective in reducing the sound pressure level in the acoustic cavity of interest because of great noise reduction by even a slight increase in insulation thickness.

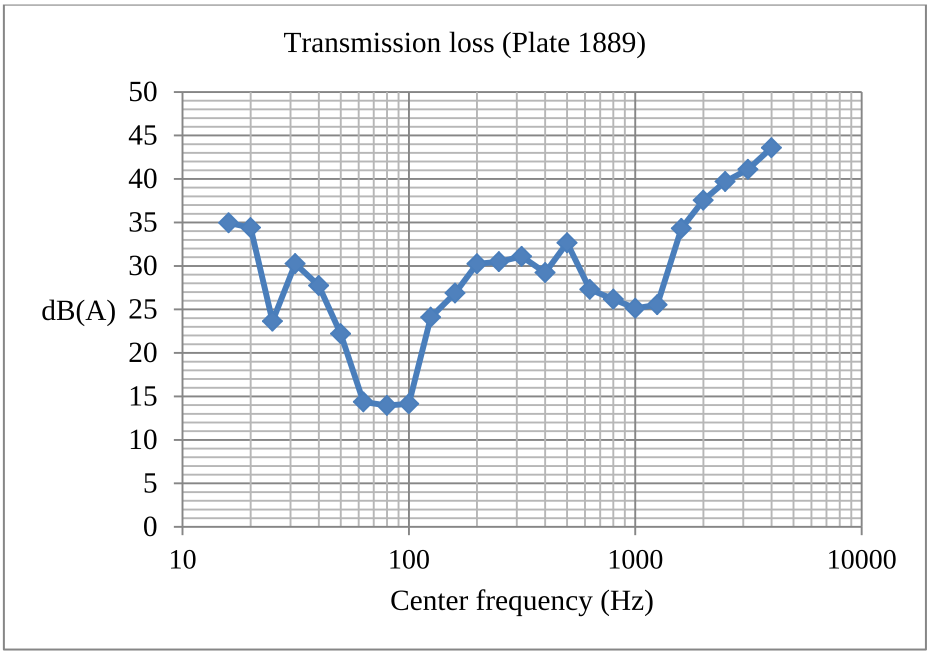


Figure 65: Transmission loss of plate 1889

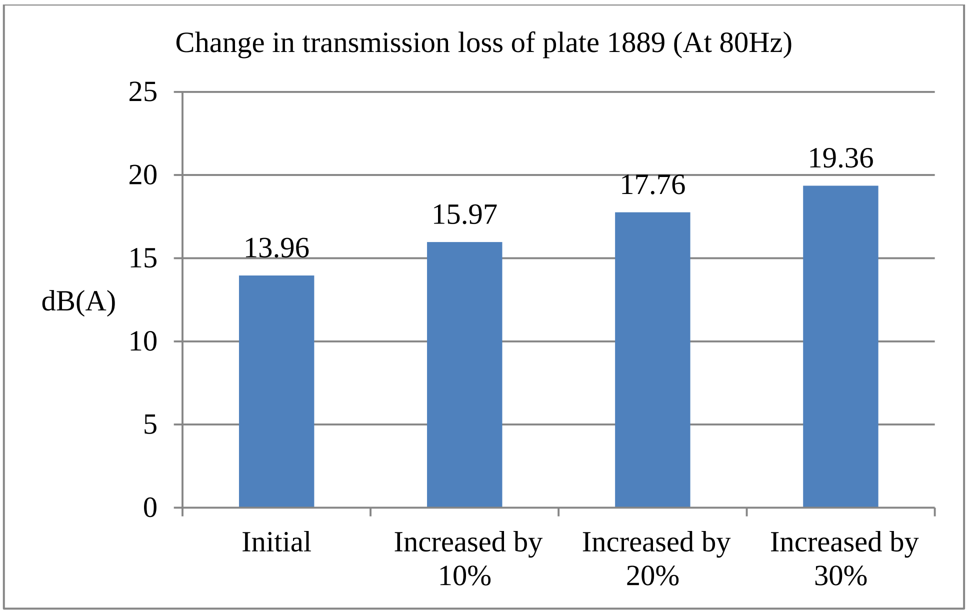


Figure 66: Increase in sound transmission loss behavior of plate 1889

## 9. CONCLUSIONS

This paper presents the results of the noise propagation throughout the structure of a 40m Ice Class motor yacht (KN Explorer) from Cerri Cantieri Navali. Three statistical energy analyses (SEA), numerical analyses based on the numerical model developed, are performed at navigation condition at cruse speed. This numerical model enables the analysis of both the structural elements and the acoustic spaces.

From the first SEA analysis, the noise levels in each room according to the general arrangement plan throughout the one-third octave frequency bands starting from 16 Hz to 4000Hz are predicted and then the highest sound pressure level in each room are checked with the noise criteria from RINA comfort class notation (COMF Yacht) for comfort and well-being of passengers and crew. According to the first analysis, most of the cabins of the yacht model satisfy the merit A noise limit: only a few does not but, at least, satisfy the merit B noise limit. However, in reality, the noise level predicted in this thesis will be even decreased because here in this thesis, when modeling the yacht, the noise absorption in the acoustic cavity is considered and calculated only from the noise control treatment. In real condition, there will be sound absorbing objects inside the room such as furniture, decorative items, floor carpet, etc.

Some of the uncertainties will emerge when referring to damping in this thesis, In order to obtain an excellent accuracy, it is advisable to perform the individual damping test of the panels which contribute the highest sound power level to the room of interest. Some of the damping loss factors defined in this thesis are based on the averaged of the average values from the damping test of each material used in the yacht model. Fortunately, the influence of damping does not have much effect in the statistical energy analysis and therefore, if one is willing to make only a prediction, SEA is apparently reliable with the advantage of decreasing cost and time consuming.

The second and third SEA analyses represent an initial step for further analysis regarding noise reduction. There are three ways to reduce the noise level such as increasing the structural thickness, adding insulation or increasing the current insulation thickness and increasing the damping. In the second SEA analysis, how the noise level changes (decreases) as a function of the structural thickness and in the third analysis, how effective increasing the insulation thickness is to decrease the noise level in the analyzed room. Depending on the cost constraint, whether to increase the particular structural thickness or the insulation thickness should be decided.

# 10.REFERENCES

1. L.L Beranek, Noise and Vibration Control, New York, McGraw-Hill Book Company, 1971.
2. J.W.E. Pettersen and J. Storm, Noise Control in Ships, Norwegian Council for Technical and Scientific Research, Oslo 1975.
3. F.Fachy and E. Lindquist, "Wave propagation in damped, stiffened structures characteristic of ship constructions", J. Sound and Vibration 1976.
4. B.S. Seland, "Propagation of structure borne sound in stiffendd plates", DNV Report 1978 (Det Norske Veritas, Oslo).
5. J.H. Janssen and J. Buiten, "An acoustical designing in naval architecture", Proceeding INTERNOISE, 1973.
6. Eugeniusz Kozaczka "Study of Noise Propagation for Small Vessels", Polish Naval Academy, Smidowicza 69, 81-103 Gdynia, Poland.
7. M. Weryk, Statistical energy analysis methods in marine applications, Hydroacoustics, vol. 8, XII Sympozjum z Hydroakustyki, Puck 2005, s. 233-246.
8. R.H. Lyon, "Statistical Energy Analysis of Dynamical Systems, Theory and Applications", MIT Press, Cambridge 1975.
9. Lisa Gragnani and Arnaud Caillet, "Evolution of predictive methodologies for Marine Acoustics".
10. Lisa Gragnani, "Dynamic Characterization of Laminated Glass For Mega Yacht Windows", University of Genoa (UNIGE), Italy, Anno Accademico 2013/2014.
11. Mateusz Weryk "Ship onboard noise propagation analysis methods", Centrum Techniki Okretowej SA ul. Szczecinska 65 80-392, Poland.
12. B.M.S Gibbs and C.L.S Gilford "The use of power flow methods for the assessment of sound transmission in building structures", J. Sound and vibration 1976, 49, 267-286.
13. Text book of wood technology. First Ed. Vol. II, McGraw-Hill Book, New York (1952), 143-317.
14. Brandon Bloss and Mohan D. Rao, Mechanical Engineering - Engineering Mechanics Department, Michigan Technological University, Houghton, MI 49931, USA.
15. Koblar, D. and Bolte_zar, M., Evaluation of the frequency-dependent Young's modulus and damping factor of rubber from experiment and their implementation in a

finite-element analysis, Experimental Techniques, published online 11 November 2013, DOI: 10.1111/ext.12066.

16. Sound transmission through buildings using Statistical Energy Analysis, Robert JM Craik.
17. A. Tonelli, D. Torre - RINA Services - Italy, G. Vergassola, D. Boote - UNIGE - Italy, Numerical Tools and Experimental Activities for the Prediction of Noise Propagation on Board Superyachts, 10-11 May 2017.
18. References Material of ESI Group, Vibroacoustic One (VA One).

# 11. APPENDIX

## Appendix I (Different types of uniform plates)

| Name | Material | Thickness (m) |
|---|---|---|
| Sundeck plate | Aluminum | 0.005 |
| Owner deck plate | Aluminum | 0.005 |
| Main deck plate | Steel | 0.005 |
| Lower deck plate | Steel | 0.004 |
| Lower deck side plate | Steel | 0.006 |
| Bottom deck side and bottom plate | Steel | 0.008 |
| Double bottom plate | Steel | 0.005 |
| Transom plate | Steel | 0.006 |
| Bulkhead fr-10 lower deck plate | Steel | 0.004 |
| Bulkhead fr-10 bottom deck plate | Steel | 0.005 |
| Bulkhead fr-15+0.55 lower deck plate | Steel | 0.004 |
| Bulkhead fr-19 bottom deck plate | Steel | 0.004 |
| Bulkhead fr-19+0.278 lower deck plate | Steel | 0.004 |
| Bulkhead fr-21 lower and bottom decks plate | Steel | 0.004 |
| Bulkhead fr-27 lower deck plate | Steel | 0.004 |
| Bulkhead fr-26 and fr-29.5 bottom deck plate | Steel | 0.004 |
| Bulkhead 34/37 plate | Steel | 0.004 |
| Bulkhead fr-37 bottom deck plate | Steel | 0.005 |
| Girder 0 (center girder) | Steel | 0.008 |
| Girder 0.45 | Steel | 0.006 |
| Girder 1.095 | Steel | 0.01 |
| Girder 1.117 | Steel | 0.006 |
| Girder 1.15 | Steel | 0.008 |
| Girder 1.6 | Steel | 0.008 |
| Girder 1.75 | Steel | 0.005 |
| Girder 2.073 | Steel | 0.01 |
| Girder 2.095 | Steel | 0.01 |
| Girder 3.059 | Steel | 0.006 |
| Owner deck upper side plate | Aluminum | 0.005 |
| Owner deck lower side plate | Aluminum | 0.012 |
| Owner deck side plate | Aluminum | 0.006 |
| Main deck upper side plate | Aluminum | 0.005 |
| Main deck lower side plate | Aluminum | 0.005 |
| Main deck side plate | Aluminum | 0.005 |
| Owner deck bow window | Laminated glass | 0.01904 |
| Owner deck stern window | Laminated glass | 0.01504 |
| Owner deck side window | Laminated glass | 0.01504 |
| Main deck bow window | Laminated glass | 0.01952 |
| Main deck stern window | Laminated glass | 0.01904 |

| | | |
|---|---|---|
| Main deck side window | Laminated glass | 0.01904 |
| Lower deck side window BL104 | Tempered Glass | 0.00876 |
| Lower deck side and stern window | Tempered Glass | 0.02704 |
| Bottom deck side window | Tempered Glass | 0.02704 |
| Skeg plate | Steel | 0.008 |
| Frame 2, 3.5, 4, 5, 6, 7 and 9 plate | Steel | 0.005 |
| Frame 8+0.48 and frame10 lower deck plate | Steel | 0.004 |
| Frame 18+0.51 lower deck plate | Steel | 0.004 |
| 0.45m longitudinal bulkhead | Steel | 0.006 |
| 3.5m longitudinal bulkhead | Steel | 0.005 |
| Longitudinal bulkhead between fr-10 and fr-15 lower deck plate | Steel | 0.004 |
| Longitudinal bulkhead between fr-15 and fr-19+0.278 lower deck plate | Steel | 0.004 |
| Longitudinal bulkheads at 0.45m (stb) and 1.31m (port) lower deck plate | Steel | 0.004 |
| Owner deck internal transverse and longitudinal walls | Aluminum | 0.005 |
| Main deck internal transverse and longitudinal walls | Aluminum | 0.005 |
| Longitudinal wall between fr-8 and fr-10 lower deck | Steel | 0.004 |
| Doors | Plywood | 0.004 |
| Watertight doors | Steel | 0.004 |
| Top plate of tanks in engine room | Steel | 0.005 |
| Side plate of tanks in engine room | Steel | 0.006 |
| Top plate of tanks (between fr-4& fr-5, fr-6& fr-7) | Steel | 0.004 |
| Pl-03 (Laricross) | Plywood | 0.016 |
| Pl-02 (Green) (Isophon light panel) | Plywood | 0.019 |
| Common bottom transverse | Steel | 0.006 |

Note: Fr-15+0.55 means 0.55m forward of frame number 15.

## Appendix II (General laminate plate)

| Name | Layers | Layer-1 | Layer-2 | Layer-3 | Total Thickness (m) |
|---|---|---|---|---|---|
| Pl-01 (Cyan) (Sandwich panel 8-6-8) | 3 | Plywood | Hard Rubber | Plywood | 0.022 |

## Appendix III (Different types of beams/stiffeners)

| Name | Material | Ixx ($m^4$) | Iyy ($m^4$) | Area ($m^2$) | Jzz ($m^4$) | Perimeter (m) | Qzz ($m^4$) | Offset Dx (m) | Offset Dy (m) |
|---|---|---|---|---|---|---|---|---|---|
| Common sundeck longitudinals (50x6) | Aluminum | 6.25E-08 | 9.00E-10 | 0.0003 | 6.34E-08 | 0.112 | 6.34E-08 | 0 | 0 |
| Common sundeck transverse (50x6) | Aluminum | 6.25E-08 | 9.00E-10 | 0.0003 | 6.34E-08 | 0.112 | 6.34E-08 | 0 | 0 |
| Sundeck transverse (100x5+90x15) | Aluminum | 1.65E-06 | 9.12E-07 | 0.00185 | 2.56E-06 | 0.41 | 2.56E-06 | 0 | 0 |
| Common owner deck longitudinals (50x6) | Aluminum | 6.25E-08 | 9.00E-10 | 0.0003 | 6.34E-08 | 0.112 | 6.34E-08 | 0 | 0 |
| Owner deck transverse (120x5+90x12) | Aluminum | 2.41E-06 | 7.30E-07 | 0.00168 | 3.41E-06 | 0.444 | 3.41E-06 | 0 | 0 |
| Owner deck transverse (120x5+90x15) | Aluminum | 2.64E-06 | 9.13E-07 | 0.00195 | 3.55E-06 | 0.45 | 3.55E-06 | 0 | 0 |

| | | | | | | | | | |
|---|---|---|---|---|---|---|---|---|---|
| Main deck longitudinals (60x4, 50x5, 200x4+100x10=132.33x10) | Steel | 1.93E-06 | 1.10E-08 | 0.001323 | 1.94E-06 | 0.2847 | 1.94E-06 | 0 | 0 |
| Main deck longitudinals (60x4,50x5, 200x4+100x10=118.1x10) | Steel | 1.37E-06 | 9.84E-09 | 0.001181 | 1.38E-06 | 0.2562 | 1.38E-06 | 0 | 0 |
| Main deck longitudinals (50x5, 200x4+100x10=122x10) | Steel | 1.51E-06 | 1.02E-08 | 0.00122 | 1.52E-06 | 0.264 | 1.52E-06 | 0 | 0 |
| Main deck transverse (200x4+60x6) | Steel | 5.30E-06 | 1.09E-07 | 0.00116 | 5.41E-06 | 0.532 | 5.41E-06 | 0 | 0 |
| Main deck transverse (140x4+60x6) | Steel | 2.08E-06 | 1.09E-07 | 0.00092 | 2.19E-06 | 0.412 | 2.19E-06 | 0 | 0 |
| Main deck transverse (200x4+80x6) | Steel | 5.85E-06 | 2.57E-07 | 0.00128 | 6.11E-06 | 0.572 | 6.11E-06 | 0 | 0 |
| Lower deck longitudinals (150x4+100x10, 60x6=90.11x10) | Steel | 6.10E-07 | 7.51E-09 | 0.0009011 | 6.17E-07 | 0.2002 | 6.17E-07 | 0 | 0 |
| Lower deck longitudinals (200x4+100x10, 50x5=105.9x10) | Steel | 9.89E-07 | 8.83E-09 | 0.001059 | 9.98E-07 | 0.2318 | 9.98E-07 | 0 | 0 |
| Lower deck longitudinals (200x4+100x10, 50x5=108.4x10) | Steel | 1.06E-06 | 9.03E-09 | 0.001084 | 1.07E-06 | 0.2368 | 1.07E-06 | 0 | 0 |
| Lower deck longitudinals (200x4+100x10, 50x5=122x10) | Steel | 1.51E-06 | 1.02E-08 | 0.00122 | 1.52E-06 | 0.264 | 1.52E-06 | 0 | 0 |
| Lower deck longitudinals (200x4+100x10, 50x5=147.5x10) | Steel | 2.67E-06 | 1.23E-08 | 0.001475 | 2.69E-06 | 0.315 | 2.69E-06 | 0 | 0 |
| Lower deck transverse(150x4+80x6) | Steel | 2.75E-06 | 2.57E-07 | 0.00108 | 3.01E-06 | 0.472 | 3.01E-06 | 0 | 0 |
| Lower deck transverse (140x4+80x6) | Steel | 2.29E-06 | 2.57E-07 | 0.00104 | 2.55E-06 | 0.452 | 2.55E-06 | 0 | 0 |
| Lower deck transverse (140x4+60x6) | Steel | 2.08E-06 | 1.09E-07 | 0.00092 | 2.19E-06 | 0.412 | 2.19E-06 | 0 | 0 |
| Owner deck side longitudinals (50x6) | Aluminum | 6.25E-08 | 9.00E-10 | 0.0003 | 6.34E-08 | 0.112 | 6.34E-08 | 0 | 0 |
| Owner deck side transverse (180x5+50x5) | Aluminum | 4.10E-06 | 5.40E-08 | 0.00115 | 4.16E-06 | 0.47 | 4.16E-06 | 0 | 0 |
| Main deck side longitudinals (50x6, 180x8+80x10=155x10) | Aluminum | 3.10E-06 | 1.29E-08 | 0.00155 | 3.12E-06 | 0.33 | 3.12E-06 | 0 | 0 |
| Main deck side transverse (180x5+80x8) | Aluminum | 5.74E-06 | 3.43E-07 | 0.00154 | 6.08E-06 | 0.536 | 6.08E-06 | 0 | 0 |
| Lower deck side longitudinals (60x4)-(Fr0-39) | Steel | 7.20E-08 | 3.20E-10 | 0.00024 | 7.23E-08 | 0.128 | 7.23E-08 | 0 | 0 |
| Lower deck side transverse (170x4+80x8)-(Fr0-39) | Steel | 4.25E-06 | 3.42E-07 | 0.00132 | 4.59E-06 | 0.516 | 4.59E-06 | 0 | 0 |
| Bottom deck side and bottom longitudinals (80x5)-(Fr0-10) | Steel | 2.13E-07 | 8.33E-10 | 0.0004 | 2.14E-07 | 0.17 | 2.14E-07 | 0 | 0 |
| Bottom deck side and bottom transverse (250x5+80x8)-(Fr0-10) | Steel | 1.36E-05 | 3.44E-07 | 0.00189 | 1.39E-05 | 0.676 | 1.39E-05 | 0 | 0 |
| Bottom deck side and bottom longitudinals (125x10, 80x5=107x10)-(Fr10-19) | Steel | 1.02E-06 | 8.92E-09 | 0.00107 | 1.03E-06 | 0.234 | 1.03E-06 | 0 | 0 |
| Bottom deck side and bottom transverse (295x8+120x12)-(Fr10-19) | Steel | 3.82E-05 | 1.74E-06 | 0.0038 | 4.00E-05 | 0.854 | 4.00E-05 | 0 | 0 |
| Bottom deck side and bottom longitudinals (125x10, | Steel | 9.10E-07 | 8.58E-09 | 0.00103 | 9.19E-07 | 0.226 | 9.19E-07 | 0 | 0 |

| | | | | | | | | | |
|---|---|---|---|---|---|---|---|---|---|
| 80x5=103x10)-(Fr19-30) | | | | | | | | | |
| Bottom deck side and bottom transverse (295x8+120x12)-(Fr19-30) | Steel | 3.82E-05 | 1.74E-06 | 0.0038 | 4.00E-05 | 0.854 | 4.00E-05 | 0 | 0 |
| Bottom deck side and bottom longitudinals (125x10, 80x5=112x10)-(Fr30-34) | Steel | 1.17E-06 | 9.33E-09 | 0.00112 | 1.18E-06 | 0.244 | 1.18E-06 | 0 | 0 |
| Bottom deck side and bottom transverse (270x8+120x12)-(Fr30-34) | Steel | 3.03E-05 | 1.739 | 0.0036 | 3.21E-05 | 0.804 | 3.21E-05 | 0 | 0 |
| Bottom deck side and bottom longitudinals (125x10)-(Fr34-39) | Steel | 1.63E-06 | 1.04E-08 | 0.00125 | 1.64E-06 | 0.27 | 1.64E-06 | 0 | 0 |
| Bottom deck side and bottom transverse (300x8+120x12)-(Fr34-39) | Steel | 3.99E-05 | 1.74E-06 | 0.00384 | 4.17E-05 | 0.864 | 4.17E-05 | 0 | 0 |
| Double bottom longitudinals (80x5) | Steel | 2.13E-07 | 8.33E-10 | 0.0004 | 2.14E-07 | 0.17 | 2.14E-07 | 0 | 0 |
| Double bottom transverse (190x4+80x6) | Steel | 5.11E-06 | 2.57E-07 | 0.00124 | 5.37E-06 | 0.552 | 5.37E-06 | 0 | 0 |
| Frame 2, 4, 5, 6, 7and 9 (Vertical - 60x4) | Steel | 7.20E-08 | 3.20E-10 | 0.00024 | 7.23E-08 | 0.128 | 7.23E-08 | 0 | 0 |
| Frame 2, 3.5, 4, 5, 6 and 7 (Horizontal - 100x10) | Steel | 8.33E-07 | 8.33E-09 | 0.001 | 8.41E-07 | 0.22 | 8.41E-07 | 0 | 0 |
| Frame 3.5 (Vertical - 80x5) | Steel | 2.13E-07 | 8.33E-10 | 0.0004 | 2.14E-07 | 0.17 | 2.14E-07 | 0 | 0 |
| Frame 9 (Horizontal - 100x10, 140x4+80x6=136x10) | Steel | 2.10E-06 | 1.13E-08 | 0.00136 | 2.11E-06 | 0.292 | 2.11E-06 | 0 | 0 |
| Frame 18 owner deck wall transverse (60x40x5) | Aluminum | 3.59E-08 | 2.01E-07 | 0.000475 | 2.37E-07 | 0.2 | 2.37E-07 | 0 | 0 |
| Frame 18 owner deck wall longitudinals (60x40x5,60x5=52.26x10) | Aluminum | 1.19E-07 | 4.36E-09 | 0.0005226 | 1.23E-07 | 0.1245 | 1.23E-07 | 0 | 0 |
| Frame 18+0.51 lower deck plate (Horizontal) -(60x5) | Steel | 9.00E-08 | 6.25E-10 | 0.0003 | 9.06E-08 | 0.13 | 9.06E-08 | 0 | 0 |
| Frame 18+0.51 lower deck plate (Vertical) -(60x5, 120x4+60x6=94.62x10) | Steel | 7.06E-07 | 7.89E-09 | 0.0009462 | 7.14E-07 | 0.2092 | 7.14E-07 | 0 | 0 |
| Frame 22+0.2 and frame 20 owner deck wall transverse (60x5) | Aluminum | 9.00E-08 | 6.25E-10 | 0.0003 | 9.06E-08 | 0.13 | 9.06E-08 | 0 | 0 |
| Frame 22+0.2 and frame 20 owner deck wall longitudinals (60x5) | Aluminum | 9.00E-08 | 6.25E-10 | 0.0003 | 9.06E-08 | 0.13 | 9.06E-08 | 0 | 0 |
| Owner deck longitudinal wall transverse and longitudinals (60x5) | Aluminum | 9.00E-08 | 6.25E-10 | 0.0003 | 9.06E-08 | 0.13 | 9.06E-08 | 0 | 0 |
| Main deck internal wall longitudinals and transverse (60x5) | Aluminum | 9.00E-08 | 6.25E-10 | 0.0003 | 9.06E-08 | 0.13 | 9.06E-08 | 0 | 0 |
| Longitudinal wall between frame 8 and 10 lower deck longitudinals (80x8) | Steel | 3.41E-07 | 3.41E-09 | 0.00064 | 3.44E-07 | 0.176 | 3.44E-07 | 0 | 0 |
| Longitudinal wall between frame 8 and 10 lower deck transverse (60x6) | Steel | 1.08E-07 | 1.08E-09 | 0.00036 | 1.09E-07 | 0.132 | 1.09E-07 | 0 | 0 |
| Longitudinal bulkhead between fr-10 and fr-15 lower deck (Horizontal) -(60x5) | Steel | 9.00E-08 | 6.25E-10 | 0.0003 | 9.06E-08 | 0.13 | 9.06E-08 | 0 | 0 |
| Longitudinal bulkhead between fr-10 and fr-15 lower deck (Vertical) -(80x5) | Steel | 2.13E-07 | 8.33E-10 | 0.0004 | 2.14E-07 | 0.17 | 2.14E-07 | 0 | 0 |

| | | | | | | | | | |
|---|---|---|---|---|---|---|---|---|---|
| Longitudinal bulkhead between fr-15 and fr19+0.278 lower deck (Horizontal and Vertical-60x5) | Steel | 9.00E-08 | 6.25E-10 | 0.0003 | 9.06E-08 | 0.13 | 9.06E-08 | 0 | 0 |
| Longitudinal bulkheads at 0.45m (stb) and 1.31m (port) lower deck (Horizontal and Vertical-60x5) | Steel | 9.00E-08 | 6.25E-10 | 0.0003 | 9.06E-08 | 0.13 | 9.06E-08 | 0 | 0 |
| 0.45m longitudinal bulkhead longitudinals (Vertical - 60x4) | Steel | 7.20E-08 | 3.20E-10 | 0.00024 | 7.23E-08 | 0.128 | 7.23E-08 | 0 | 0 |
| 0.45 longitudinal bulkhead transverse (Horizontal - 150x4+80x6) | Steel | 2.75E-06 | 2.57E-07 | 0.00108 | 3.01E-06 | 0.472 | 3.01E-06 | 0 | 0 |
| Top of tanks in engine room longitudinals (80x5) | Steel | 2.13E-07 | 8.33E-10 | 0.0004 | 2.14E-07 | 0.17 | 2.14E-07 | 0 | 0 |
| Side of tanks in engine room longitudinals (60x6) | Steel | 1.08E-07 | 1.08E-09 | 0.00036 | 1.09E-07 | 0.132 | 1.09E-07 | 0 | 0 |
| Longitudinals (60x4) for top plate of tank (Between fr-4&5, 6&7) | Steel | 7.20E-08 | 3.20E-10 | 0.00024 | 7.23E-08 | 0.128 | 7.23E-08 | 0 | 0 |
| Transverse (200x5+80x6) for top plate of tank (Between fr-4&5, 6&7) | Steel | 6.78E-06 | 2.58E-07 | 0.00148 | 7.03E-06 | 0.572 | 7.03E-06 | 0 | 0 |

## Appendix IV(a) (Different types of ribbed plates – Ribs in local x direction)

| Name | Skin | 1-Dir. Rib | 1-Dir. Spacing Mean (m) | 1-Dir. Spacing Std. Dev. (%) | 1-Dir. Height (m) |
|---|---|---|---|---|---|
| Sundeck ribbed plate | Sundeck plate | Common sundeck longitudinals (50x6) | 0.9 | 0 | 0.0275 |
| Owner deck ribbed plate (Until Fr19) | Owner deck plate | Common owner deck longitudinals (50x6) | 0.9 | 0 | 0.0275 |
| Owner deck ribbed plate (From Fr19) | Owner deck plate | Common owner deck longitudinals (50x6) | 0.9 | 0 | 0.0275 |
| Owner deck lower side ribbed plate | Owner deck lower side plate | Owner deck side longitudinals (50x6) | 0.317 | 0 | 0.0275 |
| Owner deck upper side ribbed plate | Owner deck upper side plate | Owner deck side longitudinals (50x6) | 0.317 | 0 | 0.031 |
| Main deck ribbed plate (Fr0-10) | Main deck plate | Main deck longitudinals (60x4, 50x5, 200x4+100x10=132.33x10) | 0.344 | 4.57 | 0.06867 |
| Main deck ribbed plate (Fr10-19) | Main deck plate | Main deck longitudinals (60x4, 50x5, 200x4+100x10=132.33x10) | 0.344 | 4.57 | 0.06867 |
| Main deck ribbed plate (Fr19-30) | Main deck plate | Main deck longitudinals (60x4, 50x5, 200x4+100x10=132.33x10) | 0.344 | 4.57 | 0.06867 |
| Main deck ribbed plate (Fr30-34) | Main deck plate | Main deck longitudinals (60x4,50x5, 200x4+100x10=118.1x10) | 0.342 | 5.33 | 0.06155 |
| Main deck ribbed plate (Fr34-40) | Main deck plate | Main deck longitudinals (50x5, 200x4+100x10=122x10) | 0.3412 | 5.586 | 0.0635 |
| Main deck upper side ribbed plate | Main deck upper side plate | Main deck side longitudinals (50x6, 180x8+80x10=155x10) | 0.307 | 1.57 | 0.08 |
| Main deck lower side ribbed plate | Main deck lower side plate | Main deck side longitudinals (50x6, 180x8+80x10=155x10) | 0.307 | 1.57 | 0.08 |
| Lower deck ribbed plate (Fr0-10) | Lower deck plate | Lower deck longitudinals (150x4+100x10, 60x6=90.11x10) | 0.344 | 4.57 | 0.047 |
| Lower deck ribbed plate (Fr10-19) | Lower deck plate | Lower deck longitudinals (200x4+100x10, 50x5=105.9x10) | 0.344 | 4.57 | 0.05495 |
| Lower deck ribbed plate (Fr19-30) | Lower deck plate | Lower deck longitudinals | 0.346 | 3.85 | 0.0562 |

| | | | | | |
|---|---|---|---|---|---|
| | | (200x4+100x10, 50x5=108.4x10) | | | |
| Lower deck ribbed plate (Fr30-34) | Lower deck plate | Lower deck longitudinals (200x4+100x10, 50x5=122x10) | 0.3412 | 5.59 | 0.063 |
| Lower deck ribbed plate (Fr34-40) | Lower deck plate | Lower deck longitudinals (200x4+100x10, 50x5=147.5x10) | 0.333 | 7.08 | 0.07575 |
| Lower deck side ribbed plate (Fr0-10) | Lower deck side plate | Lower deck side longitudinals (60x4)-(Fr0-39) | 0.339 | 0.73 | 0.033 |
| Lower deck side ribbed plate (Fr10-19) | Lower deck side plate | Lower deck side longitudinals (60x4)-(Fr0-39) | 0.3 | 12.23 | 0.033 |
| Lower deck side ribbed plate (Fr19-30) | Lower deck side plate | Lower deck side longitudinals (60x4)-(Fr0-39) | 0.301 | 12.01 | 0.033 |
| Lower deck side ribbed plate (Fr30-34) | Lower deck side plate | Lower deck side longitudinals (60x4)-(Fr0-39) | 0.284 | 11.07 | 0.033 |
| Lower deck side ribbed plate (Fr34-40) | Lower deck side plate | Lower deck side longitudinals (60x4)-(Fr0-39) | 0.283 | 16.03 | 0.033 |
| Bottom deck side and bottom ribbed plate (Fr0-10) | Bottom deck side and bottom plate | Bottom deck side and bottom longitudinals (80x5)-(Fr0-10) | 0.284 | 23.11 | 0.044 |
| Bottom deck side and bottom ribbed plate (Fr10-19) | Bottom deck side and bottom plate | Bottom deck side and bottom longitudinals (125x10, 80x5=107x10)-(Fr10-19) | 0.254 | 26.36 | 0.0575 |
| Bottom deck side and bottom ribbed plate (Fr19-30) | Bottom deck side and bottom plate | Bottom deck side and bottom longitudinals (125x10, 80x5=103x10)-(Fr19-30) | 0.234 | 24.42 | 0.0555 |
| Bottom deck side and bottom ribbed plate (Fr30-34) | Bottom deck side and bottom plate | Bottom deck side and bottom longitudinals (125x10, 80x5=112x10)-(Fr30-34) | 0.23 | 20.96 | 0.06 |
| Bottom deck side and bottom ribbed plate (Fr34-40) | Owner deck plate | Bottom deck side and bottom longitudinals (125x10)-(Fr34-39) | 0.2 | 0 | 0.0665 |
| Double bottom ribbed plate | Double bottom plate | Double bottom longitudinals (80x5) | 0.35 | 0 | 0.0425 |
| Frame 2 ribbed plate | Frame 2, 3.5, 4, 5, 6, 7 and 9 plate | Frame 2, 3.5, 4, 5, 6 and 7 (Horizontal - 100x10) | 1.335 | 0 | 0.0525 |
| Frame 3.5 ribbed plate | Owner deck plate | Frame 2, 3.5, 4, 5, 6 and 7 (Horizontal - 100x10) | 1.473 | 0 | 0.0525 |
| Frame 4 ribbed plate | Frame 2, 3.5, 4, 5, 6, 7 and 9 plate | Frame 2, 3.5, 4, 5, 6 and 7 (Horizontal - 100x10) | 1.51 | 0 | 0.0525 |
| Frame 9 ribbed plate | Owner deck plate | Frame 9 (Horizontal - 100x10, 140x4+80x6=136x10) | 0.808 | 0 | 0.0705 |
| Frame 7 ribbed plate | Frame 2, 3.5, 4, 5, 6, 7 and 9 plate | Frame 2, 3.5, 4, 5, 6 and 7 (Horizontal - 100x10) | 1.25 | 0 | 0.0525 |
| Frame 5 ribbed plate | Frame 2, 3.5, 4, 5, 6, 7 and 9 plate | Frame 2, 3.5, 4, 5, 6 and 7 (Horizontal - 100x10) | 0.983 | 0 | 0.0525 |
| Frame 6 ribbed plate | Frame 2, 3.5, 4, 5, 6, 7 and 9 plate | Frame 2, 3.5, 4, 5, 6 and 7 (Horizontal - 100x10) | 0.56 | 0 | 0.0525 |
| Frame 15 and 17 main deck and lower deck wall ribbed plate (starboard) | Main deck internal transverse and longitudinal walls | Main deck internal wall longitudinals and transverse (60x5) | 1.522 | 0 | 0.0325 |
| Frame 15+0.68 and 17 main deck and lower deck wall ribbed plate (port) | Main deck internal transverse and longitudinal walls | Main deck internal wall longitudinals and transverse (60x5) | 1.522 | 0 | 0.0325 |
| Frame 16 main deck and frame 15+0.55 lower deck wall ribbed plate | Main deck internal transverse and longitudinal walls | Main deck internal wall longitudinals and transverse (60x5) | 1.522 | 0 | 0.0325 |
| Frame 18 owner deck wall ribbed plate | Owner deck internal transverse and longitudinal walls | Frame 18 owner deck wall transverse (60x40x5) | 1.284 | 0 | 0.0426 |
| Frame 18+0.51 lower deck ribbed plate | Frame 18+0.51 lower deck plate | Frame 18+0.51 lower deck plate (Horizontal) -(60x5) | 1.215 | 0 | 0.032 |
| Frame 22+0.2 and frame 20 owner deck wall ribbed plate | Owner deck internal transverse and longitudinal walls | Frame 22+0.2 and frame 20 owner deck wall transverse (60x5) | 1.284 | 0 | 0.0325 |

| | | | | | |
|---|---|---|---|---|---|
| Frame 22+0.2,frame 20 and frame 24+0.56 main deck wall ribbed plate (Same in lower deck) | Main deck internal transverse and longitudinal walls | Main deck internal wall longitudinals and transverse (60x5) | 1.284 | 0 | 0.0325 |
| Transom ribbed plate | Transom plate | Transom (Horizontal-140x4+80x8) | 0.874 | 17.5 | 0.1125 |
| Bulkhead fr-10 lower deck ribbed plate | Bulkhead fr-10 lower deck plate | Bulkhead fr-10 lower deck (Horizontal) -(60x6) | 0.849 | 0 | 0.032 |
| Bulkhead fr-10 bottom deck ribbed plate | Bulkhead fr-10 bottom deck plate | Bulkhead fr-10 lower deck (Horizontal) -(60x6) | 0.281 | 27.23 | 0.0325 |
| Bulkhead fr-15+0.55 lower deck ribbed plate | Bulkhead fr-15+0.55 lower deck plate | Bulkhead fr-19 bottom deck (Horizontal) -(140x4+80x8) | 0.812 | 0 | 0.032 |
| Bulkhead fr-19 bottom deck ribbed plate | Bulkhead fr-19 bottom deck plate | Bulkhead fr-19 bottom deck (Horizontal) -(140x4+80x8) | 1.782 | 22.67 | 0.1115 |
| Bulkhead fr-19+0.278 lower deck ribbed plate | Bulkhead fr19+0.278 lower deck plate | Bulkhead fr-19+0.278 lower deck (Vertical and Horizontal) -(60x5) | 1.215 | 0 | 0.032 |
| Bulkhead fr-21 lower and bottom decks ribbed plate | Bulkhead fr-21 lower and bottom decks plate | Bulkhead fr-21 lower deck (Horizontal) -(60x5) | 1.215 | 0 | 0.032 |
| Bulkhead fr-26 and 29.5 bottom deck ribbed plate | Bulkhead fr-26 and fr-29.5 bottom deck plate | Bulkhead fr-26 and 29.5 bottom deck (Horizontal) -(60x6) | 0.857 | 0 | 0.032 |
| Bulkhead fr-27 lower deck ribbed plate | Bulkhead fr-27 lower deck plate | Bulkhead fr-27 lower deck (Horizontal)- (60x5) | 1.214 | 0 | 0.032 |
| Bulkhead 34/37 ribbed plate | Bulkhead 34/37 plate | Bulkhead fr-34/37 lower deck (Horizontal)- (50x5) | 0.616 | 0 | 0.027 |
| Bulkhead fr-34 bottom deck ribbed plate | Bulkhead 34/37 plate | Bulkhead fr-34 bottom deck (Horizontal) -(141x4+60x6) | 1.308 | 0 | 0.1011 |
| Bulkhead fr-37 bottom deck ribbed plate | Bulkhead fr-37 bottom deck plate | Bulkhead fr-37 bottom deck (Horizontal) -(80x10) | 0.405 | 8.65 | 0.0425 |
| 0.45 longitudinal bulkhead ribbed plate | 0.45m longitudinal bulkhead | 0.45 longitudinal bulkhead transverse (Horizontal - 150x4+80x6) | 1.1 | 0 | 0.1127 |
| Longitudinal bulkhead between fr-10 and fr-15 lower deck ribbed plate | Longitudinal bulkhead between fr-10 and fr-15 lower deck plate | Longitudinal bulkhead between fr-10 and fr-15 lower deck (Horizontal) -(60x5) | 1.115 | 0 | 0.032 |
| Longitudinal bulkhead between fr-15 and fr-19+0.278 lower deck ribbed plate | Longitudinal bulkhead between fr-15 and fr-19+0.278 lower deck plate | Longitudinal bulkhead between fr-15 and fr19+0.278 lower deck (Horizontal and Vertical-60x5) | 1.115 | 0 | 0.032 |
| Longitudinal bulkhead at 0.45m (stb) and 1.31m (port) lower deck ribbed plate | Longitudinal bulkheads at 0.45m (stb) and 1.31m (port) lower deck plate | Longitudinal bulkheads at 0.45m (stb) and 1.31m (port) lower deck (Horizontal and Vertical-60x5) | 1.116 | 0 | 0.032 |
| Top ribbed plate of tank (Between fr-4&5, 6&7) | Top plate of tanks (between fr-4&5, 6&7) | Longitudinals (60x4) for top plate of tank (Between fr-4&5, 6&7) | 0.35 | 0 | 0.032 |
| Owner deck longitudinal wall ribbed plate | Owner deck internal transverse and longitudinal walls | Owner deck longitudinal wall transverse and longitudinals (60x5) | 1.284 | 0 | 0.0325 |
| Main deck and lower deck longitudinal wall ribbed plate (Between fr-15 and 17) | Main deck internal transverse and longitudinal walls | Main deck internal wall longitudinals and transverse (60x5) | 1.522 | 0 | 0.0325 |
| Main deck longitudinal wall ribbed plate (Between fr-20 and 22+0.2) (Same in lower deck) | Main deck internal transverse and longitudinal walls | Main deck internal wall longitudinals and transverse (60x5) | 1.284 | 0 | 0.0325 |
| Longitudinal wall between frame 8 and 10 lower deck ribbed plate | Longitudinal wall between frame 8 and 10 lower deck | Longitudinal wall between frame 8 and 10 lower deck transverse (60x6) | 0.845 | 0 | 0.032 |

## Appendix IV(b) (Different types of ribbed plates – Ribs in local y direction)

| Name | Skin | 2-Dir. Rib | 2-Dir. Spacing Mean (m) | 2-Dir. Spacing Std. Dev. (%) | 2-Dir. Height (m) |
|---|---|---|---|---|---|

| | | | | | |
|---|---|---|---|---|---|
| Sundeck ribbed plate | Sundeck plate | Sundeck transverse (100x5+90x15) | 0.4788 | 4.928 | 0.0945 |
| Owner deck ribbed plate (Until Fr19) | Owner deck plate | Owner deck transverse (120x5+90x15) | 0.463 | 7.7 | 0.1092 |
| Owner deck ribbed plate (From Fr19) | Owner deck plate | Owner deck transverse (120x5+90x12) | 0.487 | 12.5 | 0.1049 |
| Owner deck lower side ribbed plate | Owner deck lower side plate | Owner deck side transverse (180x5+50x5) | 0.744 | 30 | 0.1126 |
| Owner deck upper side ribbed plate | Owner deck upper side plate | Owner deck side transverse (180x5+50x5) | 0.483 | 3.04 | 0.1161 |
| Main deck ribbed plate (Fr0-10) | Main deck plate | Main deck transverse (200x4+60x6) | 1.1 | 0 | 0.1345 |
| Main deck ribbed plate (Fr10-19) | Main deck plate | Main deck transverse (140x4+60x6) | 0.93 | 0 | 0.1011 |
| Main deck ribbed plate (Fr19-30) | Main deck plate | Main deck transverse (140x4+60x6) | 0.99 | 0 | 0.1011 |
| Main deck ribbed plate (Fr30-34) | Main deck plate | Main deck transverse (200x4+80x6) | 0.99 | 0 | 0.1411 |
| Main deck ribbed plate (Fr34-40) | Main deck plate | Main deck transverse (200x4+80x6) | 0.99 | 0 | 0.1411 |
| Main deck upper side ribbed plate | Main deck upper side plate | Main deck side transverse (180x5+80x8) | 0.455 | 15.12 | 0.1316 |
| Main deck lower side ribbed plate | Main deck lower side plate | Main deck side transverse (180x5+80x8) | 0.739 | 30 | 0.1316 |
| Lower deck ribbed plate (Fr0-10) | Lower deck plate | Lower deck transverse (150x4+80x6) | 1.1 | 0 | 0.1117 |
| Lower deck ribbed plate (Fr10-19) | Lower deck plate | Lower deck transverse (140x4+80x6) | 0.93 | 0 | 0.025 |
| Lower deck ribbed plate (Fr19-30) | Lower deck plate | Lower deck transverse (140x4+60x6) | 0.99 | 0 | 0.1006 |
| Lower deck ribbed plate (Fr30-34) | Lower deck plate | Lower deck transverse (140x4+60x6) | 0.99 | 0 | 0.1006 |
| Lower deck ribbed plate (Fr34-40) | Lower deck plate | Lower deck transverse (140x4+60x6) | 0.99 | 0 | 0.1006 |
| Lower deck side ribbed plate (Fr0-10) | Lower deck side plate | Lower deck side transverse (170x4+80x8)-(Fr0-39) | 1.1 | 0 | 0.1312 |
| Lower deck side ribbed plate (Fr10-19) | Lower deck side plate | Lower deck side transverse (170x4+80x8)-(Fr0-39) | 0.93 | 0 | 0.1312 |
| Lower deck side ribbed plate (Fr19-30) | Lower deck side plate | Lower deck side transverse (170x4+80x8)-(Fr0-39) | 0.99 | 0 | 0.1312 |
| Lower deck side ribbed plate (Fr30-34) | Lower deck side plate | Lower deck side transverse (170x4+80x8)-(Fr0-39) | 0.99 | 0 | 0.1312 |
| Lower deck side ribbed plate (Fr34-40) | Lower deck side plate | Lower deck side transverse (170x4+80x8)-(Fr0-39) | 0.99 | 0 | 0.1312 |
| Bottom deck side and bottom ribbed plate (Fr0-10) | Bottom deck side and bottom plate | Bottom deck side and bottom transverse (250x5+80x8)-(Fr0-10) | 1.1 | 0 | 0.1727 |
| Bottom deck side and bottom ribbed plate (Fr10-19) | Bottom deck side and bottom plate | Bottom deck side and bottom transverse (295x8+120x12)-(Fr10-19) | 0.99 | 0 | 0.2097 |
| Bottom deck side and bottom ribbed plate (Fr19-30) | Bottom deck side and bottom plate | Bottom deck side and bottom transverse (295x8+120x12)-(Fr19-30) | 0.99 | 0 | 0.2097 |
| Bottom deck side and bottom ribbed plate (Fr30-34) | Bottom deck side and bottom plate | Bottom deck side and bottom transverse (270x8+120x12)-(Fr30-34) | 0.99 | 0 | 0.1954 |
| Bottom deck side and bottom ribbed plate (Fr34-40) | Owner deck plate | Bottom deck side and bottom transverse (300x8+120x12)-(Fr34-39) | 0.99 | 0 | 0.2125 |
| Double bottom ribbed plate | Double bottom plate | Double bottom transverse (190x4+80x6) | 0.99 | 0 | 0.1354 |
| Frame 2 ribbed plate | Frame 2, 3.5, 4, 5, 6, 7 and 9 plate | Frame 2, 4, 5, 6, 7and 9 (Vertical - 60x4) | 0.35 | 0 | 0.0325 |
| Frame 3.5 ribbed plate | Owner deck plate | Frame 3.5 (Vertical - 80x5) | 0.35 | 0 | 0.0425 |
| Frame 4 ribbed plate | Frame 2, 3.5, 4, 5, 6, 7 and 9 plate | Frame 2, 4, 5, 6, 7and 9 (Vertical - 60x4) | 0.35 | 0 | 0.0325 |
| Frame 9 ribbed plate | Owner deck plate | Frame 2, 4, 5, 6, 7and 9 (Vertical - 60x4) | 0.35 | 0 | 0.0325 |

| | | | | | |
|---|---|---|---|---|---|
| Frame 7 ribbed plate | Frame 2, 3.5, 4, 5, 6, 7 and 9 plate | Frame 2, 4, 5, 6, 7and 9 (Vertical - 60x4) | 0.35 | 0 | 0.0325 |
| Frame 5 ribbed plate | Frame 2, 3.5, 4, 5, 6, 7 and 9 plate | Frame 2, 4, 5, 6, 7and 9 (Vertical - 60x4) | 0.35 | 0 | 0.0325 |
| Frame 6 ribbed plate | Frame 2, 3.5, 4, 5, 6, 7 and 9 plate | Frame 2, 4, 5, 6, 7and 9 (Vertical - 60x4) | 0.35 | 0 | 0.0325 |
| Frame 15 and 17 main deck and lower deck wall ribbed plate (starboard) | Main deck internal transverse and longitudinal walls | Main deck internal wall longitudinals and transverse (60x5) | 0.2575 | 0 | 0.0325 |
| Frame 15+0.68 and 17 main deck and lower deck wall ribbed plate (port) | Main deck internal transverse and longitudinal walls | Main deck internal wall longitudinals and transverse (60x5) | 0.2557 | 1.66 | 0.0325 |
| Frame 16 main deck and frame 15+0.55 lower deck wall ribbed plate | Main deck internal transverse and longitudinal walls | Main deck internal wall longitudinals and transverse (60x5) | 0.3 | 28.86 | 0.0325 |
| Frame 18 owner deck wall ribbed plate | Owner deck internal transverse and longitudinal walls | Frame 18 owner deck wall longitudinals (60x40x5,60x5=52.26x10) | 0.2406 | 0 | 0.02863 |
| Frame 18+0.51 lower deck ribbed plate | Frame 18+0.51 lower deck plate | Frame 18+0.51 lower deck plate (Vertical) -(60x5, 120x4+60x6=94.62x10)+ | 0.3478 | 0.647 | 0.04931 |
| Frame 22+0.2 and frame 20 owner deck wall ribbed plate | Owner deck internal transverse and longitudinal walls | Frame 22+0.2 and frame 20 owner deck wall longitudinals (60x5) | 0.3341 | 6.554 | 0.0325 |
| Frame 22+0.2,frame 20 and frame 24+0.56 main deck wall ribbed plate (Same in lower deck) | Main deck internal transverse and longitudinal walls | Main deck internal wall longitudinals and transverse (60x5) | 0.3341 | 6.554 | 0.0325 |
| Transom ribbed plate | Transom plate | Transom (Vertical-80x5) | 0.35 | 0 | 0.043 |
| Bulkhead fr-10 lower deck ribbed plate | Bulkhead fr-10 lower deck plate | Bulkhead fr-10 lower deck (Vertical) -(80x5) | 0.35 | 0 | 0.042 |
| Bulkhead fr-10 bottom deck ribbed plate | Bulkhead fr-10 bottom deck plate | Bulkhead fr-10 bottom deck (Vertical) -(80x5) | 0.346 | 16.81 | 0.0425 |
| Bulkhead fr-15+0.55 lower deck ribbed plate | Bulkhead fr-15+0.55 lower deck plate | Bulkhead fr-15+0.55 lower deck (Vertical) -(80x5, 120x4+60x6=81.02x10) | 0.3381 | 6 | 0.04251 |
| Bulkhead fr-19 bottom deck ribbed plate | Bulkhead fr-19 bottom deck plate | Bulkhead fr-19 bottom deck (Vertical)- (60x6) | 0.35 | 0 | 0.032 |
| Bulkhead fr-19+0.278 lower deck ribbed plate | Bulkhead fr19+0.278 lower deck plate | Bulkhead fr-19+0.278 lower deck (Vertical and Horizontal) -(60x5) | 0.35 | 0 | 0.032 |
| Bulkhead fr-21 lower and bottom decks ribbed plate | Bulkhead fr-21 lower and bottom decks plate | Bulkhead fr-21 lower deck (Vertical)- (60x5, 120x4+60x6=70.766x10) | 0.35 | 0 | 0.0373 |
| Bulkhead fr-26 and 29.5 bottom deck ribbed plate | Bulkhead fr-26 and fr-29.5 bottom deck plate | Bulkhead fr-26 and 29.5 bottom deck (Vertical) -(80x5) | 0.35 | 0 | 0.042 |
| Bulkhead fr-27 lower deck ribbed plate | Bulkhead fr-27 lower deck plate | Bulkhead fr-27 lower deck (Vertical) -(60x5, 120x4+60x6, 60x40x5=72x10) | 0.3151 | 16.02 | 0.038 |
| Bulkhead 34/37 ribbed plate | Bulkhead 34/37 plate | Bulkhead fr-34/37 lower deck (Vertical)- (60x4) | 0.35 | 0 | 0.032 |
| Bulkhead fr-34 bottom deck ribbed plate | Bulkhead 34/37 plate | Bulkhead fr-34 bottom deck (Vertical)- (60x4) | 0.35 | 0 | 0.032 |
| Bulkhead fr-37 bottom deck ribbed plate | Bulkhead fr-37 bottom deck plate | Bulkhead fr-37 bottom deck (Vertical) -(100x10, 300x6+100x10=248x10) | 0.3285 | 0 | 0.1265 |
| 0.45 longitudinal bulkhead ribbed plate | 0.45m longitudinal bulkhead | 0.45m longitudinal bulkhead longitudinals (Vertical - 60x4) | 0.248 | 16.22 | 0.0325 |
| Longitudinal bulkhead between fr-10 and fr-15 lower deck ribbed plate | Longitudinal bulkhead between fr-10 and fr-15 lower deck plate | Longitudinal bulkhead between fr-10 and fr-15 lower deck (Vertical) -(80x5) | 0.31 | 0 | 0.042 |
| Longitudinal bulkhead between fr-15 and fr-19+0.278 lower deck ribbed plate | Longitudinal bulkhead between fr-15 and fr-19+0.278 lower deck plate | Longitudinal bulkhead between fr-15 and fr19+0.278 lower deck (Horizontal and Vertical-60x5) | 0.31 | 0 | 0.032 |
| Longitudinal bulkhead at 0.45m (stb) and 1.31m (port) lower deck | Longitudinal bulkheads at 0.45m (stb) and 1.31m | Longitudinal bulkheads at 0.45m (stb) and 1.31m (port) lower deck (Horizontal and Vertical-60x5) | 0.35 | 0 | 0.032 |

| | | | | | |
|---|---|---|---|---|---|
| ribbed plate | (port) lower deck plate | | | | |
| Top ribbed plate of tank (Between fr-4&5, 6&7) | Top plate of tanks (between fr-4&5, 6&7) | Transverse (200x5+80x6) for top plate of tank (Between fr-4&5, 6&7) | 1.1 | 0 | 0.1354 |
| Owner deck longitudinal wall ribbed plate | Owner deck internal transverse and longitudinal walls | Owner deck longitudinal wall transverse and longitudinals (60x5) | 0.4875 | 2.664 | 0.0325 |
| Main deck and lower deck longitudinal wall ribbed plate (Between fr-15 and 17) | Main deck internal transverse and longitudinal walls | Main deck internal wall longitudinals and transverse (60x5) | 0.35 | 0 | 0.0325 |
| Main deck longitudinal wall ribbed plate (Between fr-20 and 22+0.2) (Same in lower deck) | Main deck internal transverse and longitudinal walls | Main deck internal wall longitudinals and transverse (60x5) | 0.4875 | 2.664 | 0.0325 |
| Longitudinal wall between frame 8 and 10 lower deck ribbed plate | Longitudinal wall between frame 8 and 10 lower deck | Longitudinal wall between frame 8 and 10 lower deck longitudinals (80x8) | 0.287 | 8.01 | 0.042 |

## Appendix V (Different types of insulations)

| Name | Layers | Layer-1 | Layer-2 | Layer-3 | Layer-4 | Layer-5 | Layer-6 |
|---|---|---|---|---|---|---|---|
| TT01 | 1 | Mascoat DTM | | | | | |
| TA01 (Yellow | 5 | Isover ultimate UMPN 66 slab | Promasound Tl | Isover ultimate UMPA 66 slab | Aluminum | Plywood | |
| TA01+Mascoat (Yellow | 6 | Isover ultimate UMPN 66 slab | Promasound Tl | Isover ultimate UMPA 66 slab | Aluminum | Plywood | Mascoat DTM |
| TA02 (Blue) | 4 | Isover ultimate UMPA 66 slab | Isover ultimate UMFA 24 Felt | Aluminum | Plywood | | |
| TA02+Mascoat (Blue) | 5 | Isover ultimate UMPN 66 slab | Isover ultimate UMFA 24 Felt | Aluminum | Plywood | Mascoat DTM | |
| TA02B+Mascoat (Cyan) | 4 | Isover ultimate UMPN 66 slab | Aluminum | Plywood | Mascoat DTM | | |
| TA03 (Green) | 4 | Isover ultimate UMPN 36 slab | Isover ultimate UMFA 24 Felt | Aluminum | Plywood | | |
| TA03+Mascoat (Green) | 5 | Isover ultimate UMFA 24 Felt | Isover ultimate UMPN 36 slab | Aluminum | Plywood | Mascoat DTM | |
| TA04 (Magenta) (30mm) | 3 | Isover ultimate UMPN 36 slab | Aluminum | Plywood | | | |
| TA04 (Magenta) (60mm) | 3 | Isover ultimate UMPN 36 slab | Aluminum | Plywood | | | |
| TA04 (Magenta) (90mm) | 3 | Isover ultimate UMPN 36 slab | Aluminum | Plywood | | | |
| TA04+Mascoat-2mm (Magenta) (60mm) | 4 | Isover ultimate UMPN 36 slab | Aluminum | Plywood | Mascoat DTM | | |
| TA05 (Red) | 2 | Whisper fiber | Plywood | | | | |
| TA06 (Blue) | 3 | Isover ultimate UMPA 66 slab | Aluminum | Plywood | | | |
| TF01 (Red) | 3 | Isover ultimate UMPN 66 slab | Aluminum | Plywood | | | |
| TF01B (Cyan) | 3 | Isover ultimate UMPN 66 slab | Aluminum | Plywood | | | |
| TF02 (Green) | 3 | Felt | Aluminum | Plywood | | | |
| Owner deck outer layer tempered glass (6mm) | 1 | Tempered Glass | | | | | |
| Main deck outer layer tempered glass (6mm) | 1 | Tempered Glass | | | | | |
| Main deck outer layer tempered glass (8.76mm) | 1 | Tempered Glass | | | | | |
| Doors insulation | 6 | Polyester foam - 30 $kg/m^3$ | Plywood | Rockwool | Plywood | Polyester foam - 30 $kg/m^3$ | Plywood |

| | | | | | | | |
|---|---|---|---|---|---|---|---|
| Pl-01 (Cyan) (Isover ultimate 66 slab-30mm + sandwich panel 8-6-8) | 4 | Isover ultimate UMPN 66 slab | Plywood | Hard Rubber | Plywood | | |
| Pl-02 (Green) (Isover ultimate 66 slab-30mm + Isophon-19mm) | 2 | Isover ultimate UMPN 66 slab | Plywood | | | | |
| Pl-03 (Lariphon and laricross) | 2 | Polyester foam - 30 $kg/m^3$ | Plywood | | | | |